NASA Technical Memorandum 4456

Materials Science on Parabolic Aircraft

The FY 87-89 KC-135 Microgravity Test Program

Peter A. Curreri, *Editor*
George C. Marshall Space Flight Center
Marshall Space Flight Center, Alabama

National Aeronautics and
Space Administration
Office of Management
Scientific and Technical
Information Program
1993

ACKNOWLEDGMENTS

Preparation of this volume was greatly assisted by the provision of flight data and files by Jeffrey Mullins/MSFC, EO23. Technical format editing by Tauna Moorehead and type setting by Susan Burrer and Shelby Morris/MSFC, ES01 are greatly appreciated.

PRECEDING PAGE BLANK NOT FILMED

TABLE OF CONTENTS

PRECEDING PAGE BLANK NOT FILMED

TABLE OF CONTENTS (Continued)

TABLE OF CONTENTS (Continued)

TABLE OF CONTENTS (Concluded)

TECHNICAL MEMORANDUM

MATERIALS SCIENCE ON PARABOLIC AIRCRAFT

The FY 87-89 KC-135 Microgravity Test Program

INTRODUCTION

From across the U.S. and sometimes from around the world, on a monthly basis, teams of scientists travel to Ellington Air Force Base near Johnson Space Center (JSC). In a hanger off a large airport runway, early Monday morning, they assemble an elaborate and varied array of scientific hardware and electronics. Each team tests their own hardware. Failures occur and often send technicians scrambling to on-site machine shops or off-site electronics outlets. The next morning, often after weather delays, the 22 scientists, technicians, photographers, journalists, and sometimes dignitaries sit buckled in the rear of the large KC-135 interior waiting for take-off. Before them spread throughout the cabin their apparatus hum, display lights twinkle, and heaters heat. The plane roars into the sky over the Gulf of Mexico. Parabolic maneuvers begin, always making a certain number of the passengers violently ill. The world, now, is a very different place where researchers become so light that they can fly, then 20 sec later weigh 400 pounds. And the common materials processes, on which our society relies, often change just as dramatically.

For over 20 years the NASA KC-135 and her predecessor aircraft have provided what is arguably the world's most active low-gravity materials science program. These flights are supported by NASA Headquarters scientific and commercial microgravity programs, managed by Marshall Space Flight Center (MSFC), and operated by JSC. They support foreign and domestic scientists from government agencies, NASA centers, academia, and private enterprise. The system allows ready access to low gravity, but requires that experiments be carefully designed and implemented to isolate the gravity variable and to provide meaningful scientific data in low gravity of only 25 sec duration.

This volume covers research results from the KC-135 materials science program managed by MSFC for the period FY87 through FY89. This report follows the previous report for FY 84-86 published as NASA Technical Memorandum 4059, August 1988. This volume contains over 30 reports that cover research pertinent to virtually all areas of microgravity science. As an aid to the reader the reports are grouped into eight subject areas.

Section 1 reports detail the acceleration environment to be expected onboard the KC-135. Included are the frequency dependence of g-jitter the characteristics of Martian, Lunar, and low-gravity parabolas. A method to evaluate accelerations by direct measurement of particle motion in transparent systems is also described. Information on induced curvilinear motion is deduced tht is not easily detectable by linear accelerometers. These data provide a good initial basis for planning aircraft experiments.

The KC-135, as in the past, was extensively utilized to support orbital flight experiments. These results are reported in section 2. United States Microgravity Laboratory (USML 1) Protein Crystal Growth experimental procedures were tested and modified, and the new procedures were verified. The low-gravity performance of robotic systems was evaluated for Space Station Freedom. The Casting and Solidification Technology (CAST) experimental system designed for the International Materials Laboratory (IML-1) Spacelab mission was shown to detect gravity-dependent growth variations during KC-135 parabolas. Mixing protocols for USML-1 zeolite growth experiments were tested and optimized. KC-135 tests of the ultrasonic bubble positioning experiments for the USML-1 Glovebox resulted in injection tip redesign to increase the

success probability for the space shuttle experiments. Phase partitioning systems to be flown in the space shuttle middeck were screened for optimum composition, and KC-135 low-gravity coarsening kinetics data obtained were later found to complement those taken in one gravity and in orbit. Subsequent success of the above experiments on the space shuttle is a testament to the high rate of return on NASA's instrument in the parabolic aircraft materials science program.

Transport and interfacial phenomena studies on the KC-135 are the topic of section 3. Aircraft experiments on container shape and wall coating effects on immiscible liquid demixing documented deviation from the predictions of the Concus theory. Rotating cylinder experiments validated theory for two-phase rotation fluid shape in low gravity. Bioconvection studies during low-gravity parabolas resulted in the determination of the conditions for gravity-dependent and gravity-independent cell flow patterns. In another study low gravity was used to prepare undrained soap cell boarders, an otherwise inaccessible state, to study flotation and Rayleigh-Taylor heavy over light fluid instabilities. Using a torque meter viscometer, the validity of the no slip boundary condition was tested for the low-gravity environment. Electrodeposition for nickel during multiple low-gravity parabolas did not produced an amorphous product. This is contrary to what was reported for continuous deposition in sounding rocket low gravity. Reduced sedimentation of tracer particles in low gravity enabled the quantification of the Kirkendall effect for gas diffusion. These fluid science result, in all, are extraordinarily diverse and scientifically fruitful.

Thermodynamic and combustion results are given in section 4. A holographic study of heat transfer for a fluid near its thermodynamic critical point was undertaken to calculate the heat and mass transfer and compare it with theory for near critical point systems. In this section pulse heating experiments, which can be used to determine important thermophysical materials properties, are described that have extended the melting point limit above 1500 °C, for the first time, by utilizing the advantages of low gravity. The phenomenon in which the lack of convection causes flames to take spherical shape has been documented in Drop Tower experiments. The longer low-gravity period for the KC-135, however, was utilized to study the longer-term stability of this flame morphology. The results of aircraft thermodynamic and combustion studies continue to be of fundamental importance for space system safety, combustion engineering and basic science.

Section 5 describes experiments in which the KC-135 was utilized to develop the technology for containerless processing in space. The capability of the High Temperature Acoustic Levitator (HAL) was extended to three-axis positioning of samples heated to 1500 °C. Other studies utilized acoustic levitation to study the solidification of organic samples heated to 200 °C. Experiments on the KC-135 allowed the isolation of the levitating field intensity from the gravity variables for comparison with ground experiments. The KC-135 hardware and science development effort for containerless processing has been instrumental to its success in the MPS program.

Laser and plasma arc welding experiments are described in section 6 (solidification with a free surface). Two studies report utilized the orbital arc welding apparatus. The first investigated coalescence due to arc-induced convection, Marangoni convection, and particle pushing in immiscible metal alloys. The second investigated white iron solidification and regraphitizing for FeC alloys. Another study utilized a laser welding apparatus to track microstructure variations during resolidification of stainless steel and transparent metal models solidified in the low- and high-gravity portions of the parabola. The behavior of weld pools in low gravity is not yet well understood; thus their contained study is of both practical and scientific importance.

The interaction of a liquid melt with its crucible (covered in section 7) has proved, since the first Skylab crystal growth experiments, to be of scientific interest as well as an important experimental parameter for solidification in space. Cu-Pb-Al immiscible alloys of varying composition were gas quenched during low gravity in alumina crucibles. Aluminum composition, which influences the interfacial energy between melt and crucible, was found to be a determinant factor in the alloys ability to form fine dispersions when solidified in low gravity.

Cd-Te solidification experiments were performed, using the same apparatus and sample size, to determine if melt crucible dewetting would occur in orbit. Cd-Te, however, could not be made to solidify in a single low-gravity period. Ga-doped germanium crystals directionally solidified in quartz crucibles

during continuous low-gravity parabolas yielded surface striations that are characteristic of free surface solidification. However, indium antimonide directionally solidified during low-gravity parabolas did not reveal dewetting under direct video observation of the solid liquid interface. These data suggest that the KC-135 can provide critical information on the melt crucible interactions, but limited low-gravity time make it practical only for some of the systems of interest for solidification in space.

KC-135 provides the unique capability when combined with unidirectional solidification of having in one sample a series of identifiable sections grown in low gravity or in high gravity. Section 8 describes results for metallic-based systems which are normally solidified at rates fast enough to make them particularly well suited for KC-135 study. Cu-Pb-Al immiscible alloy samples directionally solidified during low-gravity parabolas show strong gravity dependence in both phase fraction and phase alignment of microstructures. Metal matrix ceramic particulate composites solidified in low gravity (relative to high gravity) were shown to have more uniform dispersions and lower particulate engulfment rate. Immiscible alloy solidification experiments with the binary alloys Cu-Pb and Ga-Bi have determined that alignment and microstructure of phases, grain size, fiber growth initiation, and interfiber spacings are modified in low gravity. Studies with Fe-C alloys documented a strong gravity dependence for the nucleation of graphite grains. The electronic properties were measured for Al-In-Sn immiscible alloy sections solidified in low and high gravity. The sample solidified under one gravity or high gravity is normally resistively metallic, but when solidified in low gravity it became semimetallic. The superconducting transition temperature of the low-gravity sample was increased by 15%. These experiments illustrate the fact, long known in the industry, that convection effects strongly influence the properties of a casting.

1. KC-135 LOW-GRAVITY ENVIRONMENT CHARACTERIZATION

PRECEDING PAGE BLANK NOT FILMED

KC-135 ACCELERATION LEVELS DURING LOW- AND HIGH-GRAVITY TRAJECTORIES

Investigators: Guy A. Smith and Gary L. Workman, The University of Alabama in Huntsville, Johnson Research Center, Huntsville, AL

CHARACTERISTICS OF LOW-GRAVITY PARABOLAS ON THE KC-135

OBJECTIVES

The "weightless" environment experienced by occupants of the KC-135 when the aircraft flies parabolic maneuvers provides a unique testbed for a variety of experiments. The range of experiments that utilizes the reduced gravity includes physiological, scientific, and engineering experiments. The most publicized work has been the many significant results that have been obtained by physiological studies on the effects of reduced gravity on humans and animals. The KC-135 testbed can also be used for determining human factors requirements in preparing for space flight activities, particularly in practicing for the human's ability to perform particular tasks in microgravity. In preparation for space flight activities, the KC-135 has provided extraordinary service and cost-savings for pre-space flight validation of procedures and personnel.

In addition to the simulated low-gravity experiments on the human element, a number of useful experiments can be performed to check out equipment and physical concepts prior to initiating the huge expense associated with a manifested space flight. Within this concept are a number of materials processing experiments that allows a preliminary look at the effect of reduced gravity on fluid phenomena and solidification experiments. The materials processing community can and has taken advantage of the KC-135 as such a testbed quite frequently over the years.

Much can be learned about the role of reduced gravity on both the physical phenomena being studied in a materials processing experiment. The impact of electrical power and physical constraints of the aircraft itself, and the physiological effects on the personnel performing experiments in the varying gravity levels of the aircraft all effect how well an experiment works on the KC-135. The ultimate goal is usually to provide a near free-fall environment which allows one to predict how well the same experiment would operate in microgravity and in some fashion extrapolate from the 0.01 g experienced in the KC-135 to 0.00001 g experienced in space. Hence, the quality of the aircraft low-gravity period certainly affects the experimental results obtained and how it should be interpreted.

Quality of Low Gravity Experienced on the KC-135

There are a number of conditions which affect the quality of the low gravity experienced by both the experiments and the personnel performing the experiments. The most significant factor affecting the quality of low-g maneuvers is clear air turbulence, which significantly affects about 20% of all flights. It is especially prevalent during the winter months when the weather along the Louisiana coast is quite variable. During good weather conditions clear air turbulence is significant in only a few low-g maneuvers per flight, and usually without forewarning.

The KC-135 flies a parabolic trajectory to achieve low gravity. The trajectory is initiated by orienting the nose of the aircraft up at 45° during the entry into the low-g phase of the parabola and exited at 45° with the nose down. The rotation of the aircraft during this maneuver provides a small variation in the actual g level experienced by the individual experiments since the variation in g depends on the physical

PRECEDING PAGE BLANK NOT FILMED

location of the experiment in the aircraft. Figure 1 was reproduced from a chart obtained from the KC-135 Operations Office at JSC.

Instrumentation

In most experiments it is desirable to obtain acceleration data in all three axes. The data shown here were obtained from accelerometers housed in commercially available triaxial mounts. As can be seen in the charts presented here, there are significant acceleration effects in all three axes; hence, the triaxial-axial mount has been the preferred mounting for accelerometer data. Two different models were used in the data sets presented here. A set of Systron-Donner Model 4310A was used for the free-floating data sets and a Sundstrant Model 303T14 were used for the floor-mounted data sets. Their accuracies are checked annually using the Earth's gravity as a standard, corrected for the latitude of Huntsville, AL. The resolution for each set of accelerometers was less than 0.0001 g. Nominal accuracy for both sets in the instrumentation used for the measurements is ±0.5 mg.

EXAMPLES OF ACCELERATION DATA OBTAINED DURING KC-135 FLIGHTS

The University of Alabama in Huntsville has operated a variety of experiments on the KC-135 since 1983. During this time the flight personnel have experienced a full range of reduced gravity environments. A large amount of accelerometer data has been collected in performing reduced gravity experiments on the aircraft in this time frame. As mentioned above, weather is the most prominent source of a poor quality low g experienced by the experimenter. In cases where turbulence is excessive or the pilot cannot find "clear air" in which to fly parabolas, the mission is justifiably aborted.

There is a "typical parabola" for normal flight conditions and an accompanying g level profile for any experiment package which is bolted to the floor of the aircraft. Note that

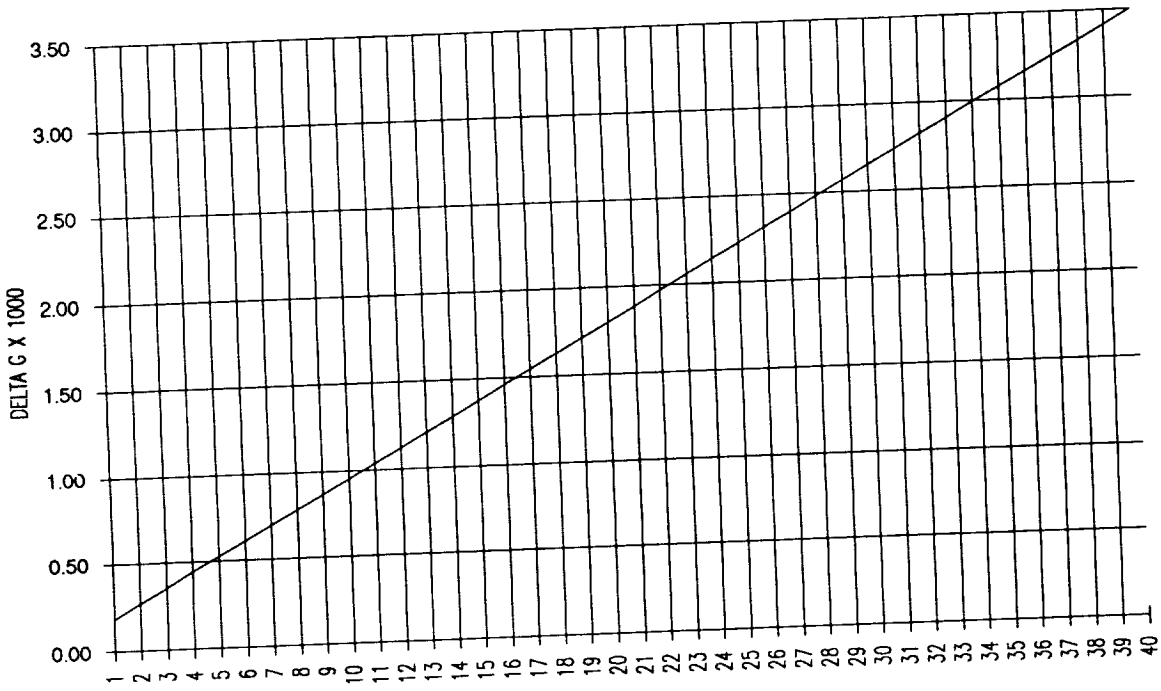

Figure 1. Variation of g level with respect to placement in the KC-135 aircraft.

there is also the possibility of free-floating an experiment in order to improve the minimum or quality of the g level for a particular type of experiment. Free-floating experiments require the operators to hold onto the experiment until the low-gravity portion of the parabola is attained, and then gently release the package. The package then floats for about 5 to 15 sec depending upon the quality of the parabola and the size of the package. The smaller the package the more room there is for it to free float prior to contacting the cabin walls. The accelerometer package used to collect the free float acceleration data was less than 1 ft^3. Even a package this small would quite often contact the walls after only a few seconds of actual free float time.

The best indicator of the effect of the parabolic trajectory is given in Figure 2. This chart shows accelerometer data from a series of parabolas. Note that the g level varies normally between 0.01 to around 1.8 g. Consequently the experimental hardware has to function uniformly throughout this range. Other constraints on the equipment and the supporting structures which are required for safety concerns are outlined in the JSC KC-135 User's Guide which is available from the KC-135 Operations Office.

It should be noted that all of the data presented in graph form have been digital filtered by a simple running average. This was done to eliminate the millivolt level signal noise and the high frequency components from the data for clarity. When needed every single data point for each channel can be recalled and analyzed.

It is interesting to note that although the KC-135 flies a parabolic trajectory, the resulting g profile more closely resembles a square wave.

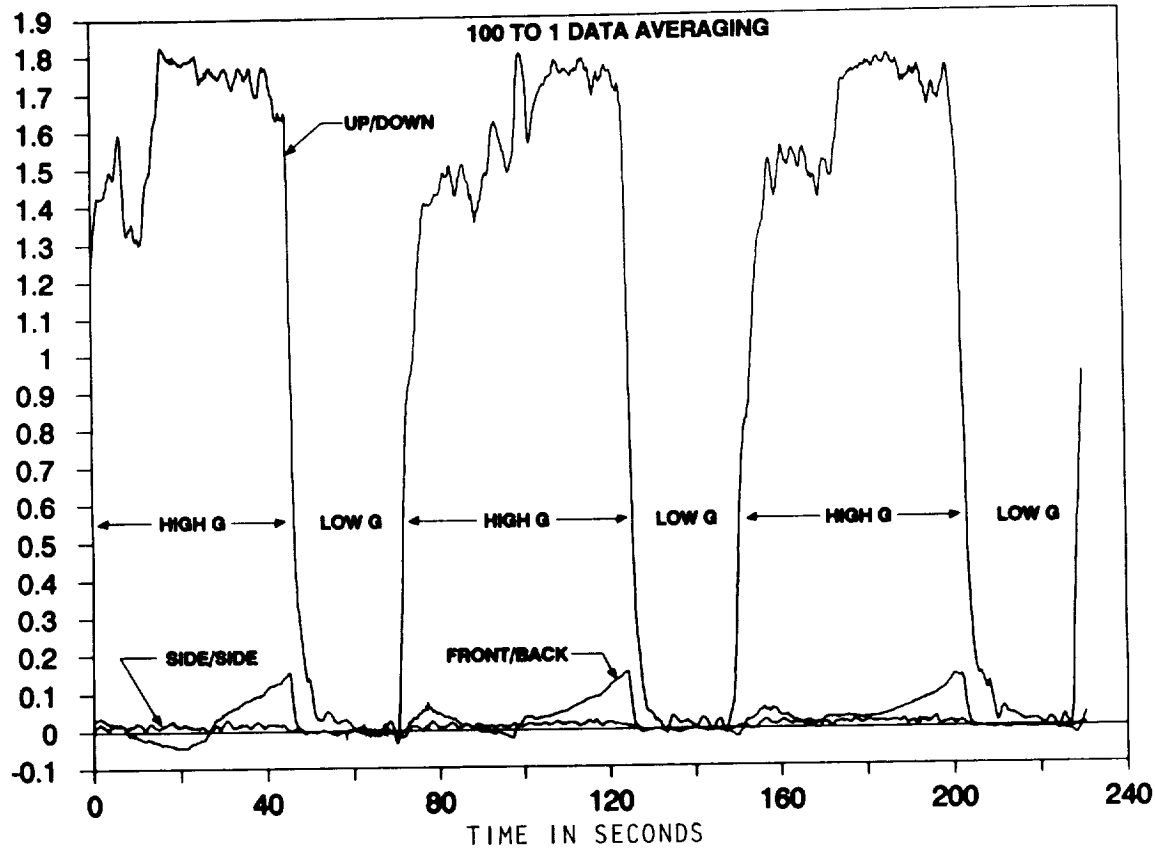

Figure 2. Typical accelerometer data obtained during a series of parabolic flights on the KC-135.

Thus if one were to model the effects of the varying g levels on a KC-135 experiment, it would be more realistic to model the g level source function like a square wave and not like the sinusoidal one that would be expected from the flight profile.

There are large g changes occurring in the high-g portion of the flight. Both the experiments and the passengers experience these changes. However, some experiments can be performed which take advantage of the higher gravity, particularly for solidification studies. The non-uniformity of the high-g profile may not allow for good scientific results, since the g level is more difficult to control.

A closer look at the low-gravity portion of the parabola typically resembles Figure 3. There are some minor excursions from 0.01 g due primarily to weather effects or instability in the aircraft's flight path. Note that there is relatively greater variation in the up/down and front/back motions than in the side/side directions. This information is useful for orienting experiments which may have specific orientation requirements.

As mentioned earlier, an improvement in the low-gravity profile can be obtained by free-floating small packages. Figure 4 gives accelerometer data for an experiment package during release and free-float. Note that in this experiment there is a data cable attached to the package which may cause some of the residual acceleration effects seen in the free-floating mode. However the g profile is obviously much

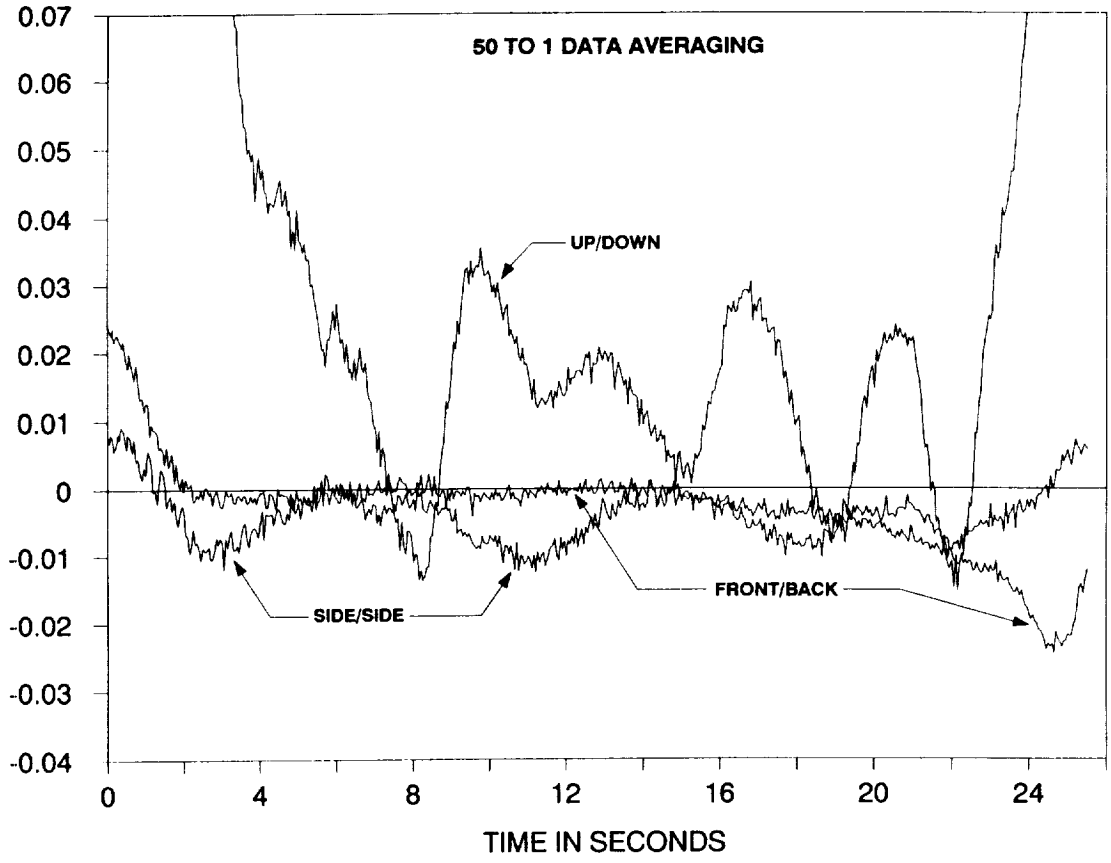

Figure 3. Accelerometer data showing a typical variation in g during the reduced gravity portion of the parabola.

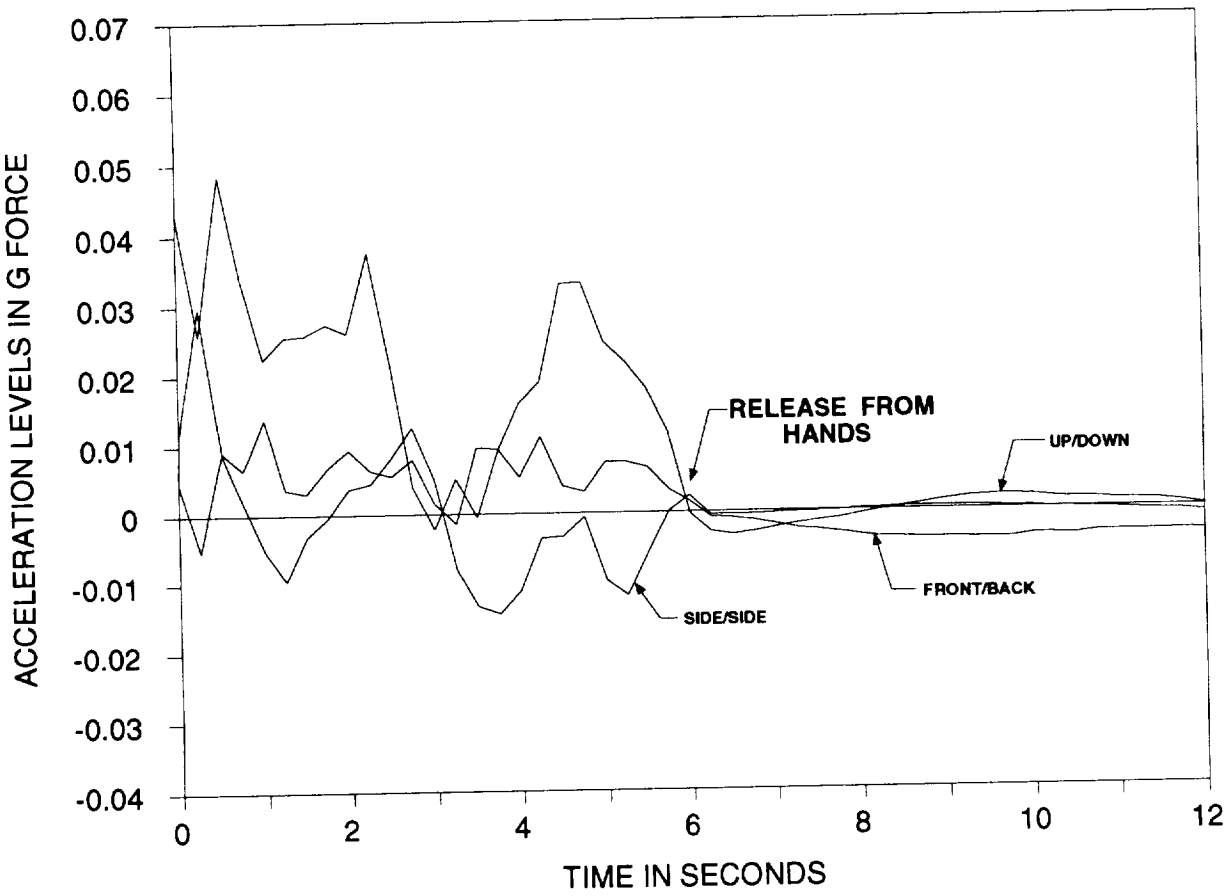

Figure 4. Example of accelerometer data from an experiment free-floating within the aircraft cabin.

smoother in the free-floating mode and would probably be even smoother without a data cable dangling from the package. In addition the package is isolated from the higher frequency vibrations originating from the engines, pumps, and high velocity airflow around the aircraft's exterior surfaces. Note that at the point marked "RELEASE..." on the graph the package free-floated from the operator's hands. Data were averaged to reduce the electrical noise level.

Comparisons of good parabolas experienced during good flying conditions with the "bad" conditions experienced in turbulent weather provide useful criteria with which to judge what kind of useful information is being obtained in an experiment during flight.

Obviously excessive motion of the aircraft due to turbulent weather will impact the data obtained from an experiment which depends upon fluid flow. Figure 5 shows such a comparison.

It is obvious from the typical worse case example that large g levels greater than 0.1 g over several seconds are going to significantly affect any materials processing experiment. Under these conditions, even the operators in the aircraft experience significant turbulent motion and bounce around in the aircraft.

As another final example, on June 4, 1991, a series of lunar and martian g parabolas were performed. These particular g levels were obtained by "stretching" out the trajectory of the

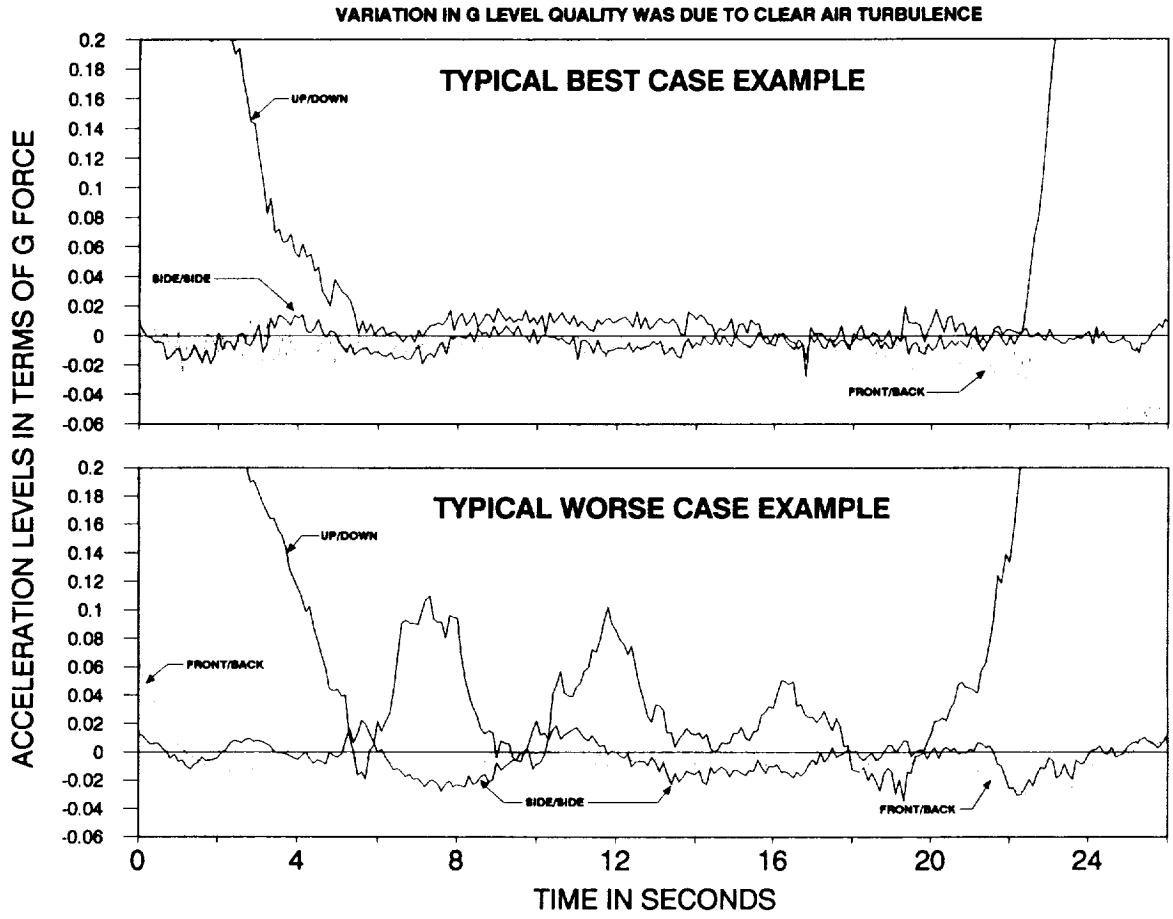

Figure 5. Comparison of the quality of the g level during a KC-135 parabolic period in good and poor weather conditions.

parabola the required amount. Accordingly the length of time increased from the typical 20-25 sec for a low-gravity period to 26-28 sec for lunar g periods and to 29-33 sec for martian g. In referring to Figure 6 there seems to be a repetitive drift in the vertical g acceleration throughout the lunar and martian g period which is absent from the low-gravity period. This is apparently due to a control problem with the aircraft at the time the data were taken.

DISCUSSION

The information provided in this report presents a good estimate as to the quality a user of the KC-135 can expect during a flight. It should be clearly noted that these graphs provide only a broad view of what one can expect - there is no way to accurately predict the quality of low g from one parabola to the next. With this in mind the inclusion of accelerometers into the experiment package is almost mandatory. A sudden g spike caused by either the aircraft or a person striking the package and its effect upon the results would otherwise be impossible to correlate.

The types of accelerometers available to the experimenter cover a wide range of applications. In determining what type of accelerometer to use, the following questions need to be addressed.

1. Is a single axis sufficient or are all three required?

2. What are the resolution requirements? Is 1 mg sufficient or should it be even better?

3. What is the frequency response needed? Piezoelectric accelerometers for instance are good for the higher frequencies but not the low.

4. What are the accuracy specifications? Factors such as temperature change will induce drift in all accelerometer output signals. In addition all accelerometers have a certain amount of nonlinearity inherent in their design.

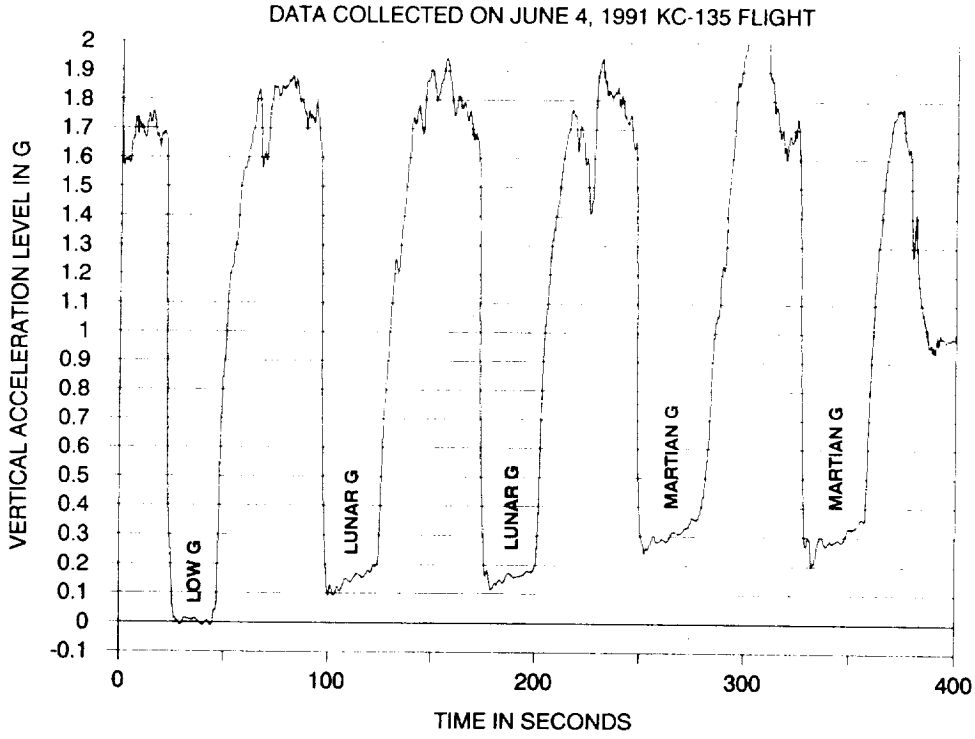

Figure 6. Comparison of low, lunar, and martian g levels.

MICROGRAVITY FLOW VISUALIZATION

Sponsor: Commercial Programs through MSFC

Investigators: Gary L. Workman and William F. Kaukler, The University of Alabama in Huntsville, Huntsville, AL

OBJECTIVES

Quantification of fluid movement which would affect microgravity materials processing experiments. Fluid motion observations are used to verify the effects of any accelerations on fluid behavior within the sample ampoule. Quantification and observation of the relaxation of the fluid motion upon going into the low-g portion of the parabola was also an objective of this study.

Flow visualization data recorded during parabolic flight can be used to evaluate fluid motions during flight or, in some cases, to provide supporting information on fluid motions occurring at specific times, such as might occur during particular parabolas or in turbulent weather conditions. The resulting KC-135 data are also useful for obtaining experimental parameters in order to develop a model that could predict fluid convective behavior in the transient g levels of the KC-135, as well as provide insight to experimental improvements expected when performed on a space-based platform. This simulation ability will also enable a better interpretation of the effects of the low-gravity environment of the KC-135 during parabolic maneuvers on various materials processing experiments.

EXPERIMENTAL PROCEDURE AND RESULTS

A video flow visualization apparatus, similar to a Stockbarger-Bridgman furnace, has been constructed using a heater/cooler combination to apply a thermal gradient through a transparent ampoule and flown in the KC-135 aircraft with vertical alignment of the temperature gradient. Simultaneous video recording from two orthogonal views of tracer particles during the parabolic maneuvers allows observation of convective and buoyant flows during changes in the gravity vector.

The apparatus constructed for this experiment is shown in Figure 1. Two simultaneous orthogonal views of tracer particles in the fluid of interest are recorded using two CCD cameras and combined into a single side-by-side image on the video tape, together with pertinent experimental data such as g level, temperature gradient, and time. Figures 2-4 show reproduced images recorded from typical KC-135 flight data. Results obtained from these flight data were expected, except for some subtle indication of rotational motion which was not attributable to gravity-driven convection. Actual flow velocities are expected to be in the range of 10^{-5} to 10^{-9} m/sec with the experimental arrangement used in this work, with the hot zone on top. These rates are difficult to measure in a reasonable length of time; hence, the computational model described below is probably easier to use to establish the flow field quantitatively.

The rotational acceleration concepts are difficult to sort out in rectangular sample containers and have not previously been of much concern to the materials processing community. However, the study of the effects of rotational acceleration may deserve some attention in future research activities.

Experimental parameters can be adjusted by varying the ampoule geometry, and materials properties, such as thermal conductivity, density, and viscosity, and thermal conditions can be selected to offer a range of values for fluid dynamic parameters (Prandtl, Schmidt, and Raleigh numbers). For example low Prandtl numbers are desired to model semiconductor

PRECEDING PAGE BLANK NOT FILMED

14 INTENTIONALLY BLANK

and metal melts as well as predict their behavior. Note also that the sample ampoule in the Microgravity Flow Visualization Apparatus can be translated during flight to allow sampling of various depths with the ampoule.

A parallel effort to develop numerical modeling capability using Easyflow software has also been done. Several models were developed for simulating water samples and germanium to determine if the software gave the same results as published work. Both steady state and transient models, as well as 2-D and 3-D, were run. Graphical outputs show both temperature and convective flows resulting from varying g level only during an experiment. Figure 3 shows how the Easyflow software displays this information. In general, the results using water sample provided much insight into the fluid motions occurring during simulated parabolic flight and compared quite well with the experimental observations. Figure 5 shows a typical sequence of how the convective flows and temperature gradients change during transition from 1.8 to 0.01 g in the numerical simulation. We were not able to study rotational acceleration in the current version of the software.

The Microgravity Flow Visualization Apparatus can provide data from fluid motions during KC-135 or space flight in order to correlate the effect of such motions on a crystal growth or some other materials processing experiment. Easyflow models also are able to provide computational capability for predicting fluid motions during g level changes. The subsequent effect of these fluid motions on an actual crystal growth process has yet to be investigated.

REFERENCES

Griffen, P. R., and S. Motakef, "Influence of Non Steady Gravity on Natural Convection During Microgravity Solidification of Semiconductors - Part 1. Time Scale Analysis," Appl. Microgravity Tech., II, 121-127 (1989).

Griffen, P. R., and S. Motakef, "Influence of Non Steady Gravity on Natural Convection During Microgravity Solidification of Semiconductors - Part 2. Implications for Crystal Growth Experiments," Appl. Microgravity Tech., II, 128-132 (1989).

Workman, G. L., Contract Final Report, NAS8-36955, D. O. 72.

Workman, G. L., and W. F. Kaukler, "Convective Flow Analysis on the KC-135 Aircraft," AIAA-92-0844.

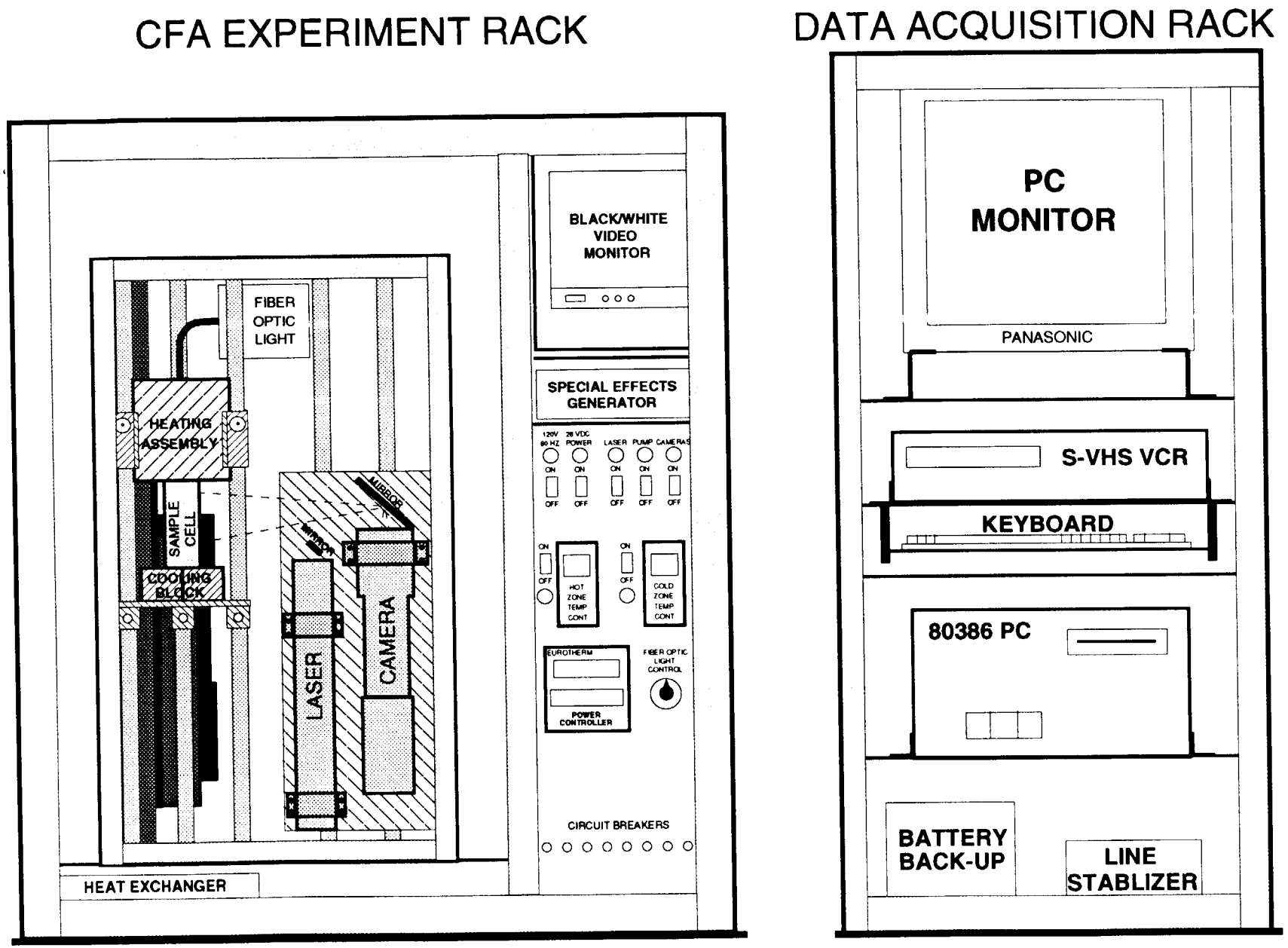

Figure 1. Experimental apparatus used to study convective flow on the KC-135.

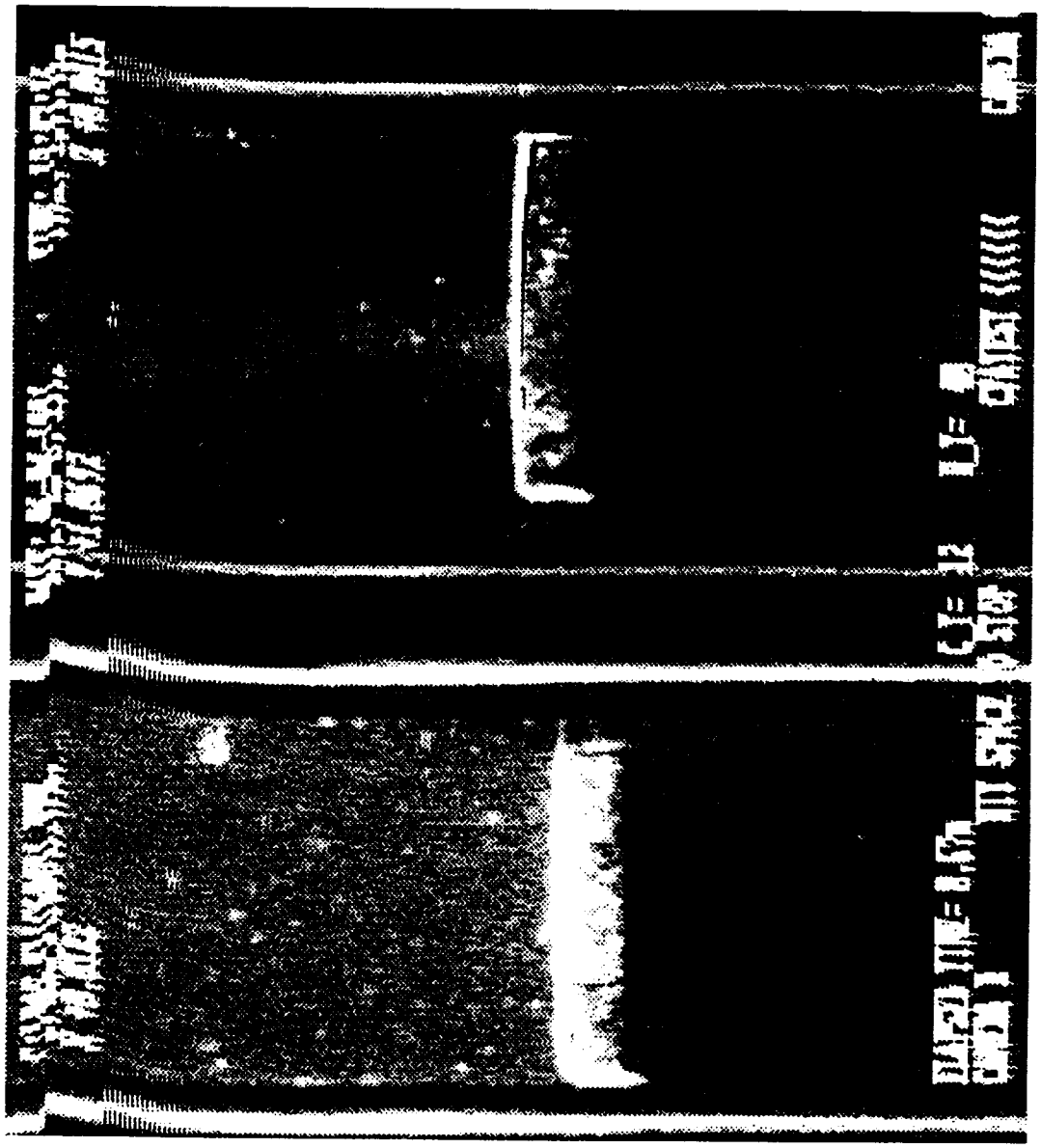

Figure 2. Dual specimen cell views and overlayed data from video. Data taken June 1991.

ORIGINAL PAGE IS
OF POOR QUALITY

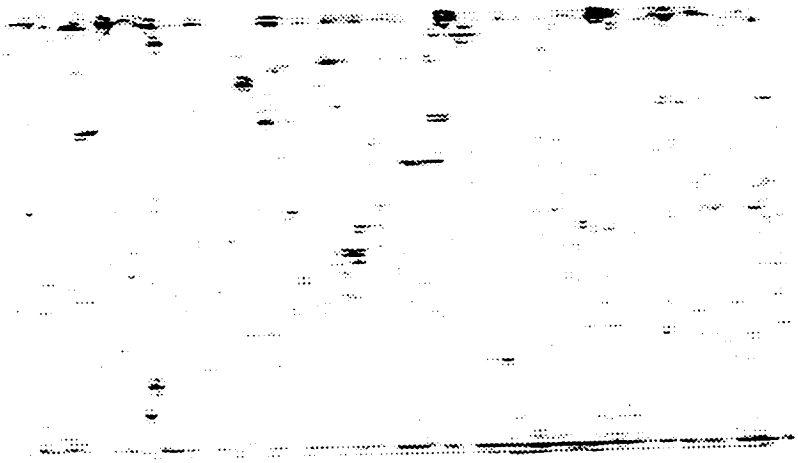

Figure 4. Same as Figure 3 with first derivative+gradient+stretch.

Figure 3. Ten frames averaged, high gravity.

ORIGINAL PAGE IS
OF POOR QUALITY

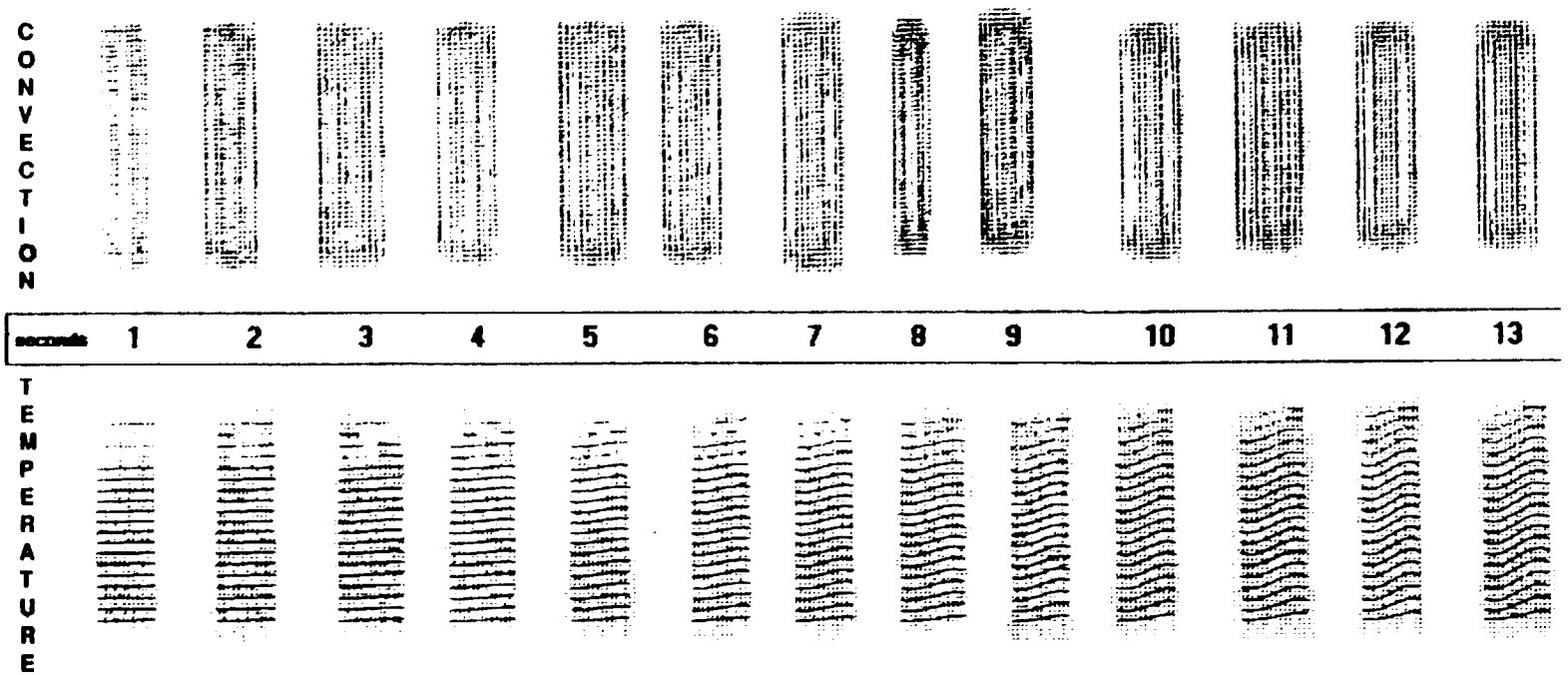

Figure 5. Sequence showing velocity flows (streamlines) and thermal gradient in 1-sec increments after going from 1 g to 0.01 g. The temperature gradient across the cell is 25 °C and velocities are on the order of 1 x 10^{-5} m/s. Easyflow software running on a PC provided the computations.

2. SPACE FLIGHT HARDWARE/EXPERIMENT DEVELOPMENT

PROTEIN CRYSTAL GROWTH KC-135 FLIGHTS

Investigator: Lawrence J. DeLucas, Associate Director, UAB Center for Macromolecular Crystallography, University of Alabama at Birmingham, Birmingham, AL

OBJECTIVES

During the last year, several new hardware concepts for protein crystal growth were designed and fabricated at the University of Alabama at Birmingham (UAB). Each hardware prototype was tested on three different KC-135 flights. The following describes the hardware that was tested and the results from these tests.

EXPERIMENTAL PROCEDURE AND RESULTS

Hardware Developed for United States Microgravity Laboratory 1

For this mission, special vapor diffusion experiment chambers were developed for use with the glovebox facility that will be located in the spacelab module. The experiment chambers were constructed using polysulfone, a material that is non-wetting and generally inert to most proteins. Using a prototype glovebox developed at UAB that can be used as a level of containment for liquids that are extruded into these experiment chambers, each experiment chamber design was tested on the KC-135. The solutions typically used to grow protein crystals along with the protein lysozyme were extruded from Hamilton syringes into depressions in each experiment chamber. The overall method of extruding the protein solution into the experiment chamber was tested and subsequently the stability of the microliter size droplets was observed. In addition, special vials that contained a rubber septum were used to house the concentrated buffers and protein solutions used for these crystallization experiments. The feasibility of withdrawing milliliter quantities of these solutions into the Hamilton syringes was tested. It was noticed from the first KC-135 flight that once the vials were 50% depleted, the remaining solution wicked along the container walls thereby preventing further liquid from being withdrawn into the syringe. Several different wicking designs were then fabricated at UAB and tested on a subsequent KC-135 flight. The second flight yielded valuable information in that one particular wicking arrangement consistently held the solution near the septum end of the bottle and allowed 95% of the contents of the bottle to be successfully withdrawn into the syringe. From these experiments we have now fabricated and approved for flight the experiment chambers and buffer and protein bottles/vials.

Hardware Developed for COMET

A batch crystallization system will be utilized for crystallization experiments to be performed on COMET currently scheduled for Septeember 9, 1992. The hardware design requires that two concentrated and viscous solutions be mixed once in orbit. It is important that the mixing occur quickly and be 100% effective. Prototype hardware was designed and fabricated at UAB and subsequently tested on the KC-135. Two methods were used to determine the effectiveness of this design in providing adequate mixing: (1) photographic documentation using colored solutions, and (2) refractive index measurements taken on the mixed solutions. The KC-135 flight verified that the prototype design provided 100% mixing with 5 seconds for the most viscous solutions that are typically used in protein crystallization experiments. Based on these data, the flight hardware is currently under construction at UAB and once completed, will again be tested on the KC-135 aircraft in 1992.

22

PRECEDING PAGE BLANK NOT FILMED

RESULTS

The KC-135 aircraft has been instrumental in allowing prototype hardware concepts to be tested, modified, and retested in a short period of time. This information has been highly beneficial in allowing us to quickly arrive at hardware which can be effectively used in the microgravity environment provided by the space shuttle. Protein crystal growth experiments are scheduled to fly on several more upcoming shuttle flights (an average of three to four shuttle flights per year over the next 5 years). During this time, additional new hardware concepts will be fabricated at UAB that will require testing on the KC-135 aircraft. Therefore, we anticipate continuing to fly an average of three times per year to accomplish this testing to support our flight program.

CHARACTERIZING MICROGRAVITY PERFORMANCE OF A LABORATORY ROBOT

Investigators: Elaine Hinman and Cynthia Coker, EB24/NASA, Marshall Space Flight Center, Huntsville, AL; Gary Workman, Carlos Rondon, Houcheng Li, and David Gilliam, The University of Alabama in Huntsville, Huntsville, AL

OBJECTIVES

Several studies have indicated the need for the use of increased automation to increase productivity in space. In many cases, these studies have concentrated on external or extravehicular uses of automation; however, telescience as a tool for increased productivity has also been cited. During the early phases of Space Station Freedom, it may be possible to exploit the projected man-tended configuration for microgravity science use.

The objective of this project has been to develop an understanding of the requirements imposed on laboratory, or high precision, robot systems by the microgravity environment. Emphasis has been placed on finding ways of reducing transient loads imparted to an object manipulated by a robot. The gathering of actual low-gravity robot acceleration data, and its use in developing an accurate dynamic simulation for use in controls work, has been a primary focus of this effort.

EXPERIMENTAL PROCEDURE

This experiment was broken into two major components: flight testing and computer simulation. Each is described below.

A robotic workcell, consisting of a Zymark Zymate II robot system, with supervisory control provided by a Commodore Ammiga 2500 computer and PC/AT bridgeboard, was developed for flight testing on the KC-135 aircraft. An accelerometer was positioned on the wrist of the robot, while base aircraft accelerations were provided by neighboring experiments. The test apparatus is shown in Figure 1.

The robot moved through various trajectories during the low-gravity portion of the aircraft's parabola. Most of the robot trajectories tested were single-axis motions. This was done in order to look at accelerations produced at the ends of those particular trajectories, and to try to examine the motion's characteristics rather than making the tests too robot-specific.

Concurrently, the computer simulation was developed. The TREETOPS software package was used to develop the dynamic model of the Zymate flight unit. This program was designed for use in dynamic analysis and control system development.

TREETOPS is designed to model and simulate multibody structures which have a tree topology. TREETOPS may be used to produce a time history of interactions which take place during the motion of the system modeled. Systems are modeled by breaking them down into "bodies" connected by "hinges." Actuators and sensors are also defined. Characteristics of each body, hinge, sensor or actuator are individually entered into the program. For example, a body's mass or the degrees of freedom of a hinge would be entered. TREETOPS allows the incorporation of outside information on a system, such as a user-written control system or NASTRAN results.

RESULTS

Several things were learned during the course of the experiment. Operationally, developing useful trajectories to fit within the short microgravity portion of a parabola can be done. In this project, short, easily-repeatable trajectories were used. These trajectories were run several times to allow for statistical analysis. Longer trajectories could be broken into component parts and "hooked together" if care was taken to account for intermediate stopping motions. FFT analyses of the flight data are currently being performed.

The initial Zymate TREETOPS model has been developed and early test cases run. Actual flight results are to be incorporated as the data are analyzed to increase simulation fidelity. Figure 2 shows the Zymate robot as defined for TREETOPS modeling. A sensor is located at point P to measure motions and accelerations of the end effector.

Results from two simulation test cases are shown in Figures 3 and 4. In this case a typical test trajectory was run, and the mass at the end effector was varied. With incorporation of the actual robot flight data, these simulations are to be used to predict performance under various conditions. These predictions can then be tested in flight. Control schemes can be tried to reduce the accelerations produced while the robot is performing different tasks.

Figure 1. KC-135 robot flight unit.

ORIGINAL PAGE
BLACK AND WHITE PHOTOGRAPH

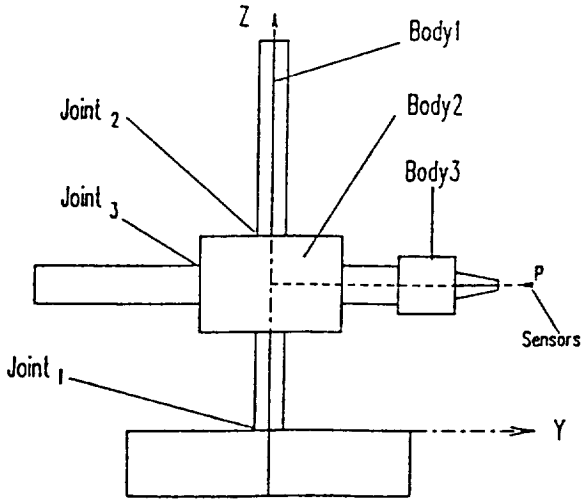

Figure 2. Zymate robot as defined for TREETOPS modeling.

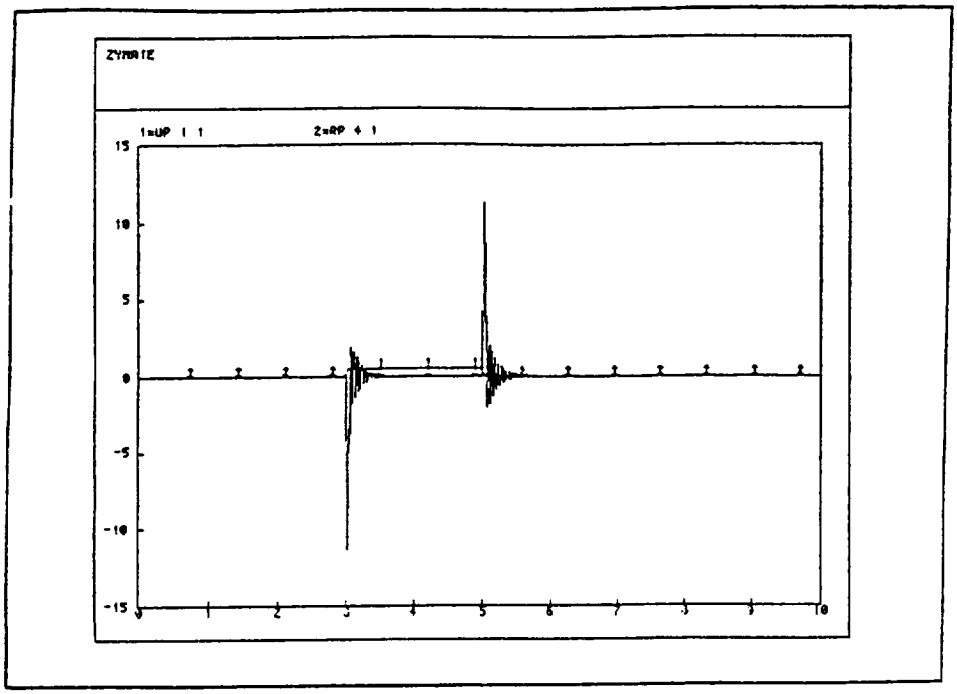

K_1=100
n=10 rad/m
k_g=100000 n/m
J_m=1 kg-m^2
m_e= 1 kg

Figure 3. Trajectory with end effector mass of 1 kg.

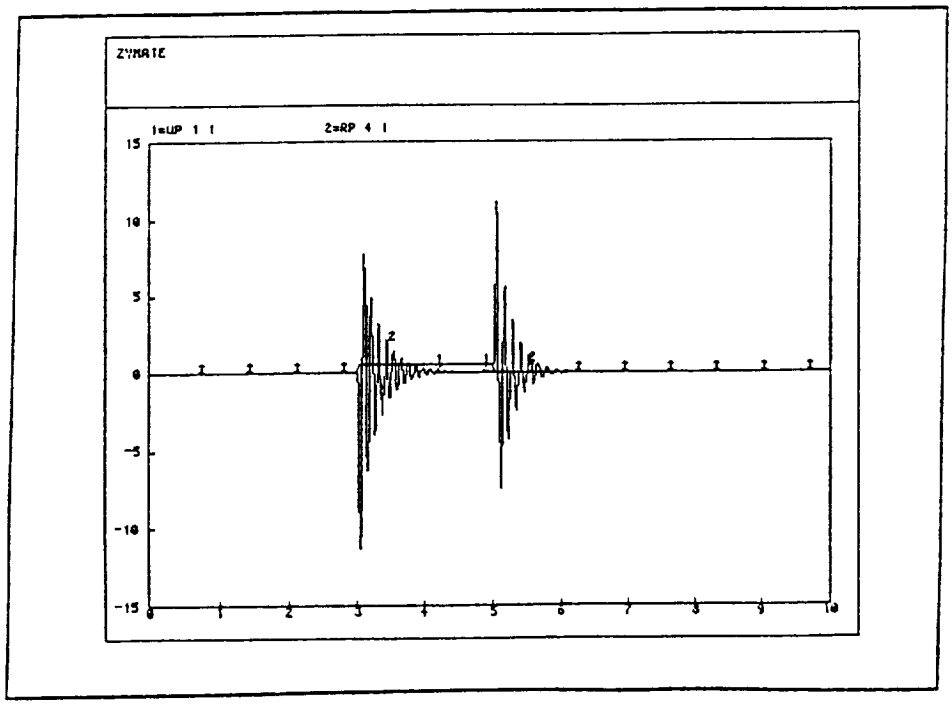

K_1=100
n=10 rad/m
k_g=100000 n/m
J_m=1 kg-m^2
m_e =50 kg

Figure 4. Trajectory with end effector mass of 50 kg.

REFERENCES

Augustine, N., et al., "Report of the Advisory Committee on the Future of the U.S. Space Program" (1990).

Fisher, W. and C. Price, "Space Station Freedom External Maintenance Task Team - Final Report" (1990).

Herrmann, F., "Advanced Protein Crystal Growth Flight Hardware for the Space Station," Proceedings of the AIAA 26th Aerospace Sciences Meeting, AIAA-88-0345 (1988).

User's Manual for TREETOPS - A Control System Simulation for Structures with a Tree Topology (Rev. 8,9), Dynacs Engineering Co., Inc. (1991).

Kotnik, P., S. Yurkovich, and U. Ozguner, "Acceleration Feedback for Control of a Flexible Manipulator Arm," Journal of Robotic Systems 5(3), 181-196 (1988).

Hinman, E. M., D. Gilliam, and G. L. Workman, "Physical and Digital Simulations for Space Robotics," The Southeastern Simulation Council - SESC 1990, Society for Computer Simulation, International, October 1990.

Li, Houcheng, G. L. Workman, and E. M. Hinman, "Characterization and Improvement of Robot Dynamics Through Simulation," The Southeastern Simulation Council - SESC 1990, Society for Computer Simulation, International, October 1990.

Hinman, E. M., "Robot-Tended Crystal Growth in a Space-Based Laboratory," International Symposium on Laboratory Automation and Robotics Proceedings (1990).

Workman, G. L., T. Grisham, E. Hinman, and C. Coker, "Robot Dynamics in Reduced Gravity Environment," Fifth Conference on Artificial Intelligence for Space Applications, NASA CP-3073 (1990).

Hinman, E. M. and G. L. Workman, "Characterizing Microgravity Performance of a Laboratory Robot," to appear in Proceedings of the 1991 International Robots & Vision Automation Conference, Detroit, MI, October 1991.

Hinman, E. M. and G. L. Workman, "Simulations for IVA Robotics," Advances in Intelligent Robotic Systems -- Sensor Fusion IV: Control Paradigns and Data Structures, to appear in Proceedings SPIE, Boston, MA, November 1991.

KC-135 EXPERIMENTAL PROGRAM CASTING AND SOLIDIFICATION TECHNOLOGY

Investigator: M. H. McCay, University of Tennessee Space Institute, Tullahoma, TN

OBJECTIVES

The use of metal models to study the solidification process is very common and is the approach used in this research. The models chosen are transparent and provide a medium easily probed by optical diagnostic techniques. The dependence of the index of refraction of the material on its density permits concentration and temperature gradients to be measured in real time through phase sensitive optical techniques. The author has used a variety of such techniques to study solidification in ammonium chloride and water and the results have been reported in several publications.[1-4] This research used a solution of 28 wt% NH_4Cl-H_2O along with the central dark ground method[5] to study the effect of varying gravity level on diffusion-limited unidirectional dendritic solidification.

EXPERIMENTAL PROCEDURE

Metal Model

The metal model chosen for this study, ammonium chloride and water, solidifies dendritically and is optically transparent with an index of refraction that is a function of both temperature and concentration. The variation of refractive index has been characterized by the equation[3]

$$n = 1.337 - 1.73 \times 10^{-4}(T - 22\ ^\circ\mathrm{C}) + 1.63 \times 10^{-3}(C - 27.07\ \mathrm{wt\%}), \quad (1)$$

where n is the index of refraction, T is the temperature in °C, and C is the concentration of ammonium chloride in wt%. In addition, the rejected solute produces a light layer within the mushy zone and thus this solution is an excellent model for superalloys which also produce a light layer as they solidify. This characteristic permits the stability of such layers to be studied using the metal model material.

Diffusion Layer Stability

The diffusion layer for the system under study is composed of water-rich liquid which is solutally lighter than the bulk. This gives rise to a classic Rayleigh-type instability which the authors have examined in detail.[1-3] One of the original purposes of performing the experiments reported here in low gravity was to reduce the Rayleigh number and permit the diffusion layer to develop fully. The NASA KC-135 low-gravity aircraft permits only 30 seconds of low gravity interlaced with 90 seconds of twice the Earth's gravity. This negates the opportunity to study breakdown of the layer; however, the 30-second low gravity should be sufficient to detect growth differences between laboratory (1 g_e) and low-gravity environments.

Solidification Assembly

Figure 1 is a schematic of the solidification assembly. The solution was sealed in a quartz cuvette instrumented with thermocouples along the side walls. Thermoelectric devices (TEDs) placed at the top and bottom surfaces were used for heating and cooling and the entire process was computer controlled to meet preselected conditions. A positive temperature gradient was applied between the TEDs, and the gradient was ramped downward at a selected rate. An expanded collimated laser beam was directed through the cuvette and optically processed to extract index of refraction data.

Optical Assembly

For both the ground-based and KC-135 experiments the solidification assembly was operated on the specially built flight-worthy optical system shown schematically in Figure 2. All processes and data acquisition were computer controlled. The optical data recording was accomplished with CID video cameras which permitted the use of image analysis equipment for post-flight data reduction. By using two cameras, both the central dark ground optical methods and a neutral buoyancy particle tracking Schlieren technique could be used simultaneously.

The video systems provided a continuous record of the optical character of the cuvette's fluid. A video card within the personal computer control and data acquisition system was used to provide video output of pertinent thermocouple data so that all absolutely required information was in video format.

Procedure

The pertinent physical parameters selected for this study are given in Table 1. A hold period of 90 minutes, consistent with the time available on the aircraft, was used for both ground and flight experiments. This was known to be sufficient to give linear thermal gradients and an acceptable interface flatness. On the flights, the initial conditions could only be set up for the first set of parabolas. After that the conditions were less than optimum due to the high gravity periods experienced during the parabolas which led to extreme convection, mixing, and general turmoil.

SUMMARY

The basic objective of these experiments was to examine the growth of the diffusion layer above the solidification front and compare that growth with ground-based growth of the layer at the same conditions. Figure 3 shows photographs of the confocal system video image during solidification. The dark band is the refraction null which corresponds to the density inversion associated with rejection of lighter fluid during solidification. The center of the null is used as the measure of the diffusion layer growth. Figures 4 and 5 present the null layer size as functions of time for the ground-based and flight experiments, respectively. The low-g portion of the flight is shown with dark symbols. The significant information on the plots is the slope. In previous experiments the flight data slopes had been significantly larger (20%) than the ground base. The slopes for the new data do not reveal that trend. Within experimental error the slopes are approximately the same, 0.89 mm/min.

Figure 6 is a photograph of fluid behavior during low gravity. The observance of a "slosh" is evidenced by the non-vertical streaming of salt finger plumes which are always observed after diffusion layer breakdown. The lateral sinusoidal behavior was also observed in accelerometer data.[6] This lateral gravity "slosh" was noted for all run conditions. Since the Rayleigh fluid configuration is inherently unstable to lateral accelerations, this reflects strongly on all the data obtained.

ACKNOWLEDGMENTS

We wish to thank the low-gravity test projects at Marshall Space Flight Center and Johnson Space Flight Center for their assistance in this project. CAST is a flight experiment supported by the Microgravity Science and Applications Division of NASA. This report was taken from AIAA Paper #89-1755.[7]

REFERENCES

1. McCay, T. D., M. H. McCay, and P. A. Gray, "Experimental Observation of Convective Breakdown of the Diffusion Layer During Alloy Solidifications," Phys. Rev. Lett., 2060-2063 (1989).

2. McCay, M. H. and T. D. McCay, "Measurement of Solutal Layers in Unidirectional Solidification," J. Thermophysics and Heat Transfer, 2(3) (1988).
3. McCay, T. D., M. H. McCay, S. A. Lowry, and L. M. Smith, "Convection Instabilities During Directional Solidification," J. Thermophysics and Heat Transfer, in press (1992).
4. McCay, M. H. and T. D. McCay, "Measurement of Solutal and Thermal Layers in Directional Solidification," AIAA-87-1494 (1987).
5. Goodman, J. W., Introduction to Fourier Optics (McGraw-Hill, San Francisco, 1968).
6. Smith, G. and G. Workman, University of Alabama in Huntsville directional solidification experiment..
7. McCay, T. D., M. H. McCay, and S. A. Lowry, AIAA 24th Thermophysics Conference, Buffalo, New York, AIAA-89-1755 (1989).

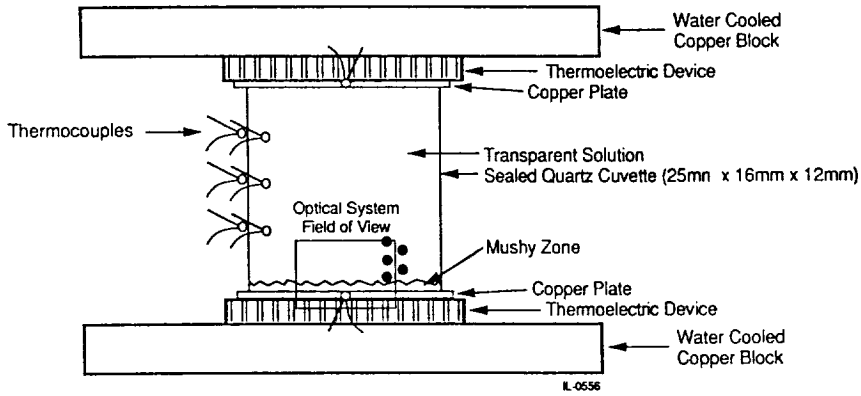

Figure 1. Schematic of cuvette solidification assembly.

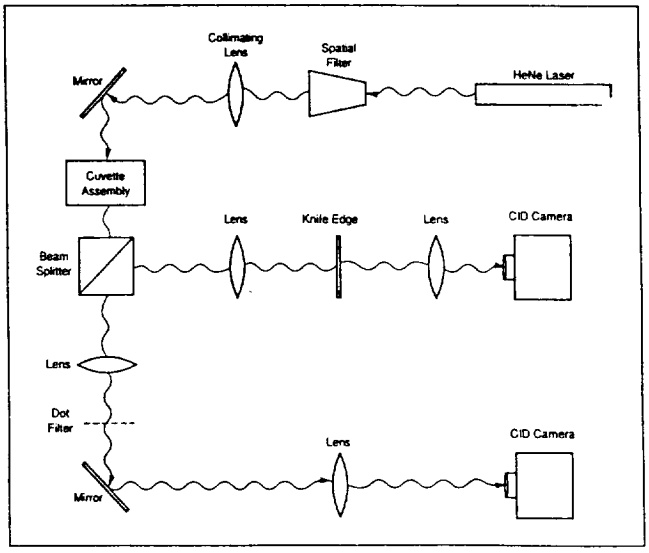

Figure 2. Schematic of KC-135 optical system.

Table 1. Solidification Run Conditions

Temperature Gradient	15 °C/cm
Temperature Ramp Rate	8 °C/min
Temperature Gradient Hold Time	90 min
Bottom Cuvette Temperature	22.5 °C
Gravity Alignment	Solidification Axis

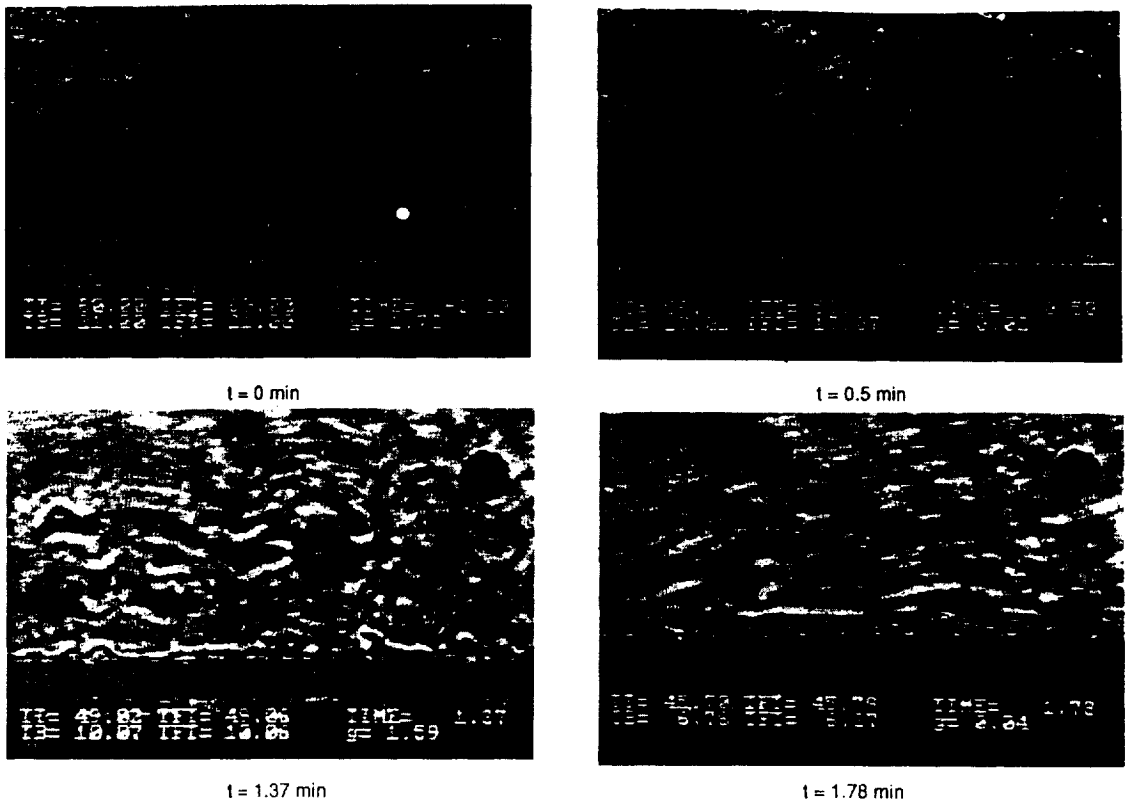

Figure 3. Time sequence of solidification during KC-135 flight (COP view).

ORIGINAL PAGE IS
OF POOR QUALITY

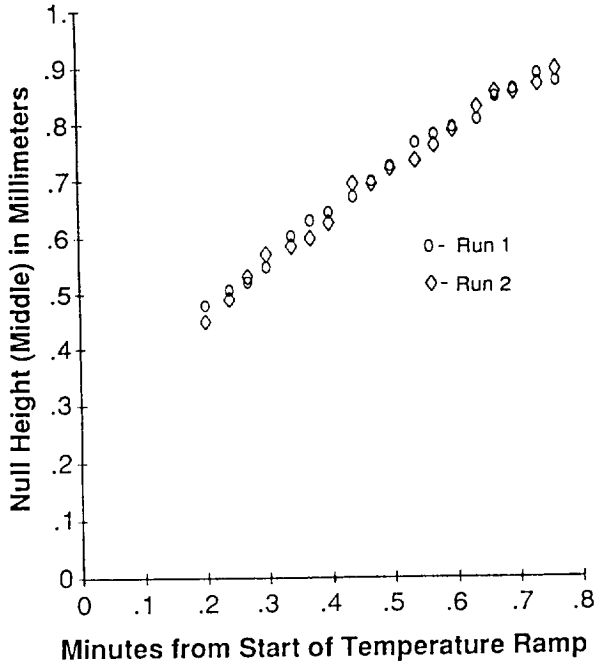

Figure 4. Null middle height as a function of time (ground base).

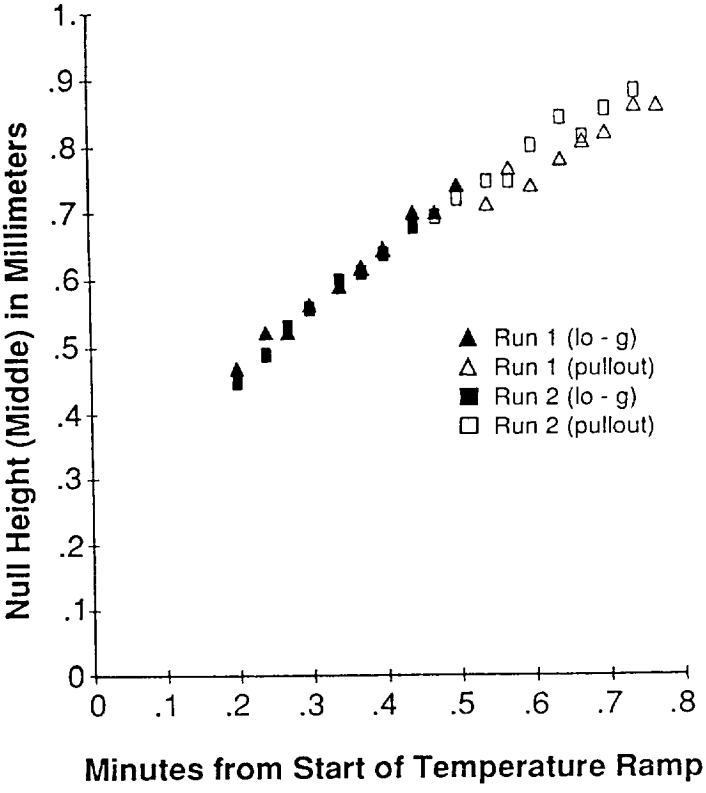

Figure 5. Null middle height as a function of time during the first parabola and pullout (KC-135).

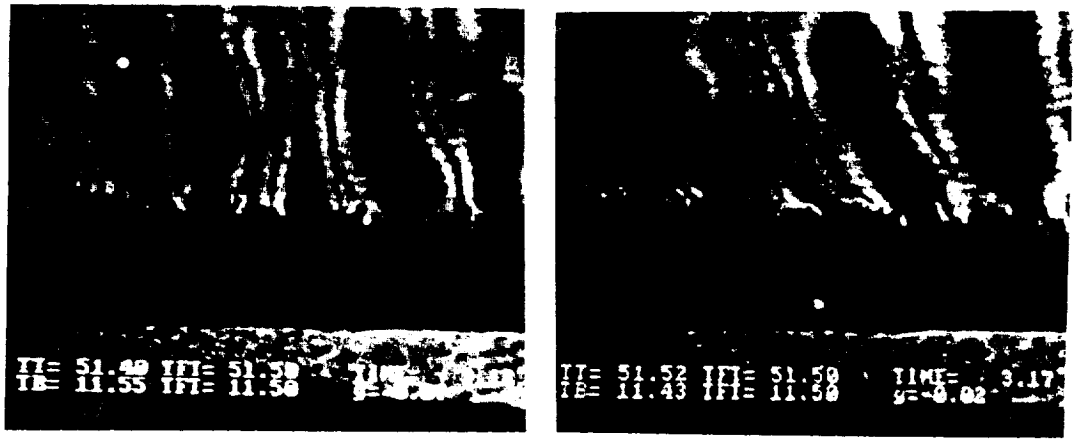

(a) (b)

Figure 6. Knife edge Schlieren views of pluming during solidification at (a) 3.12 minutes with minimal yaw acceleration and (b) 3.17 minutes with significant yaw acceleration.

EVALUATION OF MIXING TECHNIQUES AND PROTOCOLS FOR ZEOLITE A AND ZEOLITE X

Investigators: A Sacco, Jr., A. G. Dixon, and R. W. Thompson, Worcester Polytechnic Institute, Dept. of Chemical Engineering, Worcester, MA

OBJECTIVES

To observe and evaluate mixing of zeolite A and zeolite X solutions using four different mixing nozzles and numerous mixing protocols.

EXPERIMENTAL PROCEDURE AND RESULTS

Fourteen transparent autoclaves were used to test the degree of mixing of zeolite A solutions, both clear and slurries, and several zeolite X solutions. The autoclaves were activated using a power screwdriver similar to the Orbiter-supplied power screwdriver. Table 1 outlines the experimental matrix that was followed.

Observations confirmed the ease of activation of all the autoclave/nozzle designs. The bubbles observed during mixing suggest solid body rotation is taking place with some nozzle designs. In general, the Sacco Flapper and the Injector nozzle designs appeared to give the most uniform gels, as determined by visual in-flight observation and post-flight analysis. In general, zeolite X gels were not mixed as effectively as were the zeolite A gels.

Table 1. Preliminary Experimental Matrix to Establish ZCG Protocols

Type of Reactor	No.	Si/Al (ml)	Type of Solution
Sacco Flapper	1	4/5+	Zeolite A slurry
	2	3.5/5	Zeolite A slurry
	3	4/5+	Zeolite X
	4	3.5/5	Zeolite X
Piston	5	5/5	Zeolite A clear
	6	5.5/5+	Zeolite A clear
	7	5.5/5+	Zeolite X
	8	5/5	Zeolite X
Bac Flapper	9	4/5+	Zeolite A clear
	10	3.5/5	Zeolite A clear
	11	4/5+	Zeolite A slurry
	12	3.5/5	Zeolite A slurry
Injector	13	4.5/5+	Zeolite A clear
	14	4.5/5+	Zeolite A clear

KC-135 EXPERIMENTAL PROGRAM - LOW-GRAVITY TESTS FOR USML-1 GLOVEBOX EXPERIMENTS #4 AND #11

Investigators: E. H. Trinh and J. Depew,
Jet Propulsion Laboratory,
California Institute of
Technology, Pasadena, CA

OBJECTIVES

The controlled deployment of liquid samples in low gravity is determined to a large extent by the solid-liquid interfacial properties of the materials used. For liquids having low wetting angle with the solid injection mechanism, the deployment of drops having pre-determined volume and near-zero momentum must be tested under low-gravity conditions. The KC-135 environment is ideally suited for the testing of breadboard designs in preparation for the USML-1 Glovebox experiments. The second experiment under study deals with ultrasonic bubble positioning and manipulating. The testing of a bubble positioning device in low gravity prior to the USML-1 mission is also indispensable since the bubble trapping conditions are difficult to predict from 1 g experiments.

EXPERIMENT PROCEDURES AND RESULTS

Both experiments have been tested using the rack and breadboard designed for ultrasound levitation experiments carried out under another task. The apparatuses are screw fastened on the optical breadboard and are manually operated while the results are recorded by a video camera. Figure 1 is a photograph of the experimental setup for experiment #4, the low-gravity drop deployment study. Figure 2 is a photograph of the apparatus for experiment #11, the bubble dynamics investigation. Experiment #11 can be operated with the electronics included in the rack, or by using the compact control box designed for flight shown in Figure 2. Both devices are used mostly during other low-gravity periods of the parabolas, although experiment #11 also allows the trapping of large (greater than 5 mm) bubbles in normal and elevated g levels.

Experiment #4 Results

The tests carried out aboard the KC-135 have been designed to allow the experimental evaluation of various injector tips for the deployment of aqueous solutions as well as silicone oil drops. The tips have been designed such that they can be interchanged in the Drop Physics Module (DPM) deployment mechanism. The current version of the tips to be used in the DPM has been shown to be quite satisfactory for the deployment of water and aqueous solutions of glycerol, but not adequate for the deployment of silicone oil. For the latter liquid, KC-135 tests using samples having kinematic viscosity of 50 and 100 cSt have suggested that a flat plate design allowing the deployment of a floating zone also permits the deployment of large (greater than 1 cc) drops with minimal initial linear momentum. Figure 3 reproduces a series of photographs depicting the various stages of drop deployment.

The same approach has been shown to allow the reliable deployment of liquid shells, i.e., drops containing a gas bubble, but no test involving liquid-liquid combinations (compound drops) has yet been carried out.

Experiment #11 Results

A unique design of an ultrasonic cell has been shown to allow the consistent trapping of gas bubbles of up to 1 cm in diameter in 1 g laboratories. The same approach was planned for the Glovebox experiments in microgravity.

PRECEDING PAGE BLANK NOT FILMED

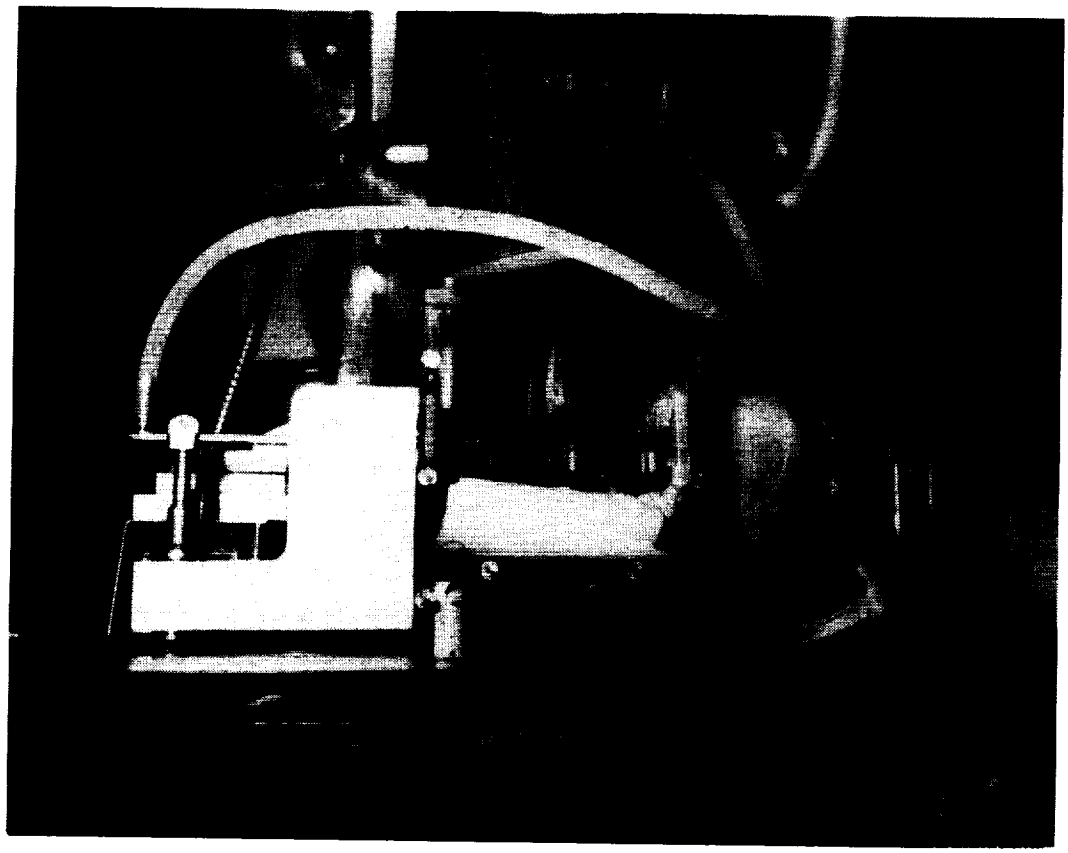

Figure 1. Experimental apparatus for GBX experiment #4. A large drop is shown being deployed following the break-up of a floating zone.

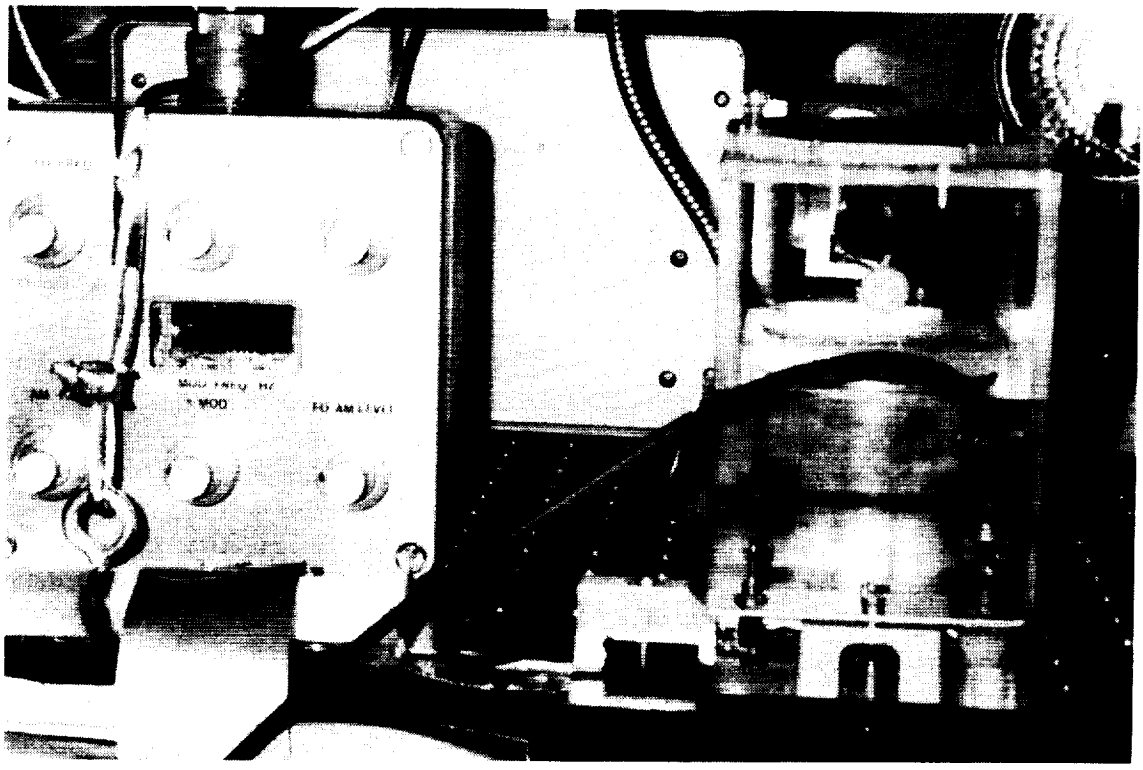

Figure 2. Experimental apparatus for GBX exerpiment #11.

ORIGINAL PAGE
BLACK AND WHITE PHOTOGRAPH

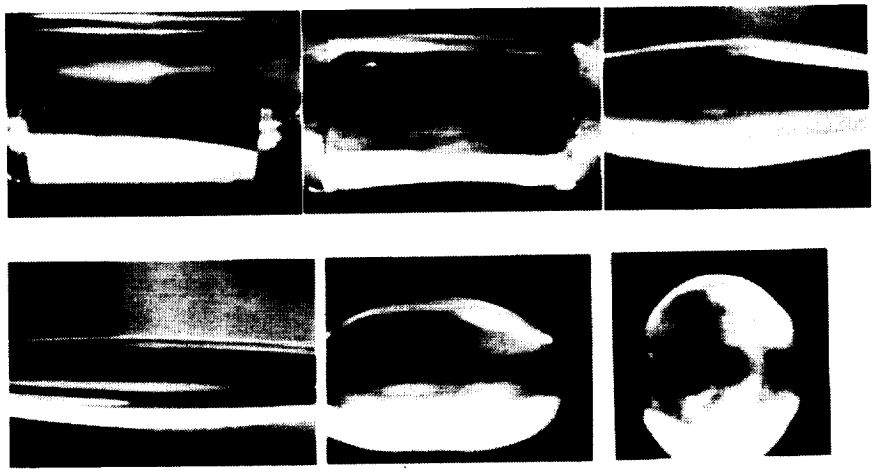

Figure 3. Photographs of various stages of the break-up of the floating zone.

The series of tests conducted in 1991, however, have shown that this would not lead to stable positioning of the bubbles in low gravity, and that a different set of parameter settings will be required. In particular, recent experiments have shown that the acoustic cell resonance at 22.5 kHz cannot be used, and that the third harmonic at 65 kHz will be required. Although both modes of operation were initially planned, some modifications in the flight experiment design have been necessary.

The test runs have shown, however, that air bubbles of about 1 cc in volume have been trapped and that the bubbles have been driven into shape oscillations, thus demonstrating the basic feasibility of the experimental objectives for USML-1. Further tests will be carried out in order to fix the parameters for the flight unit, and for the accurate definition of the flight crew procedures. Figure 4 are photographs of 8 mm bubbles trapped in 1 g and in low g during testing aboard the KC-135.

SUMMARY

The low-gravity periods provided by the KC-135 parabolas have proved to be valuable in the design of both experiments #4 and #11. In the first case, low-gravity tests have prompted the redesign of injector tips for the deployment of silicone oil in microgravity, and have allowed verification testing. In the second case, the low-gravity studies have revealed that the planned approach was not adequate, thus leading to an alternate and successful mode of operation for microgravity. In both cases, the KC-135 experiments have greatly enhanced the probability of success of the shuttle flight experiments.

ACKNOWLEDGMENTS

We thank the low gravity tests projects at Marshall Space Flight Center and at Johnson Space Flight Center for accommodating our equipment aboard the KC-135. This task is funded by the Microgravity Science and Applications Division of the National Aeronautics and Space Administration. The tests described above were carried out during FY91.

ORIGINAL PAGE
BLACK AND WHITE PHOTOGRAPH

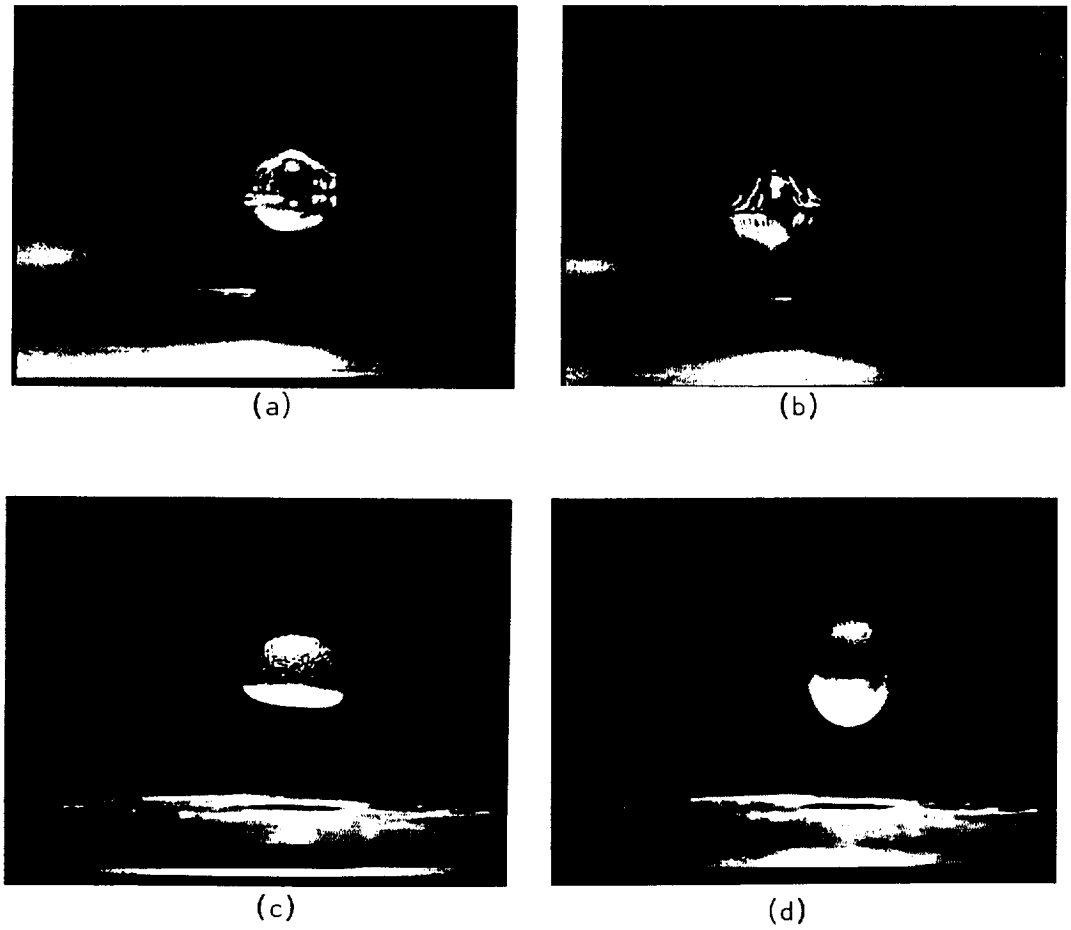

Figure 4. Low-gravity experiment carried out in the KC-135 airplane. 8 mm bubble trapped in an ultrasonic sound field excited in a water-filled cell. (a) non-oscillating stationary bubble; (b) same bubble undergoing shape oscillation driven by modulated ultrasonic radiation pressure; (c)-(d) 8 mm bubble trapped in an ultrasonic standing wave in 1 g. The oblate and prolate shapes have been captured on the photograph by strobed lightning. Capillary waves on the upper surface are excited by the ultrasonic field used for the positioning of the bubbles.

ROLE OF KC-135 EXPERIMENTS IN DEVELOPING LOW-GRAVITY POLYMER PHASE SYSTEM DEMIXING AND BIOPROCESSING RESEARCH

Investigators: J. M. Van Alstine, The University of Alabama in Huntsville, Huntsville, AL; R. C. Cronise, S. Bamberger, and P. A. Curreri, NASA, Marshall Space Flight Center, Huntsville, AL

OBJECTIVES

The objectives of KC-135 phase partition research are to identify and screen candidate polymer phase systems, and experimental variables, for low-gravity bioprocessing and basic science experiments. In addition KC-135-based research supports hardware/procedure development and crew training associated with the Partition Bioprocessing Program (Figure 1).

EXPERIMENTAL PROCEDURES AND HARDWARE

Experimental procedures have been described in detail elsewhere.[1-3] Phase systems (of varied salt and polymer, type and concentration) possessing different physical properties[1] are placed into clear chambers (glass, Plexiglas, or Lexan). Chamber inner surfaces may be modified whole or in part with various polymer coatings.[4,5] Other chamber variables include volume and geometry. Just prior to, and after, entering low gravity the systems are emulsified using manual (mixing ball) or automated (magnetic stirring). Demixing is then recorded

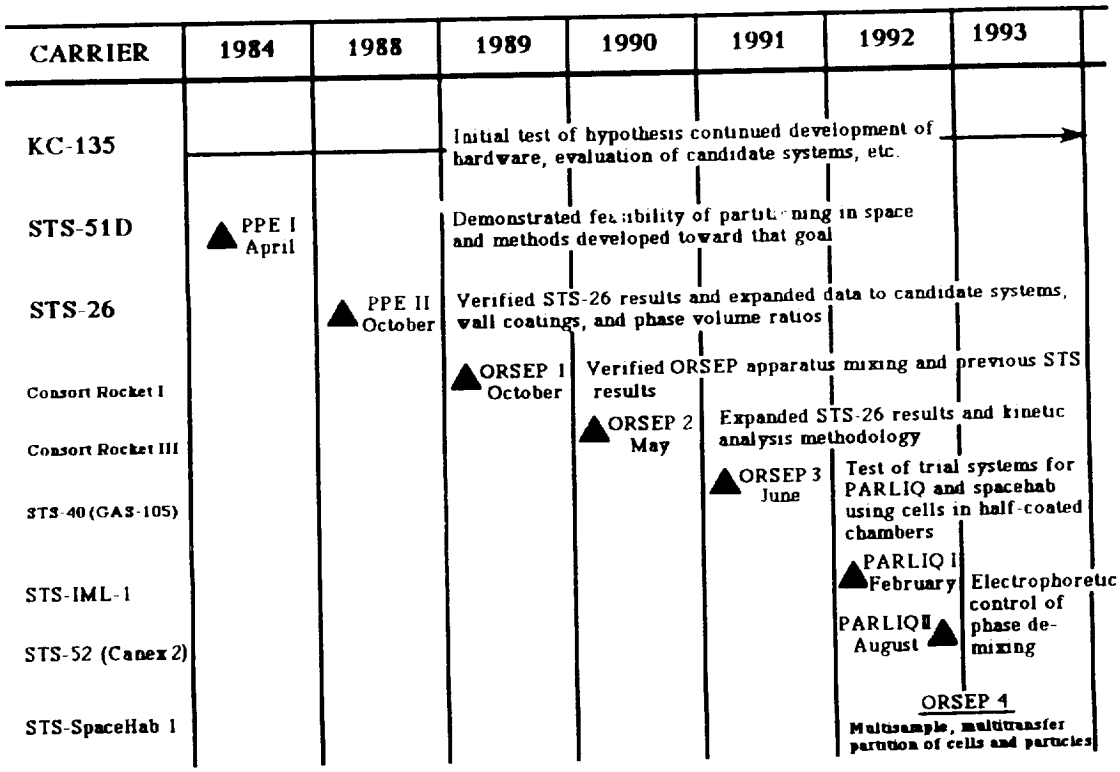

Figure 1. Low-gravity phase partitioning experiments.

using a camera or a video recorder. Hardware used for KC-135 experiments formed the basis for shuttle/rocket hardware and has been discussed previously.[1-3,6,7]

Experimental photographs, coded on the negative with hr:min:sec data, are digitized and subjected to computer-aided analysis (Figure 2 and references 2 and 3). Analysis involves image enhancement followed by fast Fourier transformation to yield a power spectrum which peaks at a frequency proportional to the inverse of the average distance between adjacent domains (Figure 2). Results expressed in terms of average phase region diameter (or radius) versus time (t) are fit to various models of demixing and used to estimate time for demixing to occur in space. The latter allows accurate planning of shuttle and rocket experiment time lines.

Phase system preparation and properties have been presented in detail elsewhere.[1-3,8] The pH 7.4 phase systems discussed here are a 7% (w/w) Dextran 40 (Pharmacia), 5% (w/w) PEG 8000 (Union Carbide), 150 mM NaCl, 7.3 mM Na_2HPO_4, 2.3 mM NaH_2PO_4 system designated as (7*,5,0)V or "G" and a 5.5% (w/w) Dextran 500, 0.7% (w/w) PEG 8000, 9.5% (w/w) Ficoll 400 (Pharmacia), 85 mM Na_2HPO_4, 25 mM NaH_2PO_4 system designated (5.5,0.7,9.5)VI or "J." Use of the neutral poly-sucrose Ficoll reduces the density differences between the phases creating an "isopycnic" control system whose demixing is not appreciably affected by gravity. The PEG or Ficoll rich phase is typically dyed with Trypan Blue (Aldrich) 0.05 mg/ml.

RESULTS AND DISCUSSION

On Earth polymer phase system emulsions demix by a complicated sequence of events. The initial emulsion consists of micron-sized phase droplets which rapidly coalesce and within seconds begin to sediment. Sedimentation promotes the growth of larger domains, the demixing rapidly evolving into a convective process with active "phase streaming."[1-3] In low gravity, coalescence, initiated as in 1 g, continues in an apparently self-driven manner. After a time period, which can vary from a minute to hours (for a 3 ml sample) demixing is complete. Some systems exhibit appreciable demixing over the 15 to 20 seconds of low gravity obtainable on the KC-135. Due to small phase density differences (e.g., 0.04 g/cc) and appreciable phase viscosities (e.g., 4-30 cP), KC-135 results are similar to those obtained in space at lower gravity levels (see below).

Low-g coalescence demixing suggests that the kinetic data for different systems should have similar slopes when domain growth is expressed as a function of log t. Figure 3 illustrates the expected result for the isopycnic system (J) in 1 g and the (7,5,0)V system (G) on the KC-135. Different symbols refer to independent experiments. Figure 4 illustrates the same data (versus t) in relation to that obtained on a shuttle flight. One can see that the isopycnic system is a valid control/model system, while the KC-135 is able to provide quality low g demixing data.

ACKNOWLEDGMENTS

The authors gratefully acknowledge R. Chassay, R. Shurney, and all NASA/Marshall and NASA/Johnson Space Center personnel whose efforts support the KC-135 program. Fellowship support was provided by the Universities Space Research Association (JVA) and the National Research Council (SB).

REFERENCES

1. Van Alstine, J. M., S. Bamberger, J. M. Harris, R. S. Snyder, and D. E. Brooks, in Proceedings of the VIIth European Symposium on Materials and Fluid Sciences Under Microgravity, ESA Publication SP-295, pp. 399-407 (1989).
2. Bamberger, S., J. M. Van Alstine, D. E. Brooks, J. B. Boyce, and J. M. Harris, in Progress in

Low-Gravity Fluid Dynamics and Transport Phenomena, J. N. Koster and R. L. Sani, Eds., AIAA, Washington, pp. 603-630 (1990).
3. Bamberger, S., J. M. Van Alstine, J. M. Harris, J. K. Baird, R. S. Snyder, J. Boyce, and D. E. Brooks, Sep'n. Sci. and Technol., 23, 17-34 (1987).
4. Boyce, J. F., B. A. Hovanes, J. M. Harris, J. M. Van Alstine, and D. E. Brooks, J. Colloid Interf. Sci., in press (1991).
5. Herren, B. J., S. G. Shafer, J. M. Van Alstine, J. M. Harris, and R. S. Snyder, J. Colloid Interf. Sci., 115, 46-55 (1987).
6. Deuser, M. S., J. M. Van Alstine, J. C. Vellinger, F. C. Wessling, and C. A. Lundquist, in Proceedings of the VIIIth European Symposium on Materials and Fluid Sciences Under Microgravity, ESA Publications, Noordwijk (1992).
7. Karr, L. J., J. M. Harris, S. G. Shafer, J. M. Van Alstine, and R. S. Snyder, J. Chromatog., 442, 219-227 (1987).
8. Walter, H., D. Fisher, and D. E. Brooks, "Partitioning in Aqueous Two-Phase Systems. Theory, Methods, Uses, and Applications in Biotechnology," Academic Press, Orlando (1986).

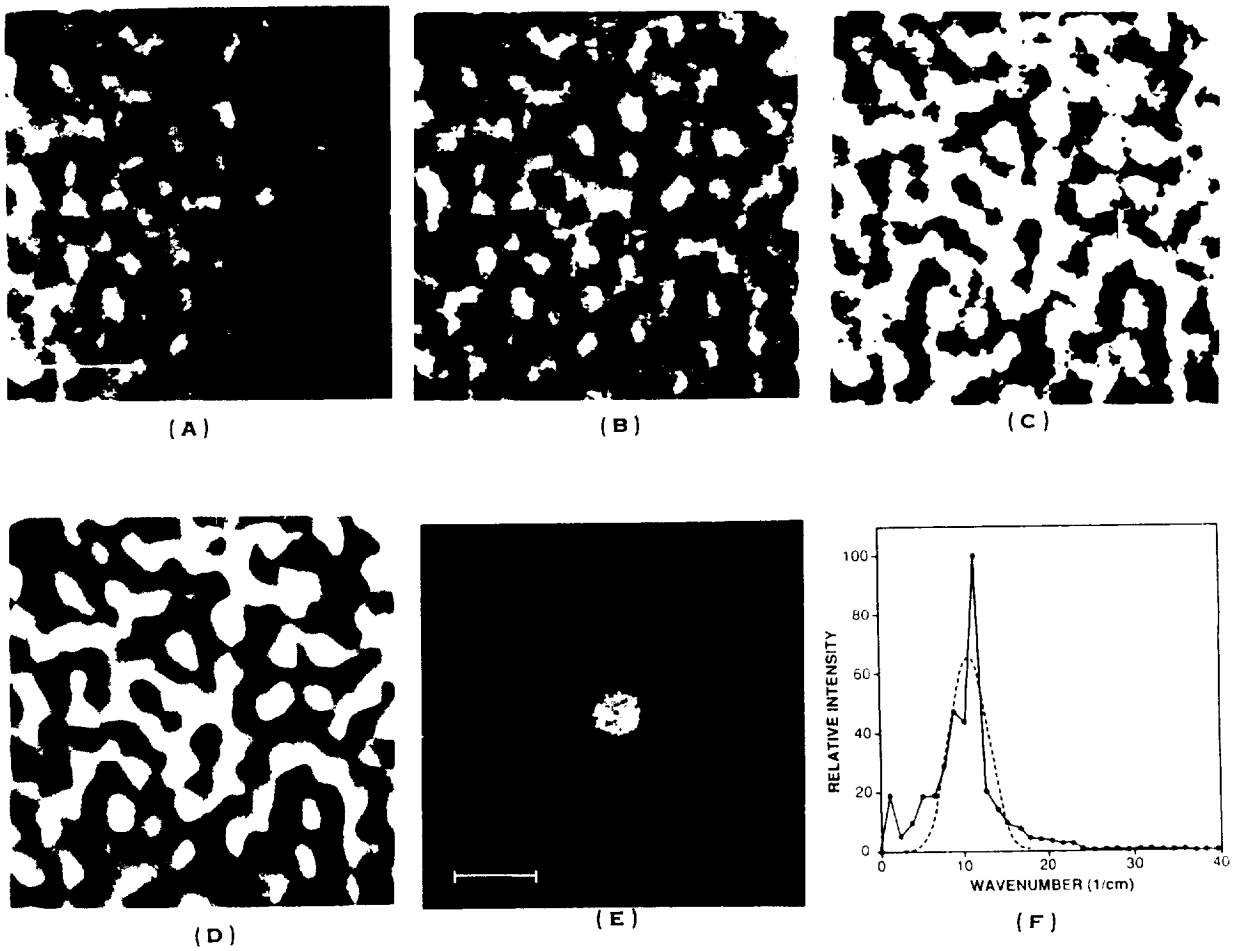

Figure 2. Kinetic analysis of system 1 [2,3] at 70 s after mixing in low g on STS-26. The photographic image (a) was corrected for uneven illumination, (b) its contrast was enhanced by setting an upper and lower intensity threshold, (c) and high-frequency noise was reduced by image smoothing (d). Panel e indicates the two-dimensional intensity distribution of the FFT of the image in panel d. Panel f indicates the power spectrum (——) and its Gaussian approximation (- - -). The bars in panels a and e represent 0.2 and 50 cm^{-1}, respectively.

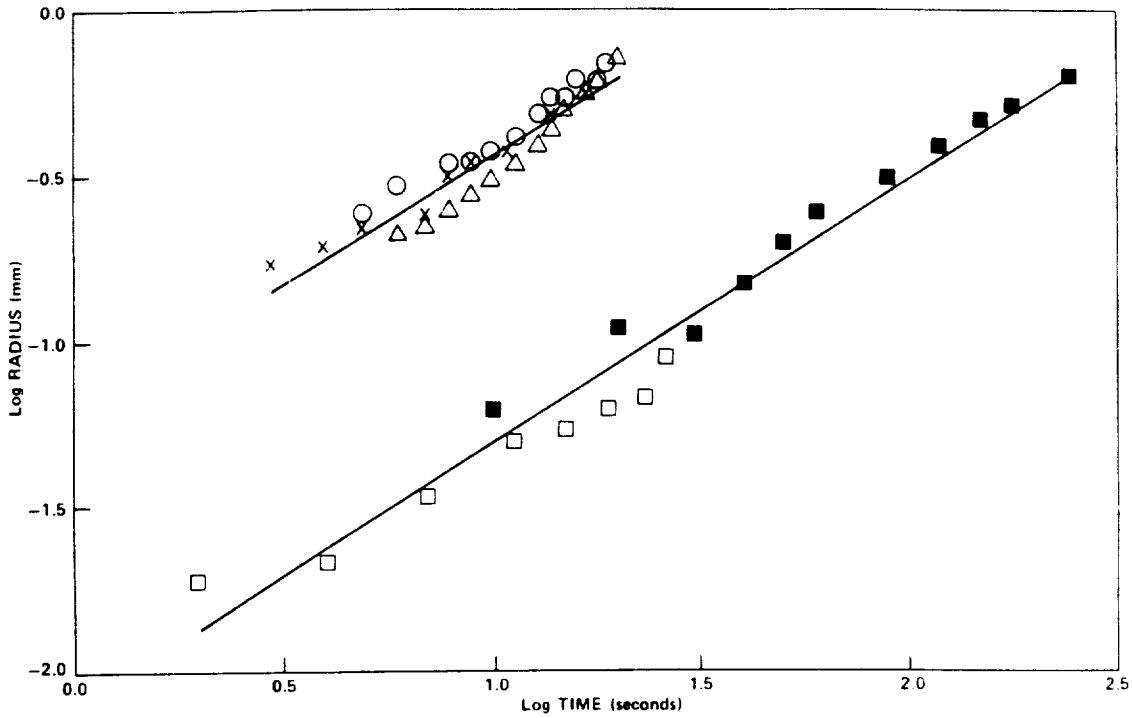

Figure 3. Plot of log time after shaking versus log radius (based on equivalent domain diameter) for (7*,5,0)V system at low g (O,Δ,X) and isopycnic (5.5,0.7,9.5)VI system at unit g (□, ■). Symbols represent individual experiments.

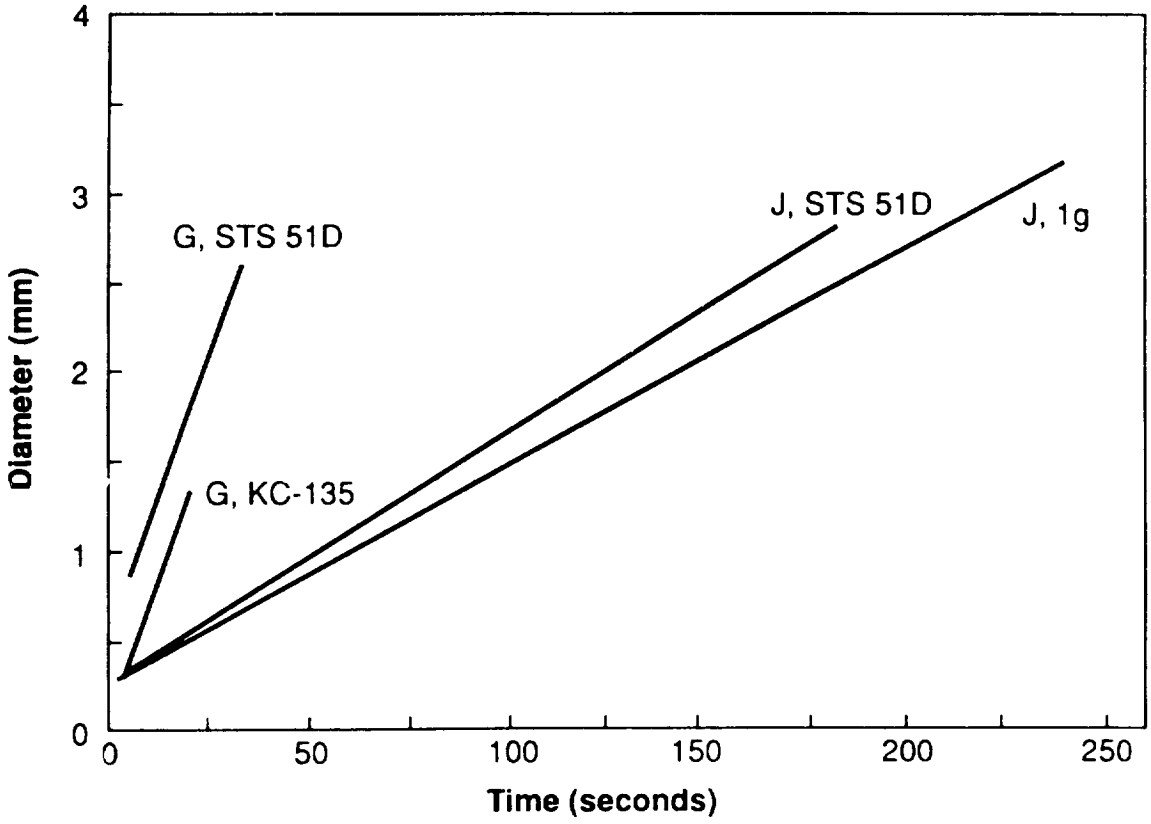

Figure 4. Linear regression lines of mean droplet size vs. time in phase system G on STS-51D and KC-135, and phase system J on STS-51D and on Earth.

3. TRANSPORT AND INTERFACIAL STUDIES IN TRANSPARENT SYSTEMS

PRECEDING PAGE BLANK NOT FILMED

46 INTENTIONALLY BLANK

CONTROL OF DEMIXING OF IMMISCIBLE LIQUIDS BY CONTAINER SHAPER

Investigators: J. M. Harris, B. A. Hovanes, and M. Mori, Department of Chemistry, The University of Alabama in Huntsville, Huntsville, AL

OBJECTIVES

This project is concerned with gaining understanding and control of the fluid physics of demixing immiscible liquids in low g. In particular we are interested in the effects of container shape and wall coatings on location and rate of demixing. We have done many experiments on the important system made from aqueous solutions of poly(ethylene glycol) and dextran. These phase systems are, however, relatively viscous and do not demix rapidly enough to be useful for KC-135 flights. Thus the current experiment was performed with water versus air and was designed to test the ability of a tub-shaped container to control the location of the demixed phases.

EXPERIMENTAL PROCEDURE AND RESULTS

This work has been stimulated by the investigations of Paul Concus and coworkers (UC Berkeley) and their theories guide understanding of the shape effects. We recently flew an experiment with tub-shaped containers on the KC-135. These containers were filled half with water and half with air. In one case a small drop of detergent was added to the water. In this case the water-wall contact angle was 2°. In the second case, clean water without detergent was used and the glass was coated with a commercial nonwetting silicone treatment to give a water-wall contact angle of 105°. According to the Concus' theories, removal of the g force should result in movement of fluids in the first case, but not in the second case.

The results of the KC-135 flight experiment with the tub-shaped containers are shown in Figures 1 and 2. Interestingly, the water did move in the first (wetting) case, to give the final configuration shown. Note that the Concus theories do not predict the final configuration. It is also interesting that in the second (non-wetting) case the fluids also move but not to the same final configuration.

PRECEDING PAGE BLANK NOT FILMED

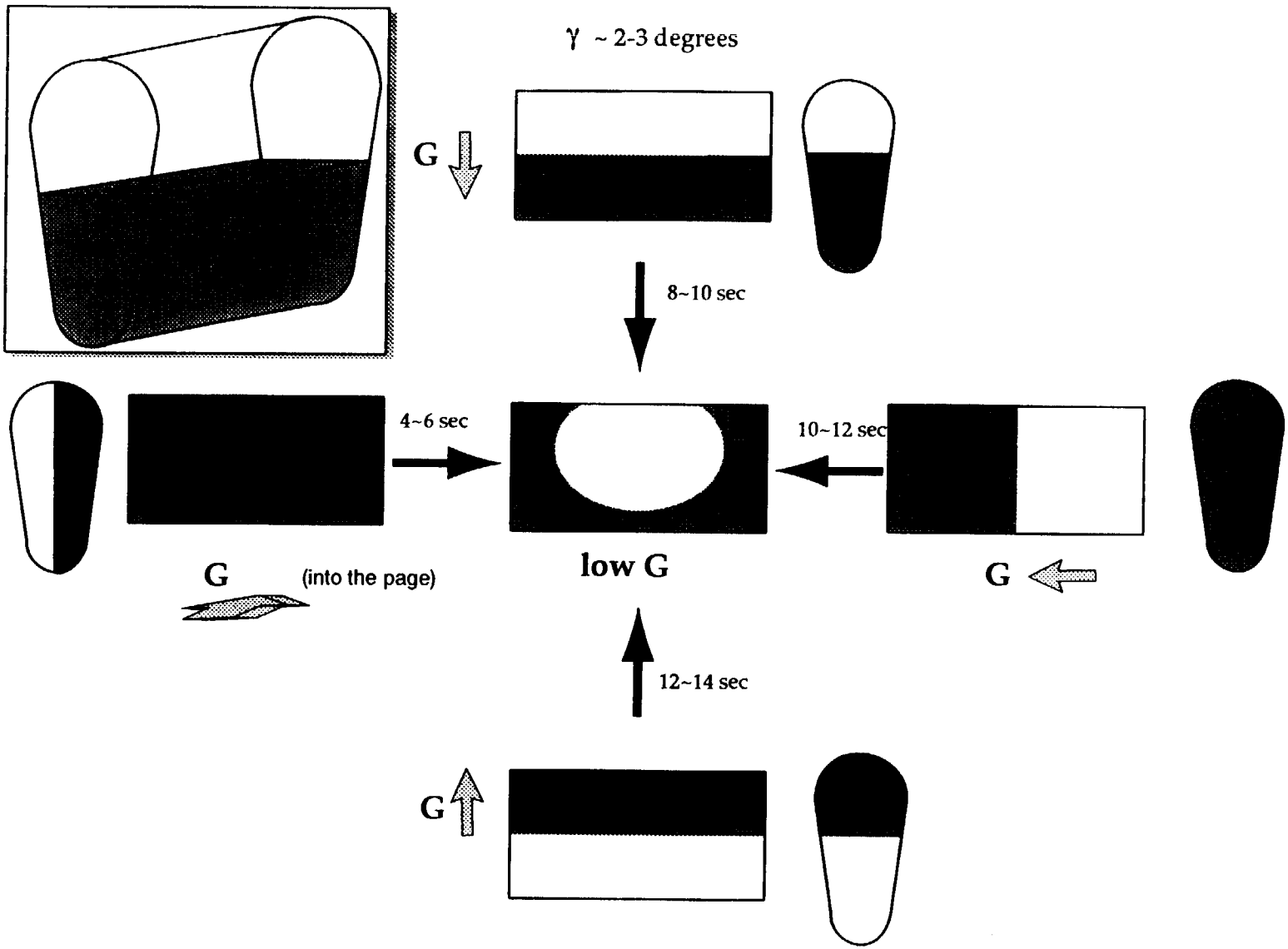

Figure 1. Results for KC-135 flight experiments for tub-shaped containers (wetting case).

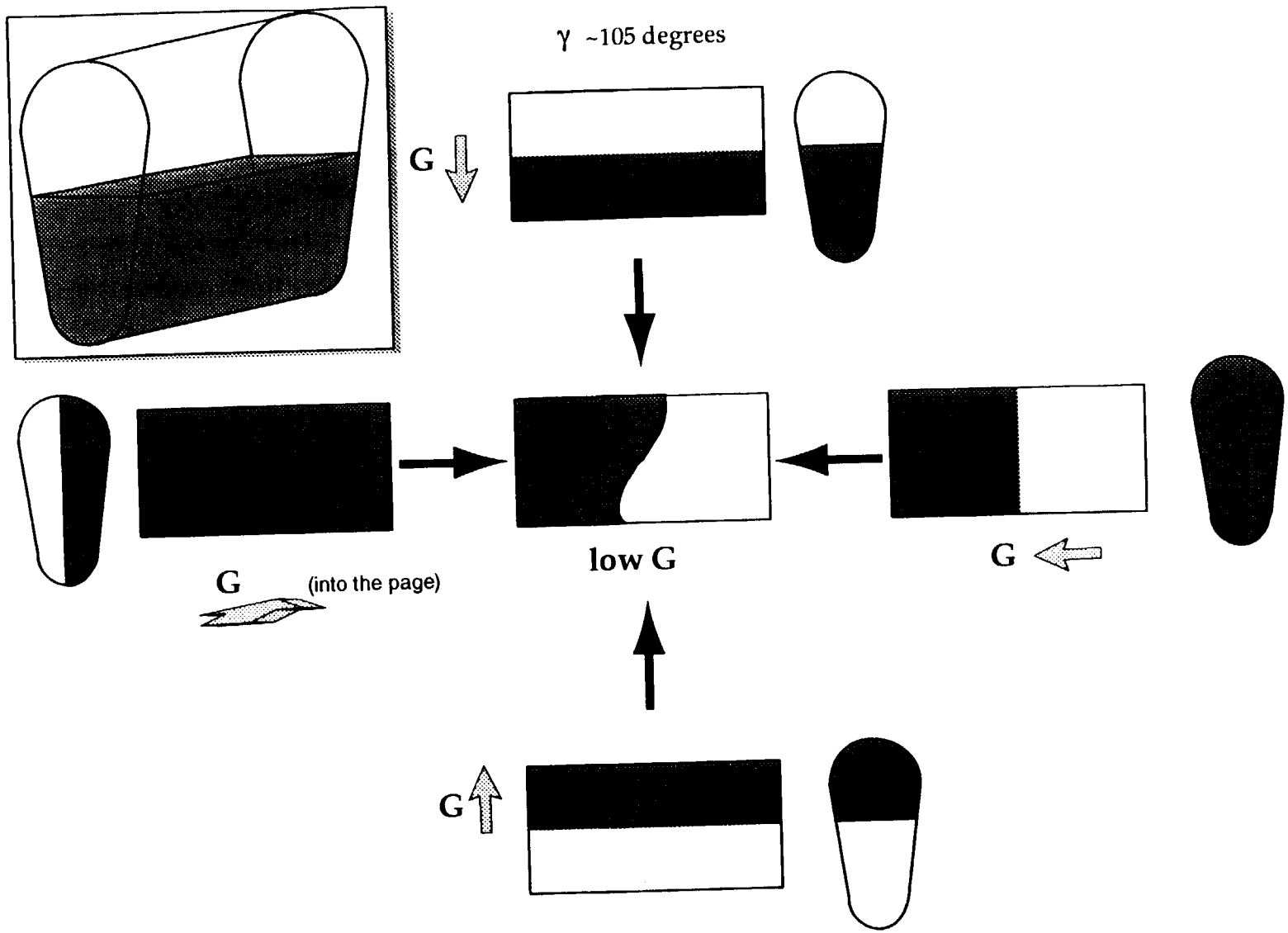

Figure 2. Results for KC-135 flight experiments for tub-shaped containers (nonwetting cave).

FLUID INTERFACE AND BUBBLE EXPERIMENT

Investigators: Fred W. Leslie, NASA, Marshall Space Flight Center, Huntsville, AL; Roger F. Gans, University of Rochester, Rochester, NY

OBJECTIVES

The objective of these exerpiments is to validate models of the equilibrium configuration of two phase rotating fluids in a low-gravity environment.

EXPERIMENTAL PROCEDURE AND RESULTS

One way to control large amounts of liquid in near-Earth orbit is to rotate the container, holding the liquid against the outer wall. In many applications it is important not only to know where the vapor is, but to know that it is symmetrically distributed. A bubble that is small compared to the size of the container is free to move within the container, though remaining near the axis. The Fluid Interface and Bubble Experiment was conducted to investigate the behavior of a free liquid surface undergoing rotation in a low-gravity environment. Of particular interest is the shape and stability of a free surface in contact with boundaries. Both of these phenomena are controlled by the magnitude of the surface tension, the centrifugal force, and to a lesser extent the low gravity. Three different approaches were used in this research: analytical, numerical, and experimental. An equation for the equilibrium shape of the bounded interface was derived using LaPlace's relation between the pressure drop across the interface and its total curvature. The equation was solved analytically for simple cases in which gravity, surface tension, or centrifugal force individually dominated. In order to obtain solutions, an experimental apparatus to measure free surface shapes in low gravity was flown in the low-gravity environment of NASA's KC-135 aircraft.

Figure 1 shows a comparison between the observed and computed surface shape. For this case, a cylinlder 4 cm deep with a 20 cm radius was partially filled with a known amount of ethanol and rotated about the cylinders axis. In the low-gravity environment, the capillary and centrifugal forces compete for controlling the shapes of the interface. The measurements of the observed shape were obtained by digitizing a photograph of the interface, scaling it, and passing the data through a ray trace program to eliminate the optical distortions created by the cylindrical container. The comparison shows good agreement for the steady state case.

REFERENCES

Leslie, F., C. Schafer, and R. Gans, "Classical Model of Liquid Helium Management for Gravity Probe-B," Proceedings of 1983 Space Helium Dewar Conference, edited by John B. Hendricks and Gerald R. Karr, University of Alabama in Huntsville, 199-210 (1983).

Gans, R. and F. Leslie, "Low Gravity Liquid Management: A Hydrostatic Stability Problem," 37th Annual Meeting of the Division of Fluid Dynamics, American Physical Society, Providence, RI, November 18-20 (1984).

Leslie, F. W., "Measurements of Rotating Bubble Shapes in a Low Gravity Environment," J. Fluid Mechanics, 161, 269-279 (1984).

Leslie, Fred, Roger Gans, and Charles Schafer, "Fluid Surface Behavior in Low Gravity," NASA TP-2486 (1985).

Leslie, F. and R. F. Gans, "Interface Stability in a Slowly Rotating Low Gravity Tank: Experiments," AIAA 24th Aerospace Sciences Meeting, January 6-9, 1986, Reno, NV, AIAA-86-0197 (1986).

Gans, R. F. and F. W. Leslie, "Interface Stability in a Slowly Rotating Low Gravity Tank: Theory," AIAA 24th Aerospace Sciences Meeting, January 6-9, 1986, Reno, NV, AIAA-86-0198 (1986).

Gans, R. F. and F. W. Leslie, "Interface Stability in a Slowly Rotating Tank: Theory," J. of Spacecraft and Rockets, 24, 232-235 (1987).

52

PRECEDING PAGE BLANK NOT FILMED

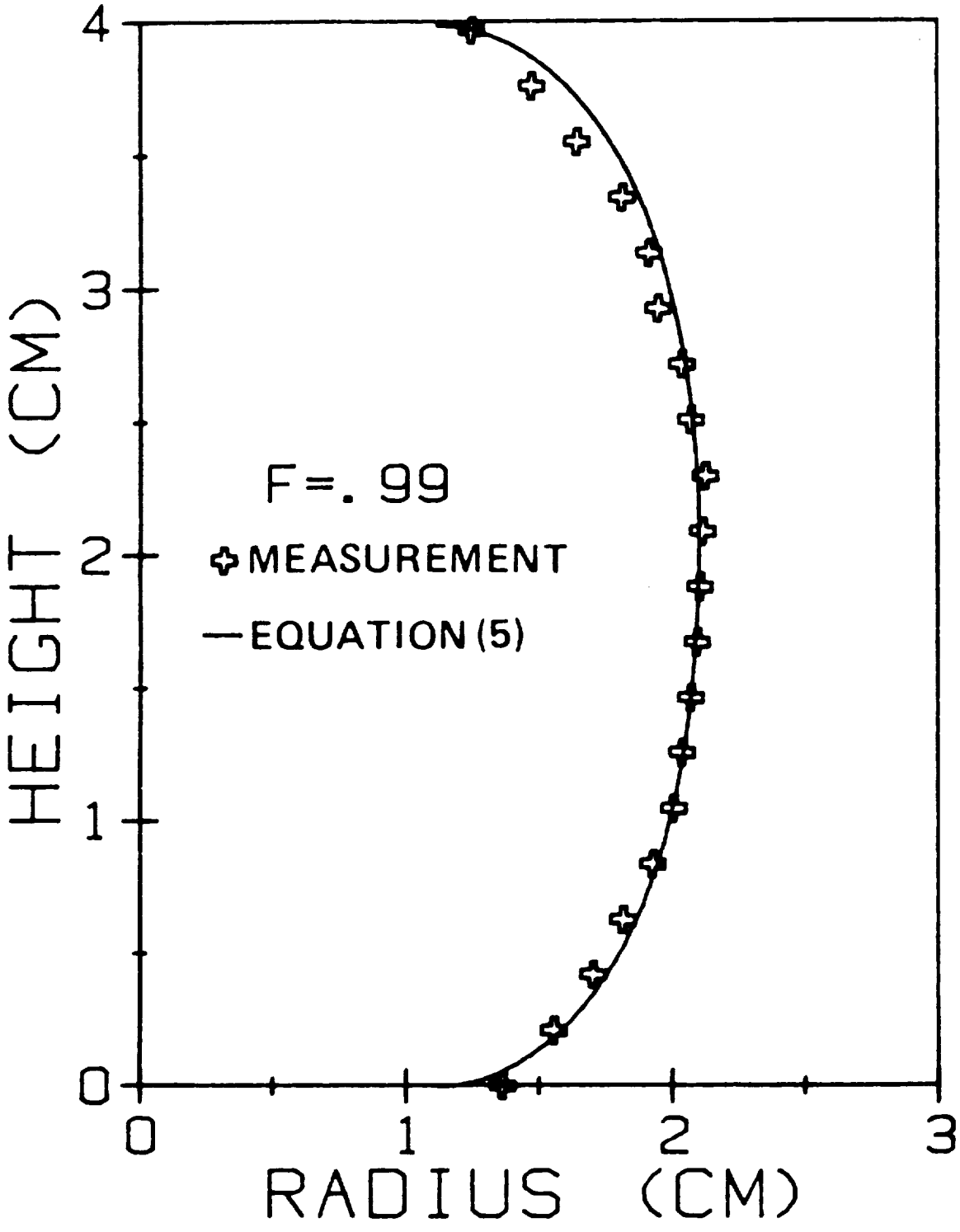

Figure 1. Comparison between observed and computed surface shape.

DECISIVE TEST OF BIOCONVECTION IN VARIABLE GRAVITY

Investigators: Helen C. Matsos, David A. Noever, and Raymond J. Cronise, NASA, Marshall Space Flight Center, Huntsville, AL

OBJECTIVES

The objective of this study is to determine the mechanism (gravity-dependent or-independent) causing bioconvective pattern formation in dense cultures of swimming cells. The term bioconvection[1] describes the curious streaming patterns observed in dense cultures of free-swimming cells. Such cultures are observed to concentrate spontaneously into remarkable flowing polygons and triangles.

EPERIMENTAL PROCEDURES

The experiment was conducted on the KC-135 aircraft during successive parabolas such that the same culture acted as its own control.[2-3] Neither fluid properties, organism count, age, nor motility was altered. Unlike an isopycnic test, viscosity[4] and osmolarity applied to identical titers in flexible geometries. Three types of bioconvecting cells were tested: a ciliate (Tetrahymena), a flagellate (Polytomella), and sperm (Caprine goat). Patterns were video-recorded, then digitized for image analysis (Figures 1 and 2).

RESULTS

To explain the cause of bioconvection, three schools of thought have been put forward: (1) the gravity hypothesis, that cells swim upward against gravity and since they are heavier than water, subsequently turn over or stir their fluid culture into elaborate networks of rising and sinking cells; this is akin to Benard cells of thermal convection; (2) the drafting hypothesis that cells draft or otherwise become linked together in their swimming by fluid viscosity; and finally (3) the chemical hypothesis, that cells detect and self-assemble in response to chemical (e.g., oxygen) gradients near their neighbors. Previous attempts to isolate and study these causes without at least one other mechanism interfering have failed. For example, the preparation of equidensity; isopycnic cultures introduce changes in both fluid density (gravity hypothesis) and viscosity (drafting hypothesis) with uncertain effects on the cells' chemistry (chemical hypothesis). However, by observing pattern formation in modulated gravity during parabolic flights, the cause of bioconvection can be identified decisively.

Flight results indicate that (1) those cells biologically capable of remaining active at extremely high concentrations (e.g., 10 billion cells per ml) form patterns by drafting for each other, while (2) cells at lower concentrations (e.g., one million cells per ml) form patterns by sinking and rising in response to gravity. The chemical mechanism did not generally lead to pattern formation in the absence of gravity or drafting.

By understanding the mechanism causing bioconvection, new applications can be designed for pharmacological studies and cell separations.[6-10] For example, bioconvective patterns have been used successfully to monitor cadmium toxicity in polluted water and to construct strategies to counter cadmium's lethal activity by supplementing protective calcium, nickel, or copper. In addition, for cell separations, 200-300% fractional splits have been obtained routinely in a rotating spectrometer in a single pass on bioconvecting cultures.

REFERENCES

1. Platt, J. R., "Bioconvection Pattern in Cultures of Free-Swimming Organisms," Science, 133, 1761-2 (1961).

2. Noever, D. A., "Evolution of Bioconvective Patterns in Variable Gravity," Phys. Rev. A, 44, 5279-5291 (1991).
3. Noever, D. A., H. C. Matsos, J. U. Johnson, and R. J. Cronise, "A Decisive Test of Gravity's Role in Biologically Generated Cellular Patterns," Phys. Rev. Lett. (submitted) (1991).
4. Fornshell, J. A., J. Protozool, 25, 125-133 (1978).
5. Pedley, T. J. and J. O. Kessler, J. Fluid Mech., 212, 155-180 (1990).
6. Noever, D. A., "A Rotating Spectrometer for Separation/Concentration of Bioconvecting Microorganisms," Rev. Scien. Instrum., 62, 229-232 (1991).
7. Noever, D. A. and H. C. Matsos, "A Bioassay for Monitoring Cadmium Cased on Bioconvective Patterns," J. Environ. Sci. Health, A26, 273-286 (1991).
8. Noever, D. A. and H. C. Matsos, "Calcium Protection Against Cadmium Poisoning: Bioconvective Indicators in Tetrahymena," J. Environ. Sci. Health, A26, 1105-1113 (1991).
9. Noever, D A. and H. C. Matsos, "The Rotating Spectrometer: New Biotechnology for Cell Separations," NASA TM-103522, November 1990.
10. Noever, D. A. and H. C. Matsos, "A Biosensor for Cadmium Based on Bioconvective Patterns," NASA TM-103523, November 1990.

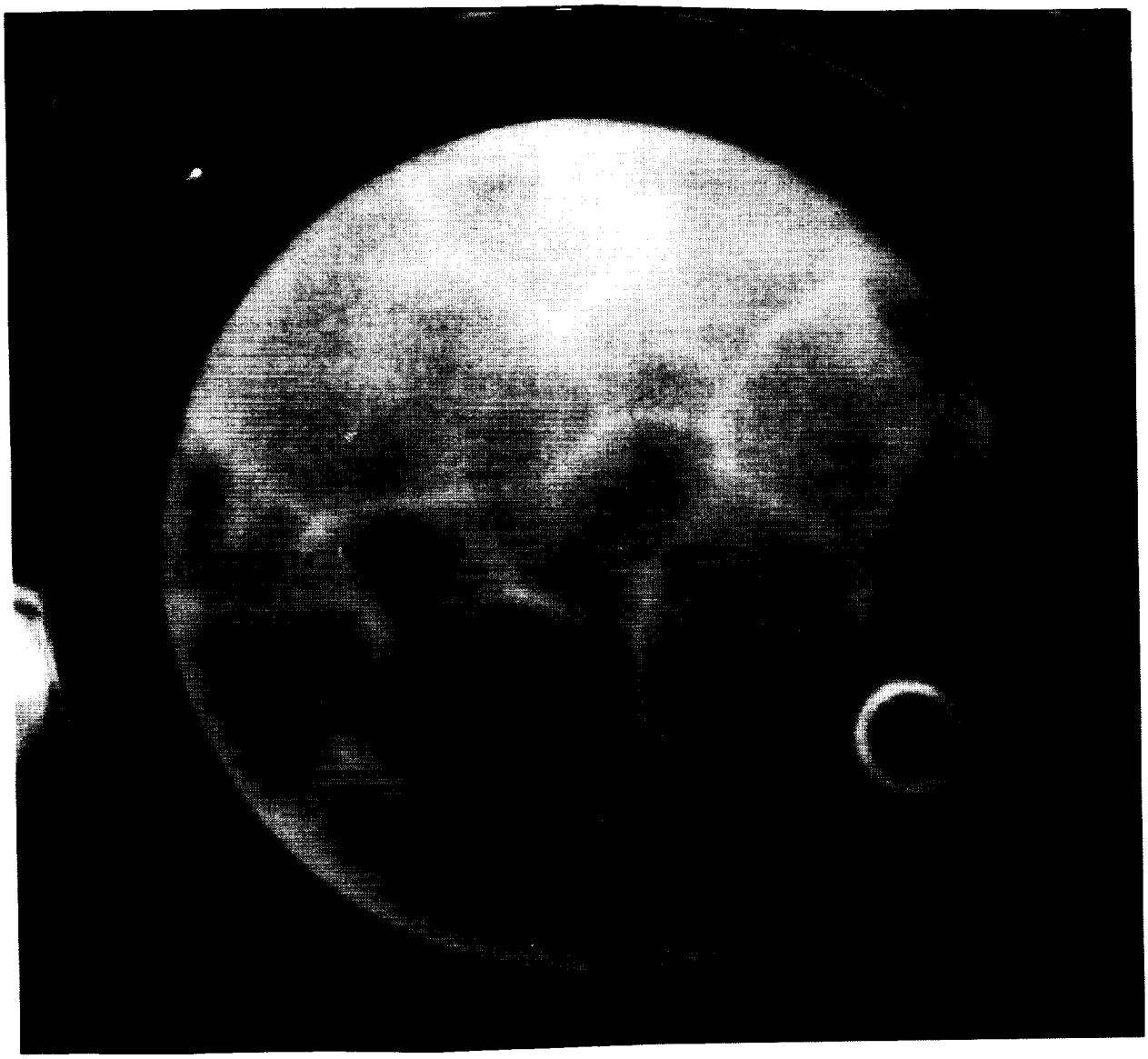

Figure 1. Video-recorded bioconvection pattern.

ORIGINAL PAGE
BLACK AND WHITE PHOTOGRAPH

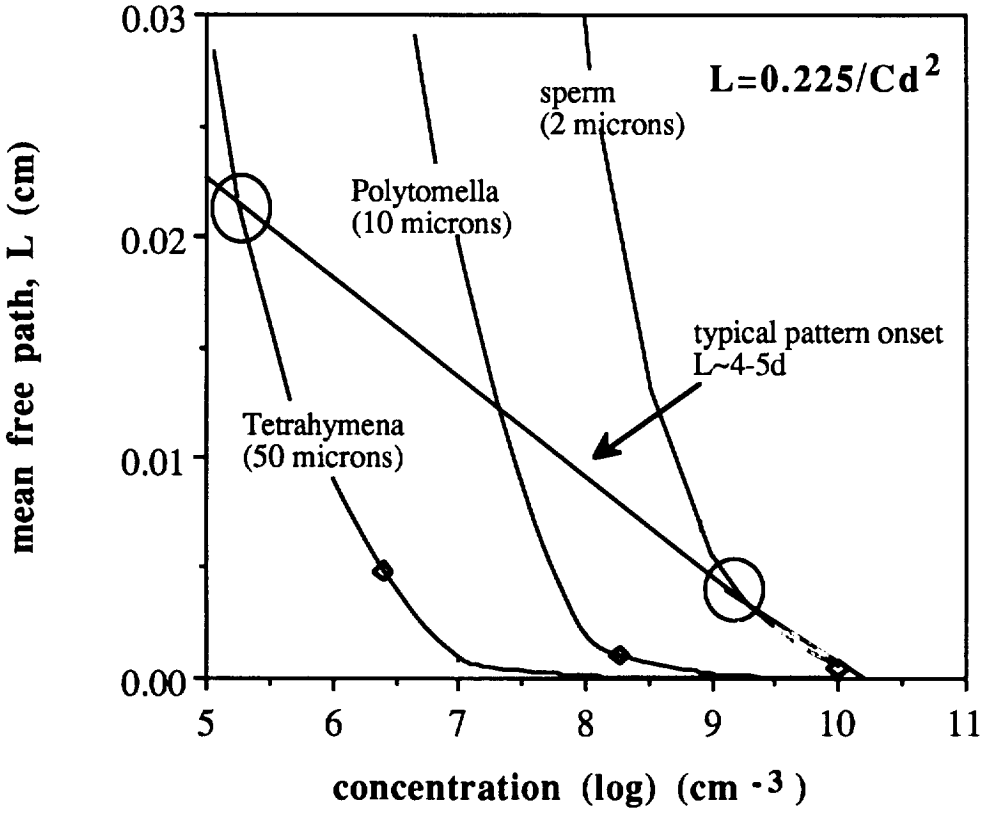

Figure 2. Digitized bioconvection data.

FOAM FRACTIONATION OF LARGE PARTICLES IN LOW GRAVITY

Investigator: David A. Noever, NASA,
Marshall Space Flight Center,
Huntsville, AL

OBJECTIVE

The objective of this study is to foam fractionate large, heavy particles in low gravity as model systems for separations of premium biologicals and whole cells with minimal surfactants.

EXPERIMENTAL PROCEDURE AND RESULTS

Gravity affects foam floatation in several ways: gravity (1) limits floatable particle sizes, (2) leads to bubble coalescence from film drainage, (3) increases surfactant requirements, and (4) increases bubble-particle collision velocities. Gravity sets an upper limit on particle sizes which can be adsorbed effectively on bubble surfaces. For large particle sizes adhered on bubbles, Scheludko [1] derived a theoretical limit which scales as the inverse one-half power of gravity; an order of magnitude increase in particle sizes is predicted for each two-order magnitude reduction in effective gravity.

Three materials were used for sample tests: stainless steel cut wire shot (Pellets, Inc., Tonawanda, NY, 0.0584 cm), uncoated glass beads (Jaygo, Mahwah, NJ, 0.04 cm), and silica sand (Activa Products, Marshall, TX, > 0.035 cm). Volumes of the particulate suspension (50 ml) were foamed in a Plexiglass apparatus (Figure 1), consisting of a vertical-sided tube 12 cm long and 1.3 cm in diameter. A sidearm served as feed source for an air pump (max. 10 ml s^{-1}) and excess gas was vented from a raised exit port. Solids from the product stream (foamate) were sampled at the conclusion of a low-gravity batch run without introducing a foam-collapsing agent. All experiments were conducted using a foaming suspension of 50 ml DI water, 1 ml glycerine, and 5 ml Dawn brand liquid detergent. Each test was performed between 26-28 °C. The gas foaming rate was adjusted to the highest level which avoided liquid entrainment of feed material.

Foam fractionation of heavy particles has been obtained in low gravity. Results for large silica, glass, and steel pellets (> 0.2 mm), Table 1, show that by using minimally supporting froths, both mass transport and separation are possible. For single-pass batch separations in low gravity, concentration factors reached a three-fold (compared to a nine-fold theoretical limit and no separation in unit gravity, Figure 2). Better understanding of gravity effects is aimed toward splitting large particle sizes from low surfactant fluids; possible interest includes bubbling premium biologicals (whole cells, proteins, and viruses, etc.) from native solutions without surfactant addition or membrane disruption.

REFERENCES

Scheludko, A., B. V., Toshev, and D. T. Bojadjiev, "Attachment of Particles to a Liquid Surface," J. Chem. Soc. Faraday Trans., 172, 2815-2825 (1976).

PRECEDING PAGE BLANK NOT FILMED
PAGE 58 INTENTIONALLY BLANK

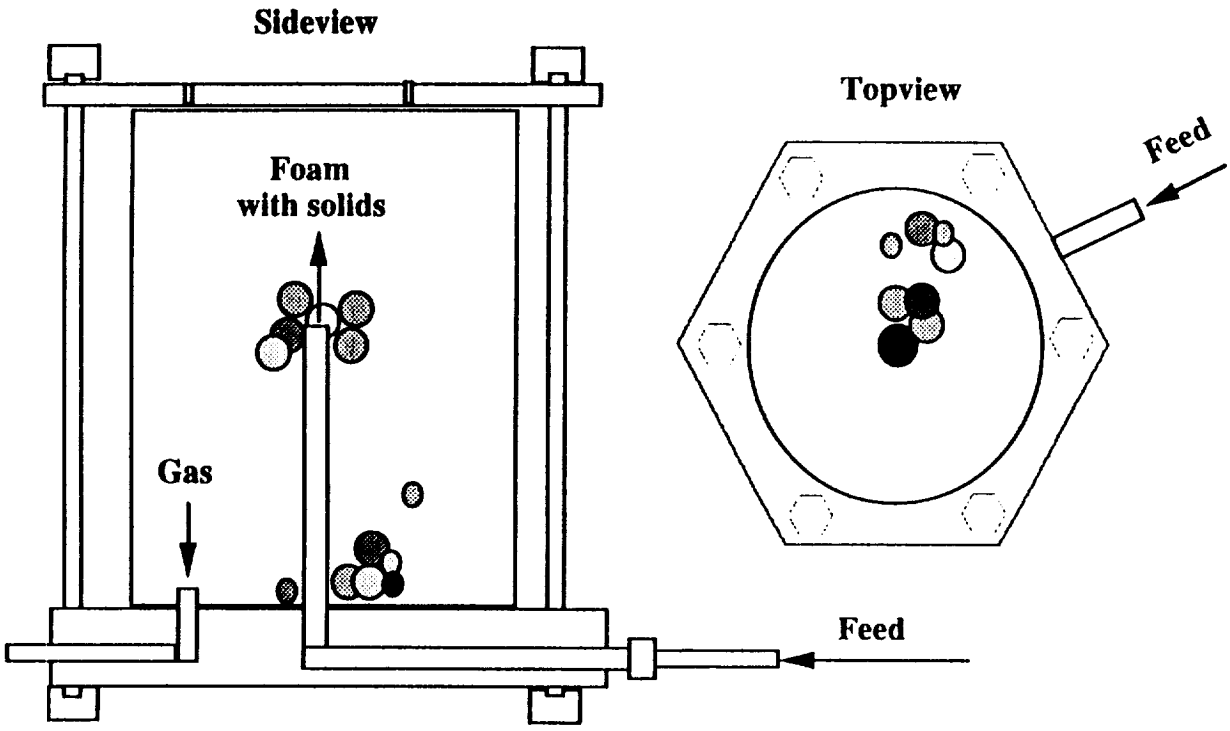

Figure 1. Schematic of foam fractionator, top and side view. Apparatus dimensions are described in text.

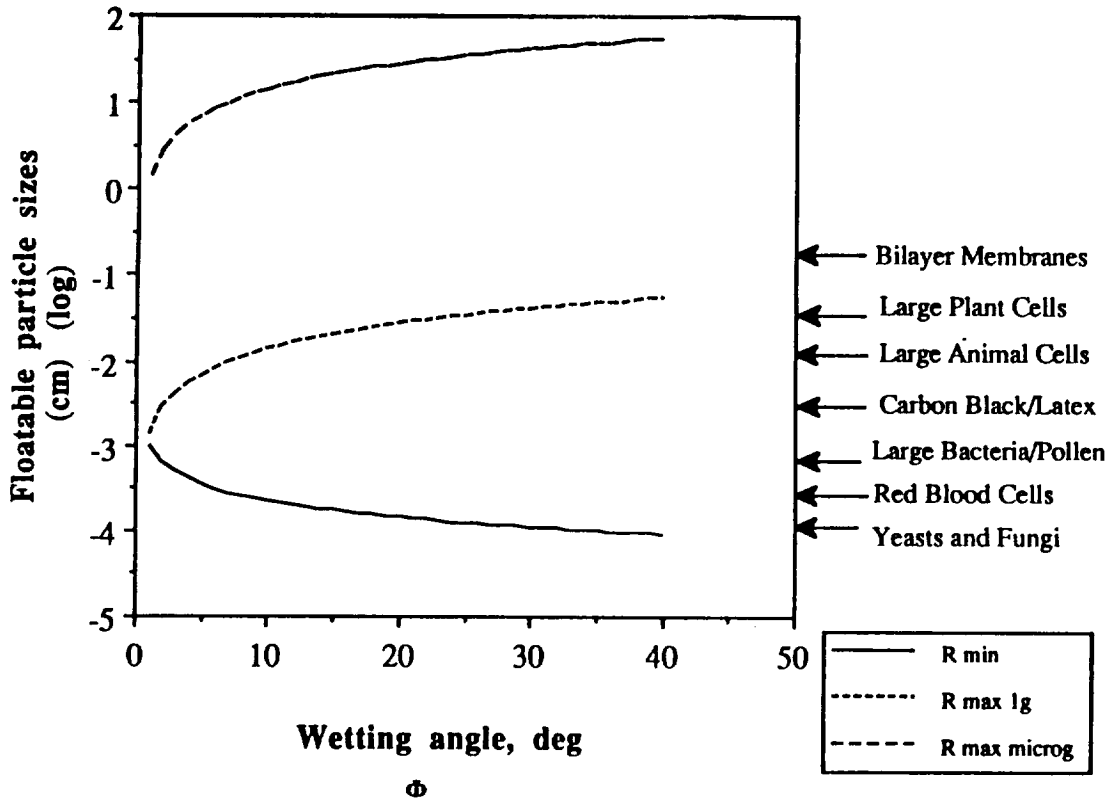

Figure 2. Theoretical upper and lower bounds on floatable particle sizes for different wetting angles. The top line corresponds to microgravity fract compared to the central dotted line for unit gravity fractionation. Typical particle sizes for biological materials are shown right.

Table 1. Concentration Factors and Recoveries of Particles by Foam Floatation at Room Temperatures

Material (g/ml density)	Gravity (980 cm/s^2)	Gas Volume (ml)	Foamate Volume (ml)	Particles in Foamate (g)	Concentration Factor	Percentage Recovery	Mean Bubble Diameter (cm)	Mean Particle per ml Foam (70% packing)	Particle Concentration Adsorbed ($part/cm^2$)
All	1	300	5	0	-1	0	0.8	0	0
Steel beads (4.59)	0.01	300	5.2	4.43	3.19	42	0.8	2×10^3	1.6×10^6
Glass beads (1.775)	0.01	300	5.2	2.35	1.11	21	0.8	0.95×10^3	0.76×10^6
Sand (1.705)	0.01	300	5.1	0.41	0.3	13	0.8	1.2×10^3	9.6×10^6

SMALL-OVER-LARGE FLUID INSTABILITY IN TWO-DIMENSIONAL SOAP FROTHS

Investigators: David A. Noever and
Raymond J. Cronise, NASA,
Marshall Space Flight Center,
Huntsville, AL

OBJECTIVE

Random networks of cellular patterns abound in nature. Examples include polycrystalline boundaries,[1] magnetic bubble domains,[2] acidic monolayers,[3] and biological membranes.[4] A striking universality among these networks has been identified; its basis derives not so much from any specific materials property, but more broadly from mathematical restrictions on completely filling n-dimensional space.[5-7]

The nature of bubble flow is studied as a novel fluid instability; bulk flow in this case is driven by the heavier fluid mass associated with smaller bubbles supported by larger bubbles, a "small-over-large" instability. Low gravity is used to prepare the otherwise inaccessible initial state of uniformly-wetted, but undrained soap cell borders. Subsequent high gravity is applied as a step function without otherwise disturbing the chamber (e.g., tilting). Bulk bubble flows are found to describe the lattice rearrangements and analogies are drawn to a "heavy-over-light" fluid Rayleigh-Taylor (R-T) instability.[8]

EXPERIMENTAL PROCEDURE

A rectangular Plexiglass chamber confined the soap froth (Figure 1). Inner dimensions were 14.5 x 19.5 x 0.32 cm^3; five fill ports provided direct access to the interior fluid and bubble lattice. In composition, the soap solution was similar to Glazier, et al.;[9] 5 ml of Dawn brand liquid detergent was added to 50 ml of deionized water and 0.2 ml blue food coloring. Like previous reports, froth dynamics did not depend on the exact recipe. The bubble lattice was formed using an annealing procedure. Prior to testing, 10 ml of solution was injected. The cell was tipped on edge, such that a fluid pool gave a corner reservoir for air bubble injection.

The chamber was initially placed horizontally in brackets and subsequently in low gravity given a perpendicular tip (Figure 2). This tipping procedure was found not to disturb the initial network nor the fluid distribution; low-gravity cell borders remained thick with soap solution. In this perpendicular position, the evolution of the bubble lattice was videotaped during successive steps between high, low, and unit gravity. Gravity-induced fluid drainage occurred perpendicularly to the cell borders. The random lattice was occasionally refreshed between parabolas by rapidly shaking the chamber. This gave a new initial network (with approximately the same cell dimensions as those blown with air directly). In all cases examined, the network showed a broad spread in both non-hexagonal cell sides and cell areas. These networks could properly be termed, disordered.[5,9]

RESULTS

When a heavy fluid is layered over a lighter fluid (e.g., water over oil), conditions are set for a classical instability, the (R-T) instability.[8] Small perturbations of the top, heavy fluid grow to form downstreaming fingers, such that the layers begin to exchange positions (if viscosity and surface tension effects do not dominate). In its simplest one-dimensional case, the instability's driving force is a vertically applied acceleration (e.g., gravity) and the relative density difference $[(\rho-\rho_o)/(\rho+\rho_o)]$ determines the evolution of both fluids.

Similar conditions for froth redistributions can be formulated in bubble lattices. Like a R-T mechanism, applied acceleration is the driving force, but flow is predicted even in an equal

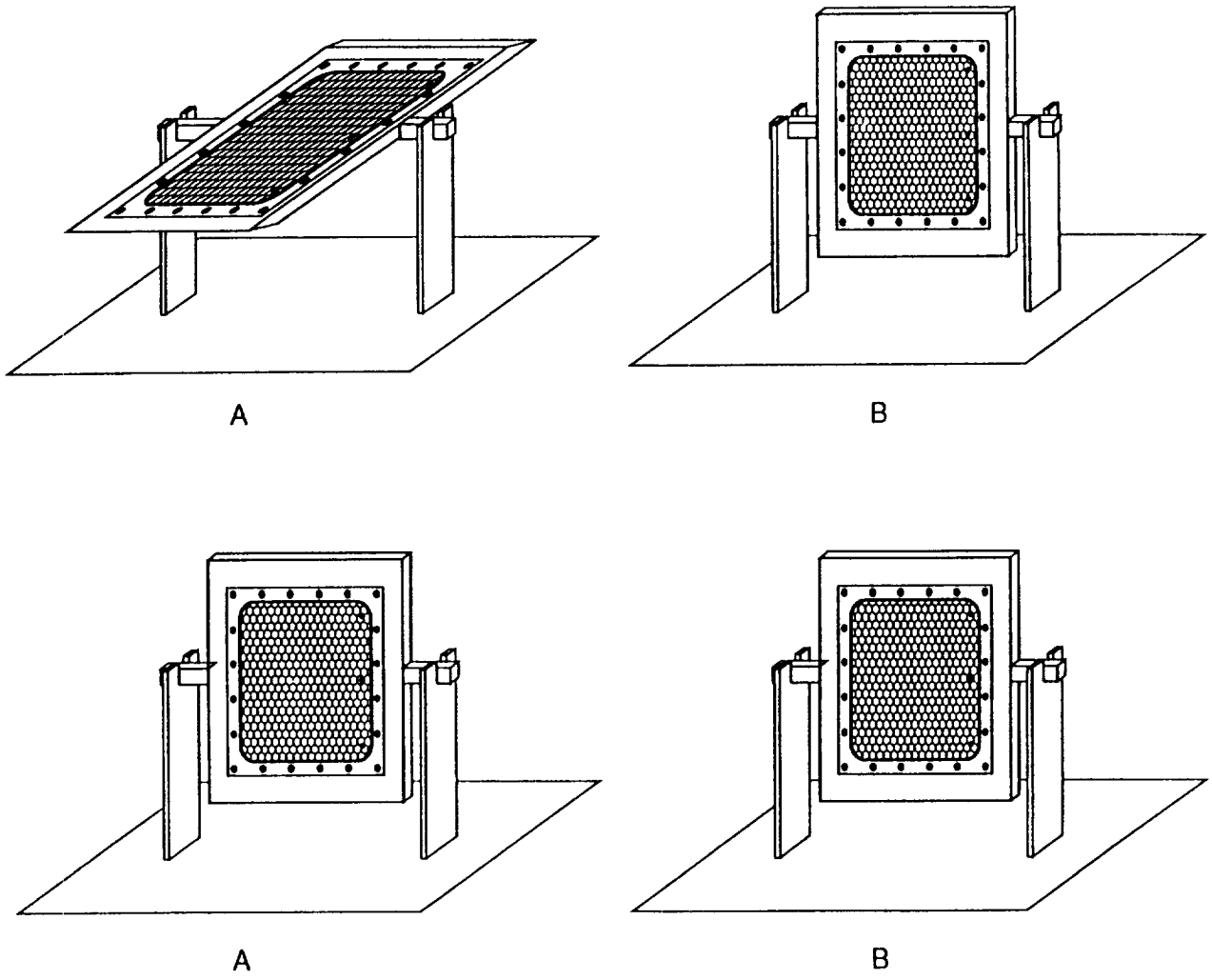

Figure 1. Apparatus orientation with respect to applied gravity force for (i) gravity drainage and (ii) capillary uptake. For the top series (i) of gravity drainage, step A corresponds to 1 g "horizontal" orientation before tipping in low gravity; step B corresponds to 2 g "vertical" orientation following reapplication of gravity. For the bottom series (ii) of capillary uptake, the orientation is always vertical with respect to applied gravity in step A in 1 g and step B in 10^{-2} g.

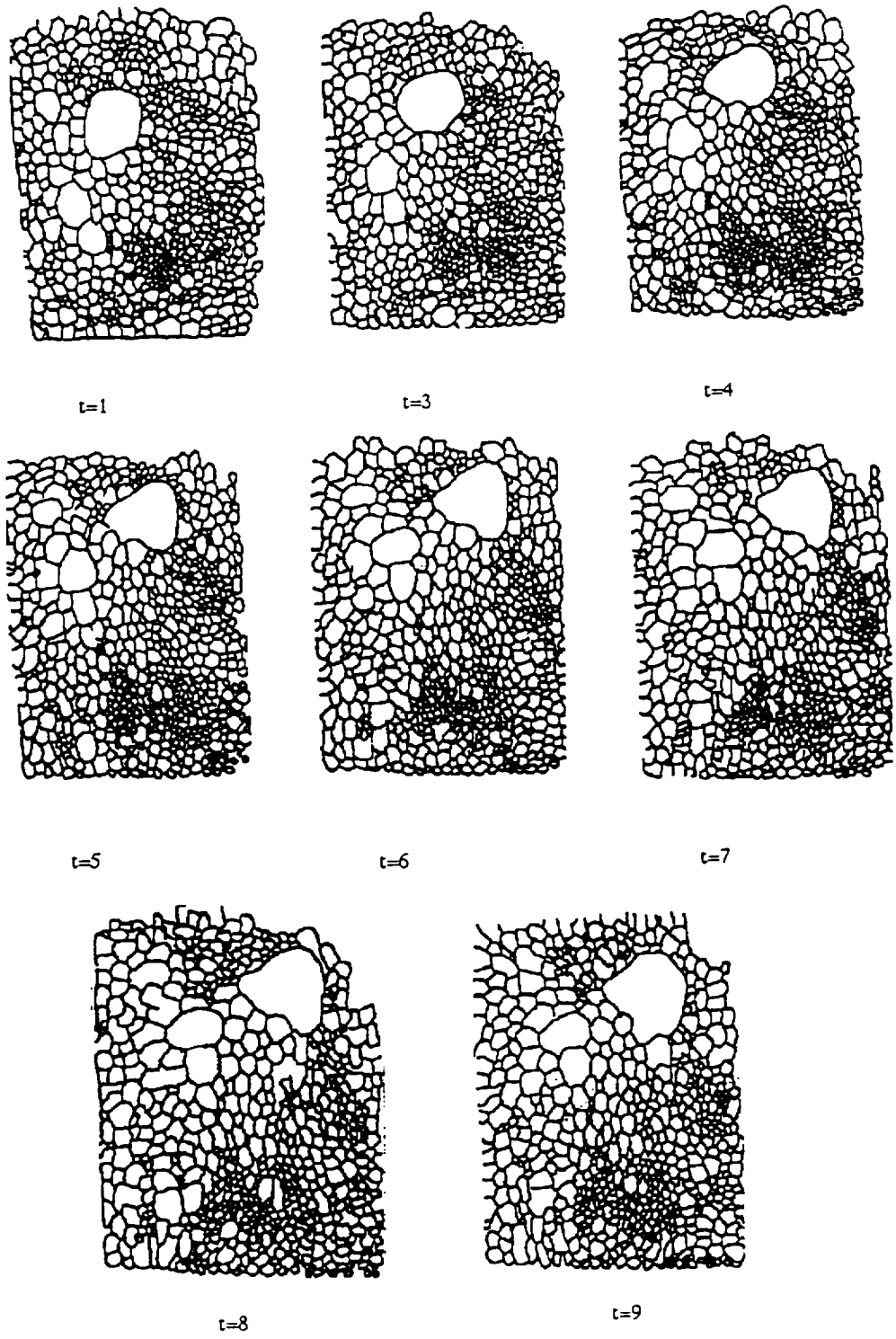

Figure 2. Digitized bubble lattices for different times (s). The bulk direction of bubble reorientation is clockwise, with the majority of smaller bubbles (with maximum perimeter to area ratios) settling to the bottom in high gravity.

density fluid. The key feature is bubble size. For a uniformly wetted lattice, areas occupied by smaller bubbles carry more net fluid than equivalent areas of larger bubbles. Hence regions of an accelerated lattice in which larger bubbles support smaller bubbles will tend to redistribute or turn over. The greater fluid mass on smaller wetted bubbles moves to a more stable, bottom configuration.

Rayleigh originally suggested such a technique to solve for the stability of a liquid cylinder.[10] Here we use a similar approach to quantify conditions for instability between two superposed and accelerated liquid masses which wet bubbles of different sizes.

The bubble lattice is modeled as two overlying fluid masses with effective densities (ρ,ρ_o) subjected to varying gravity (g) acting in a vertical (z) direction. The interface between the fluid masses is perturbed by a one-dimensional, infinitesimal disturbance. The arbitrary disturbance is expanded in a Fourier series, one term of which will be considered, η = a sin kx.

Then a "small-over-large" instability results for disturbances with wavenumber,

$$\frac{k}{k_o} < [\frac{<D_o>}{<D>} - 1]^{1/2}$$

As shown in Figure 3, the model predicts unstable wavenumbers k for infinitesimal perturbations as a function of bubble size ratio; $<D_o>/<D>$, $k_o = (\rho g/\sigma)^{1/2}$ is the unstable wavenumber[9] for an equivalent fluid of density ρ and surface tension α overlying a fluid of vanishing relative kinematic effect (e.g., vanishing viscosity and density). Region I includes the bubble configuration which is density-stable (large-over-small bubbles); region II includes a density-unstable bubble configuration (small-over-large), but which is stabilized by surface tension; and region III is unstable for all perturbations.

For experiments, the instability can be described by a modified form of the dimensionless Bond number, B_o,

$$B_o = \frac{\rho g \zeta^2}{\alpha} (\frac{<D_o>}{<D>} - 1)$$

For stability, this describes the relative importance of competing gravity and surface tension. Here, we treat the stability limit where ζ is the layer thickness of small bubbles overlying an infinite network of large bubbles. As shown in Figure 4, small (large) Bond numbers are stable (unstable). Negative Bond numbers correspond to regions which are density-stable (region I of Figure 3). The lower right inset to Figure 4 shows digitized experimental images of overturning random networks wherein small bubbles cascade over larger ones (see Figure 2). A similar effect may exist in large bubble columns which are misaligned with the vertical gravity. A 1° tilt leads to changes in fluid composition and channeling, akin to the overturning we observe.[11]

REFERENCES

1. Aboav, D. A., Metallography, 13, 43 (1980).
2. Babcock, K. L., R. Seshadri, R. M. Westervelt, Phys. Rev. A, 41, 1952 (1990).
3. Berge, B., A. J. Simon, and A. Libchaber, Phys. Rev. A, 41, 6893-6900 (1990).
4. Lewis, F. T., Amer. Scientist, 77, 358 (1945).
5. Weaire, D., and N. Rivier, Contemp. Phys., 25, 73 (1984).
6. Rivier, N., Philos. Mag., B52, 795 (1985).
7. Stine, K. J., S. A. Rauseo, B. G. Moore, J. A. Wise, and C. M. Knobler, Phys. Rev. A, 41, 6884 (1990).
8. Plesset, M. S. and C. G. Whipple, Phys. Fluids, 17, 1-7 (1974).
9. Glazier, J. A., S. P. Gross, nd J. Stavans, Phys. Rev. A, 36, 1-7 (1974).
10. Rayleigh, Lord, Proc. Roy. Soc. (London), A29, 71 (1879).
11. Valdes-Krieg, E., C. J. King, H. G. Sephton, AICHE J., 21, 400 (1975).

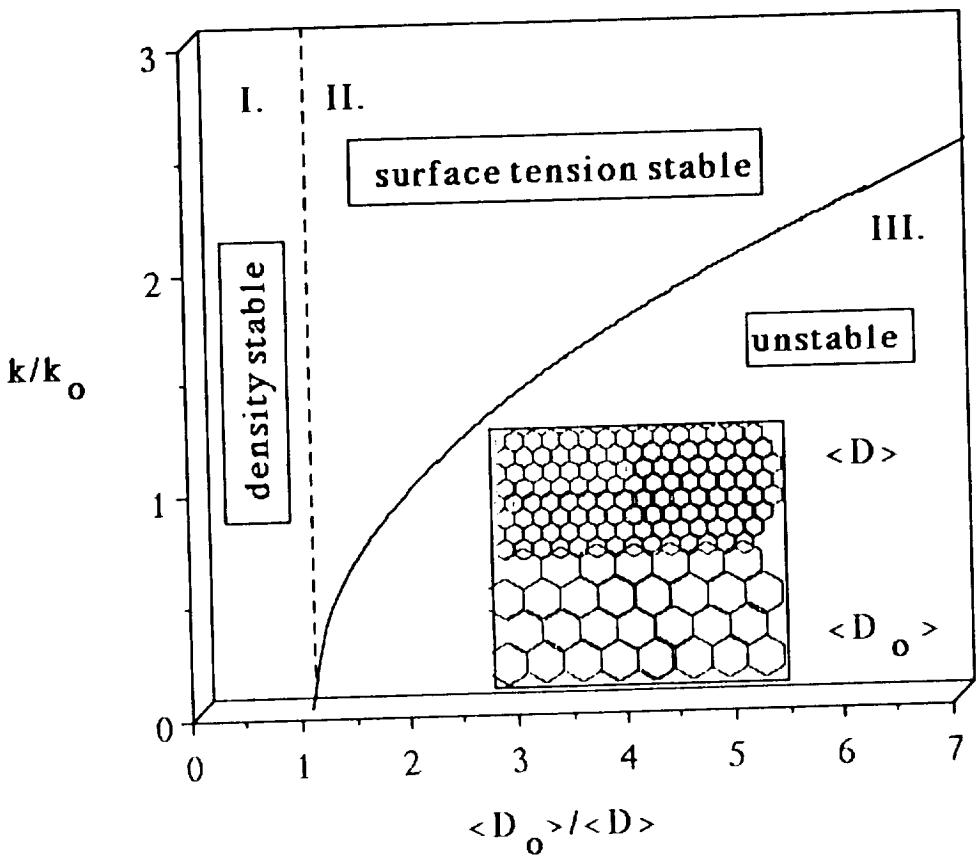

Figure 3. "Small-over-large" bubble instability. Model prediction for unstable wave-numbers k for infinitesimal perturbations as a function of bubble size ratio; $\langle D_o \rangle / \langle D \rangle$, $k_o = (\rho g/\alpha)^{1/2}$ is the unstable wavenumber for an equivalent fluid of density ρ and surface tension α overlying a fluid of vanishing relative density (ρ_o-->0).

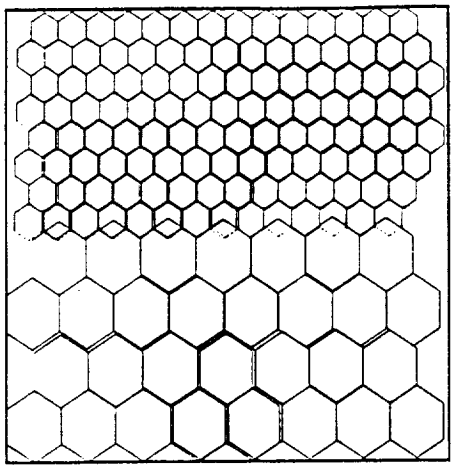

$B_o << 1$
Surface tension stable

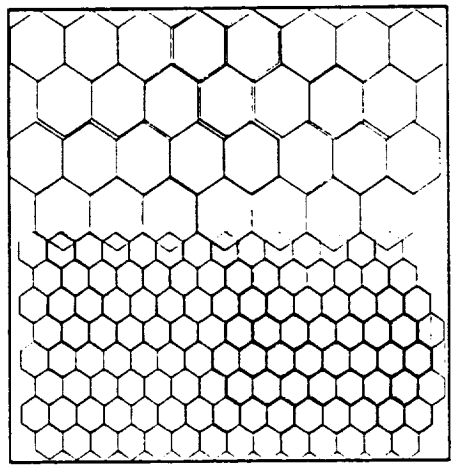

$B_o < O$
Density stable

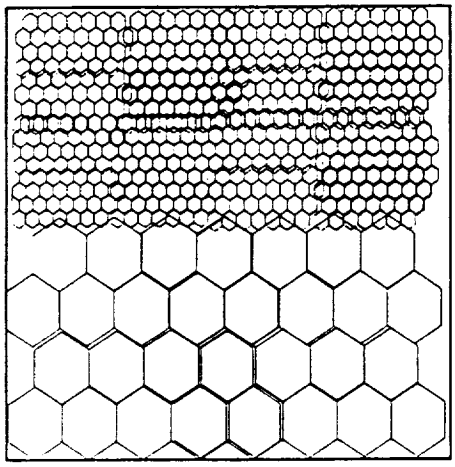

$B_o >> 1$
Gravitationally unstable

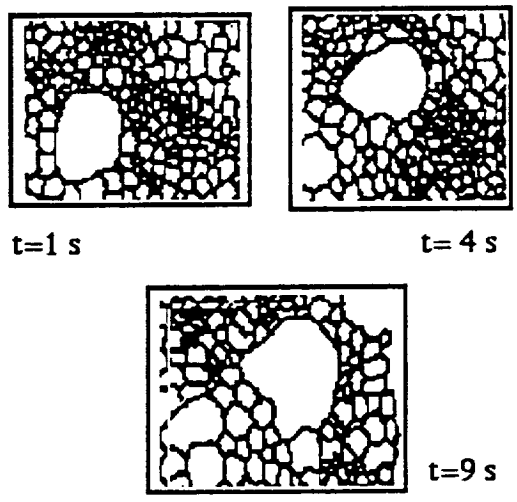

Experimental
Evidence

Figure 4. Cases for "small-over-large" bubble instability for varying Bond number. Inset lower right are experimentally digitized images of overturning bubble networks. The region of small bubbles layered on top of the large bubble tends to cascade downward when accelerated.

EFFECT OF NEAR ZERO GRAVITY ON THE FLUID-WALL BOUNDARY CONDITION FOR SILICONE OIL ON GLASS AND TEFLON

Investigator: Donald R. Pettit, Los Alamos National Laboratory, Los Alamos, NM

OBJECTIVE

The objective of this study is to measure the boundary condition between a moving wall and a viscous fluid as a function of gravity.

EXPERIMENTAL PROCEDURE AND RESULTS

The boundary condition was calculated from torque measurements required to rotate the inner cylinder of a concentric cylinder pair with silicone oil filling the annular gap and the outer cylinder fixed. The torque was continuously measured in the cyclic gravity environment aboard the NASA KC-135 airplane. The outer cylinder was a precision bore Pyrex tube with an internal diameter of 28.994±0.010 mm and was 115 mm long. Two inner cylinders were used; one made from precision bore Pyrex with an outside diameter of 25.440±0.010 mm and the other made from centerless ground Teflon with an outside diameter of 25.400±0.025 mm. Both inner cylinders were 114.3 mm long. A Brookfield torque meter model RVT, with a linear scale from 0 to 7187 dyne-cm and an accuracy of ±1% of full scale, was used. Silicone oil viscosity standards with viscosity of 47.8 and 95.8 mPa-s at 25 °C were used. The inner cylinders were supported by magnetic bearings and made to be neutrally buoyant in the silicone oil, thus preventing bearing load changes during the cyclic gravity.

Results showed no significant changes in torque for shear rates of 10, 20, and 50 rpm for both viscosities of silicone oil and both cylinders of glass and Teflon for gravity levels varying from about 0.01 g (low gravity phase of flight) to 1.8 g (high gravity phase of flight). The conclusion is drawn that the no-slip boundary condition is valid for near zero gravity fluid apparatus that involve silicone oil wetting glass and Teflon.

ELECTRODEPOSITION OF NICKEL FROM AN AQUEOUS SOLUTION IN LOW GRAVITY

Investigators: C. Riley, B. Benson, and H. Abi-Akar, Dept. of Chemistry, The University of Alabama in Huntsville, Huntsville, AL; George Maybee, McDonnell Douglas Corporation, Huntsville, AL

OBJECTIVES

It has been reported that electrodeposition in low gravity produces deposits that have differences relative to those produced in 1 g. Ehrhardt[1,2] found that nickel deposited at a high rate under low gravity over a 6-min period during a suborbital rocket flight had some peculiar properties that were indicative of an amorphous form. A major reason for the present work is to attempt to reproduce Ehrhardt's results in the low-gravity trajectories produced on a KC-135 aircraft.

EXPERIMENTAL PROCEDURE AND RESULTS

Figure 1 shows the simple apparatus constructed for this study. It consisted of eight 1.5-V batteries, and off/on switch, relay, and a plug-in board for electrodepsoition cells at voltages of 1.5 V, 3 V, 4.5 V, 6 V, and 12 V. The two battery boxes are evident. From right to left in front are the switch, relay, and plug-in board for the cells. Three cells are shown mounted on the board. The entire apparatus which is ~24 x 10 in. was secured by tape to the padded floor of the aircraft during flight. The cells have been described previously.[3-5] Since we were restricted to 20-25 s of low gravity on each parabola, multiple electrodepositions were carried out until 5.5 min of plating time was accummulated, which was comparable to that produced on a sounding rocket. Ehrhardt[1,2] used only one cell during each mission and deposited at a rate of approximately 80 mA/cm^2. Since this high rate of electrodeposition could affect the crystalline form (or lack of) a method varying the electrodepsotion rate was required. The different voltages supply this variation with the 12-V deposiiton, for example, corresponding to a cell current of approximately 300 mA/cm^2.

Figure 1. KC-135 electrodeposition apparatus.

Figure 2 shows a reproduction of x-ray diffraction spectra from nickel deposited in 1 g (top) and low gravity (bottom) in experiments by Ehrhardt.[2] Except for the lack of gravity, the experimental conditions were reported to be the same. The upper spectrum for 1 g, showing intensity vs. detector angle, has the typical fcc structural planes for crystalline nickel. In the lower spectrum, the peaks corresponding to those planes are gone or weak. It was interpreted as having a low-gravity deposit as nearly clear or invisible to the x-rays and thus mostly amorphous in nature. Figure 3 shows the x-ray diffraction spectrum of nickel electrodeposited on a gold-coated copper plate. The deposition was carried out in the low-gravity environment produced on a KC-135 aircraft. The plating potential was 6 V; the plating time was approximately 5.5 min. Accumulations from multiple 20-25 s low-gravity parabolas were utilized to give the total electrodeposition time, which is comparable to that utilized by Ehrhardt. The peaks corresponding to the face-centered curbic (fcc) nickel crystal line

PRECEDING PAGE BLANK NOT FILMED

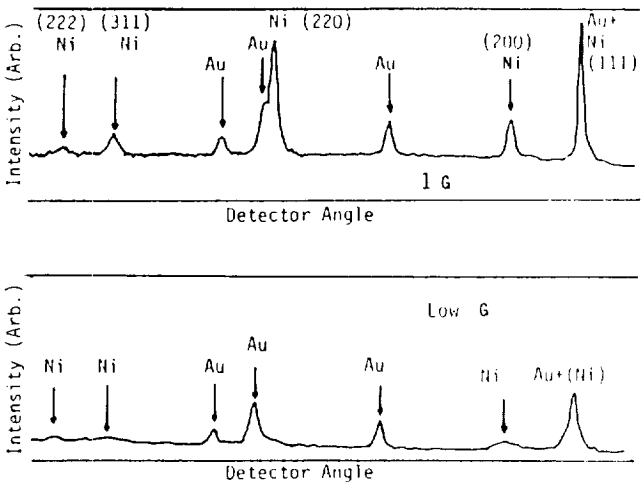

Figure 2. X-ray diffraction spectra of Ni determined by Ehrhardt.

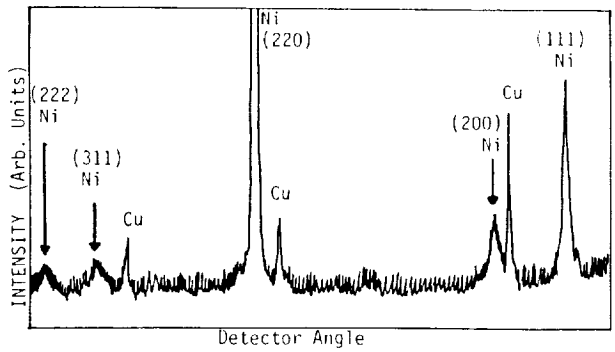

Figure 3. X-ray diffraction spectrum of Ni deposited on KC-135.

REFERENCES

1. Ehrhardt, J., "Versuche zur electrolytishem Metallabscheidung under Schwerelosigheit *Galvanotechnik*," D, 7968 Sauligan 72, NO., pp. 13-18 (1981).
2. Ehrhardt, J., "Dispersion Electrolysis Under Zero Gravity Under the SPACELAB Rocket Program TEXUS IV," Battelle Institute, BMFT Reference No. QV 219-AK-AN/A-ALN7910-5, April 1982; TEXUS VII, BMFT Reference No. 01QV219-AK-AM/A-SLN7910-5, November 1983; and TEXUS IX, BMFT Reference No. 01 QV014-AK/SN, November 1984.
3. Riley, C., H. D. Coble, and G. Maybee, Electrodeposition of Metal/Cemet Composites in Low Gravity," AIAA Paper 87-0510, January 1987.
4. Riley, C., H. Abi-Akar, B. Benson, and G. Maybee, "Low-Gravity Electrodeposition of Metals and Metal/Composites," Journal of Spacecraft and Rockets, 27(4), 386-398 (1990).
5. Riley, C., H. Abi-Akar, B. Benson, and G. Maybee, "Electrodeposition of Metals and Metal/Cermet of Composites on a Sub-Orbital Rocket," AIAA Paper 89-0308, January 1989.

THE KIRKENDALL EFFECT IN BINARY GAS DIFFUSION

Investigators: William Witherow, David A. Noever, and Raymond J. Cronise, NASA, Marshall Space Flight Center, Huntsville, AL

OBJECTIVES

The Kirkendall effect is a bulk, piston-like convective motion directed from heavier toward lighter fluids. Its bearing on nearly all diffusion-limited crystal growth experiments has been noted. Terrestrial studies have been unable to verify its existence previously, because of gravity-driven sedimentation of the tracer particles used to visualize the boundary.

As a lighter gas diffuses rapidly into a heavier gas, the resulting pressure increase causes returning bulk flow. This flow can be observed directly by photographing entrained smoke particles as they move with the diffusion boundary. Unit gravity experiments using this arrangement have been unable to quantify the Kirkendall effect in a fashion consistent with theory (several hundred percent error). Since the diffusion boundary consists of variously sized smoke particles, it does not move as a thin layer; instead, heavier particles settle rapidly under gravity. Some particles even fall at once into the lower cylinder and form a faint cloud. The only experimental way around this is to track the movement of fine particles at the top of the cloud boundary. However, even this method does not give the correct theoretical dependence of the boundary motion (on the square root of time). Attempts to correct for smoke settling have failed. When measured at the end of the experiment, the rate of sedimentation is too large (since coarsening has increased compared to early stages of the diffusion experiment). Hence, by substantially reducing sedimentation of tracer particles, low gravity should yield a quantitative existence test of a fluid Kirkendall effect.

EXPERIMENTAL PROCEDURE

The apparatus consists of two glass cylinders (4 in. diameter, 7 in. length) sealed with circular steel plates dividing two gases. By sliding one plate over the other, flow pores are opened and the two gas components meet to form a diffusional boundary. To give widely different diffusion rates, the two gases are helium and CF_2Cl_2, in proportion $D[He]/D[CF_2Cl_2] = 32.5$. As a marker, finely divided particles of ammonium chloride salt would be formed by reaction at the diffusion boundary. This salt is produced by adding 1% HCl(g) to CF_2Cl_2 in the lower cylinder and 1% NH_3(g) to He in the upper cylinder. The diffusion front will travel the length of the upper cylinder (7 in.) in 200 sec.

The apparatus is loaded with the gases on the ground before flight and the experiment is initiated upon entry into low g by manually opening the sliding plates separating the two gases. Photography using both still and video will document the diffusion movement for later analysis.

RESULTS

Theoretical results include prediction of diffusion boundary velocities for various gas mixtures and geometries. In particular, a third, non-diffusion component cannot only alter the magnitude, but also the diffusive direction from light to heavy.

REFERENCES

3-M Space Research Center, Minneapolis, MN, "Applying Momentum Boundary Conditions to Binary Gases" (1989).

Center for Microgravity and Materials Research, The University of Alabama, Huntsville, "Boundary Effects and Low Pressure Microgravity Experiments" (1989).

Noever, D. A., "A Note on the No-Slip Boundary Condition Applied to Diffusing Gases," Phys. Lett. A, 144, 253-255 (1990).

Noever, D. A., "The Baroeffect and an Appropriate Momentum Boundary Condition," Physics of Fluids A: Fluid Dynamics, 2, 863-865 (1990).

Noever, D. A., "Ternary Baroeffect with a Nondiffusing Component," Phys. Rev. Lett., 65, 1587-1590 (1990).

Noever, D. A., "Diffusive Slip and Surface Transport Properties," J. Coll. Interfac. Sci., 147(1), 186-191 (1991).

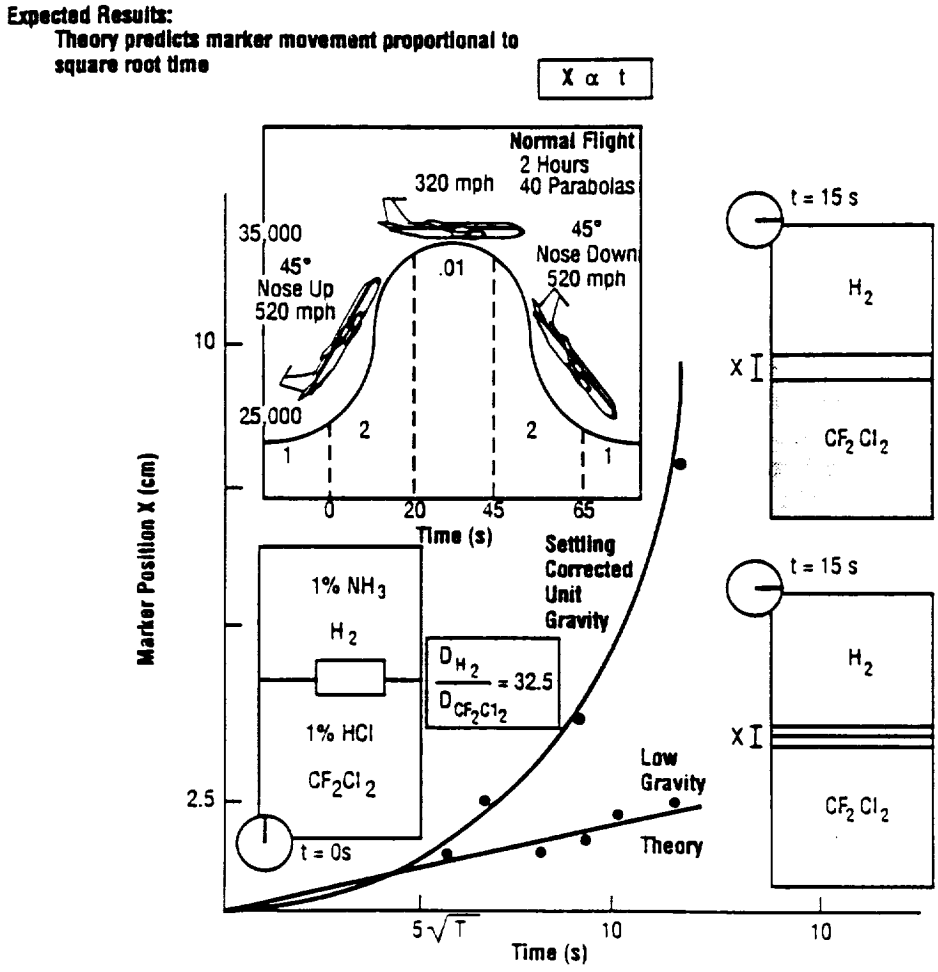

Figure 1. KC-135 experiment.

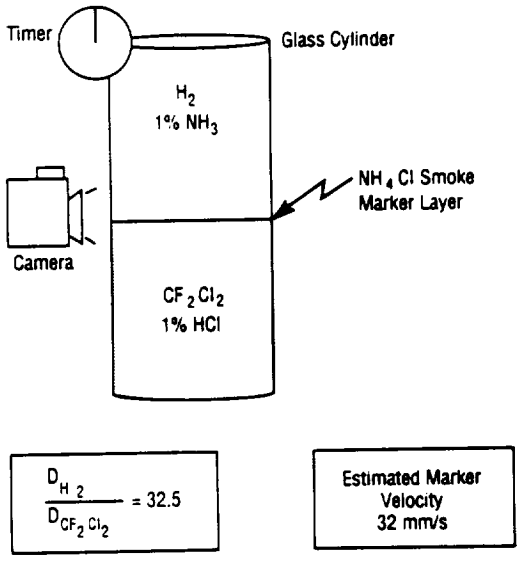

Figure 2. How to define a moving fluid boundary.

4. THERMODYNAMICS AND COMBUSTION

PRECEDING PAGE BLANK NOT FILMED

TRANSIENT HEAT TRANSFER STUDIES IN LOW GRAVITY USING OPTICAL MEASUREMENT TECHNIQUES

Investigators: Patricia J. Giarratano and Vincent D. Arp, National Institute of Standards and Technology, Boulder, CO; A. Kumakawa, Chemical Engineering Science Division, National Aerospace Laboratory, Miyagi, Japan; and Robert B. Owen, Optical Research Institute, Boulder, CO

OBJECTIVES

The objectives of this study are to investigate thermally induced motion and temperature fields in a compressible fluid during a transient heat input from a heater surface in the fluid, and to employ a non-intrusive optical technique to measure the temperature profiles in the fluid adjacent to the heater.

EXPERIMENTAL PROCEDURE AND RESULTS

A test cell with windows contained Refrigerant 13 test fluid near its thermodynamic critical point. A titanium metal strip, located in the fluid and in the view of the windows, served as a heater surface and thermometer. In the experiments, the heater was subjected to an electrical current pulse during which its electrical resistance was recorded as a function of time. From these measurements, both the heat flux and surface temperature were obtained. Simultaneously, holographic interferometry with diffuse light source was employed to measure the temperature field in the fluid adjacent to the heater surface (where steep thermal gradients occur). The experimental temperature measurements obtained during low-g experiments on the KC-135 were compared with predictions from a mathematical model which included heat transfer induced motion but not gravity-driven motion. The measurements were also compared with those obtained in the laboratory at 1 g.

Due to a limited number of test runs in low g, the holographic measurements were not highly refined and quantitative evaluation of fringe patterns was not possible. However, we were satisfied that the holographic optical technique could be further optimized to obtain the desired results. The electrical measurements of surface temperature substantiated the prediction of the surface temperature from the mathematical model.

A complete description of the experiment and results is published in the reference below.

REFERENCE

Giarratano, P. J., A. Kumakawa, V. D. Arp, and R. B. Owen, "Transient Heat-Transfer Studies in Low-Gravity Using Optical Measurement Techniques," J. of Thermophysics and Heat Transfer, 4(1), 53-58 (1990).

PRECEDING PAGE BLANK NOT FILMED

DYNAMIC THERMOPHYSICAL MEASUREMENTS IN MICROGRAVITY

Investigators: A. Cezairliyan and A. P. Miiller,
Thermophysics Division,
National Institute of Standards and Technology, Gaithersburg, MD

OBJECTIVES

The objectives of this study are to investigate main objective of the proposed research is to develop accurate millisecond-resolution dynamic techniques which, in a microgravity environment, will enable the performance of thermophysical measurements on high-melting-point electrically-conducting solids and liquids at temperatures above 1500 °K. When completed the techniques will, for the first time, extend the limit (melting point) of the highly successful ground-based millisecond-resolution pulse-heating experiments. Thermophysical properties of interest include heat of fusion, heat capacity, electrical resistivity, thermal conductivity, surface tension, hemispherical total, and normal spectral emissivities.

EXPERIMENTAL PROCEDURE AND RESULTS

The basic experimental technique involves resistively heating the specimen in a microgravity environment from room temperature up to its melting point and above in approximately 1 sec by passing a large current pulse through it, and simultaneously recording the pertinent experimental quantities with millisecond resolution. The compact pulse-heating system (Figure 1), designed for microgravity simulations with the KC-135 aircraft, utilizes two major diagnostic instruments: a high-speed pyrometer for measuring the specimen temperature and a high-speed framing camera for recording the specimen behavior during rapid melting. Experiments were performed during eight series of flights, yielding valuable information regarding the parameters affecting speciman stability above the melting point.

As a natural extension of the work on specimen stability, a novel technique for measuring surface tension of liquid metals at high temperatures in a microgravity environment was successfully demonstrated. The specimen geometry involves a tubular specimen mounted in a triaxial configuration (Figure 2) in which a fraction of the heating current "i" is returned along the tube axis. Adjustments to the current split "f" enable a balance between magnetic and surface tension forces acting on the molten specimen. Values for surface tension are determined from measurements of the equilibrium dimensions of the melt zone and the magnitudes of the currents.

The specimens were fabricated from 99.99% pure copper tube stock and had the following nominal dimensions: thickness, 0.1 mm; diameter, 6 mm; lenght between electrodes, 25 mm. Each specimen was mechanically treated to remove surface oxides and then mounted in an experiment chamber (in argon at ~0.2 MPa) prior to the KC-135 flight experiments. Depending on the experiment, the duration of the heating period varied between about 0.5 and 2 sec. The magnitude of the current pulse used to melt the specimen ranged from approximately 700 to 1100 Å, yielding heating rates in the range 500 to 2000 $K \cdot s^{-1}$.

In a typical experiment, the specimen tube softened after an initial period during melting and its melt zone radius changed from R_o (at the onset of melting) to an equilibrium value R_E, indicating that a balance between magnetic and surface tension forces had been achieved. The surface tension of copper at its melting point was successfully determined in eight microgravity experiments (Figure 3) corresponding to values of R_E/R_o in the range from 0.99 to 1.07 and current split "f" in the range 0.77 and 1.0. The results yielded an average

80

PRECEDING PAGE BLANK NOT FILMED

value of 1.27 $N \cdot m^{-1}$ which is in reasonably good agreement with literature data.

Preliminary microgravity experiments were also performed on tantalum specimens to provide baseline data for future definitive measurements of the surface tension of high-melting-point refractory metals for which there is a paucity of data. Changes in the design and construction of the measurement system are underway to improve the accuracy of the surface tension measurements and to enable the development of techniques for measuring other thermophysical properties (listed under objectives) of metals in their liquid phase.

REFERENCES

Cezairliyan, A. and A. P. Miiller, "A Dynamic Technique for Thermophysical Measurements at High Temperatures in a Microgravity Environment," Int. J. Thermophysics, 11, 653-662 (1990).

Miiller, A. P. and A. Cezairliyan, "A Dynamic Technique for Measuring Surface Tension at High Temperatures in a Microgravity Environment," Int. J. Thermophysics, 11, 663-674 (1990).

MacDonald, R. A., "The Stability of a Current Carrying Hollow Liquid Metal Cylinder," J. Appl. Phys., 66, 5302-5308 (1989).

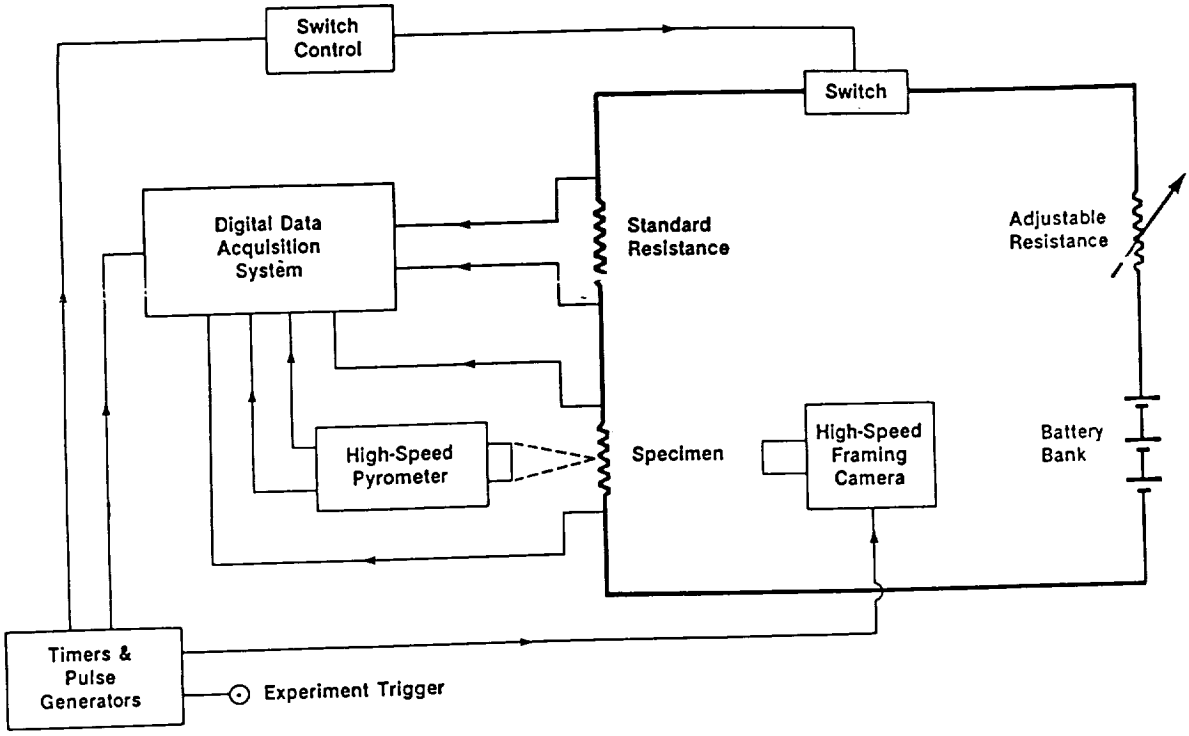

Figure 1. Functional diagram of a compact pulse-heating system designed for rapid-melting experiments during microgravity simulations with the KC-135 aircraft.

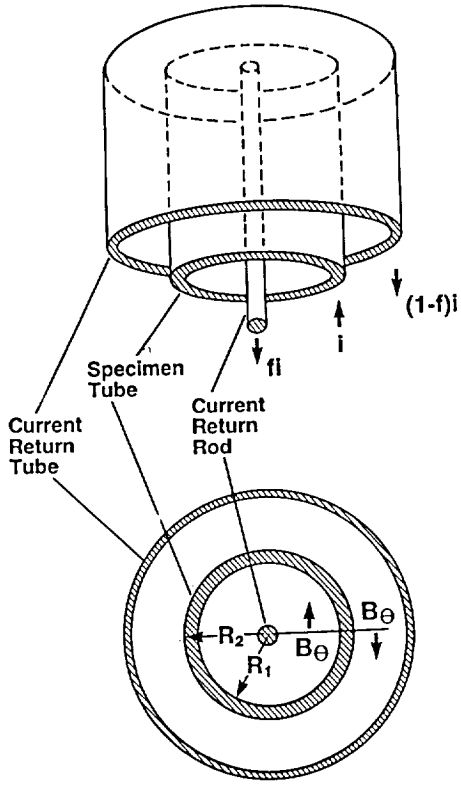

Figure 2. A schematic diagram of the triaxial configuration in which a tubular specimen is mounted concentrically with respect to the current return paths. During melting, the (inward) pressure due to surface tension may be counter-balanced by selecting a suitable return current split f to provide a net (outward) magnetic pressure.

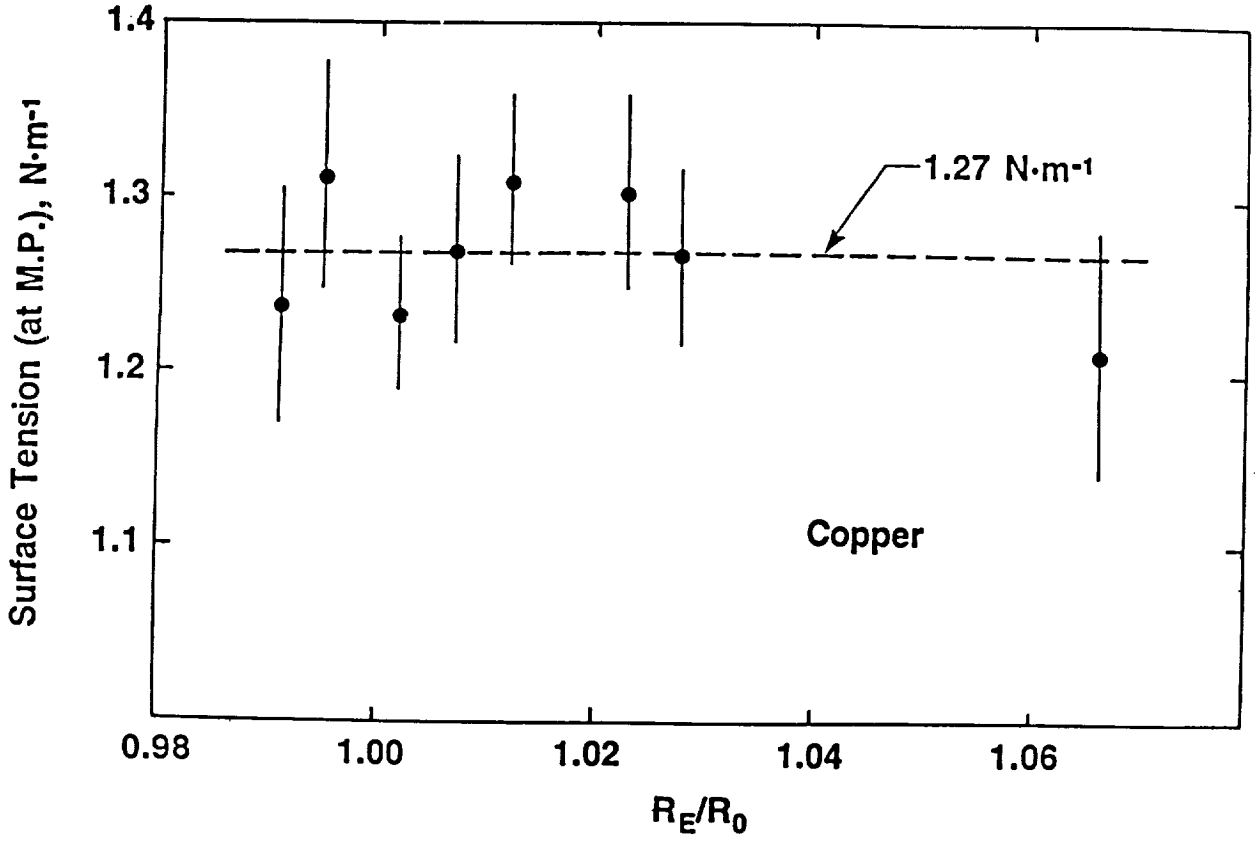

Figure 3. Results from eight microgravity experiments for surface tension of copper (at its melting point) as determined from measurements of the equilibrium dimensions of the molten tube and the magnitudes of the currents.

PREMIXED GAS COMBUSTION AT REDUCED GRAVITY

Investigator: Paul D. Ronney, Department of Mechanical and Aerospace Engineering, Princeton University, Princeton, NJ

OBJECTIVES

In previoius work in drop towers, we had discovered that in lean hydrogen-air mixtures near flammability limits, cellular flame fronts resulting from diffusive-thermal instabilities could evolve into spherical, apparently stationary "flame balls" (Figure 1). Because of the short time of microgravity available in drop towers, it could not be conclusively determined whether such structures were indeed stable, or would extinguish or evolve slowly to some other structure. Two distinct sizes of flame balls were observed (Figure 2); however, theory predicted that only the larger balls should be stable (Figure 3). Also, because pure hydrogen-air flames are invisible, and because only film cameras could be used in drop towers (due to impact loads), a "coloring agent" (CF_3Br) had to be added to all test mixtures. The impact of this coloring agent was unknown. Hence, the objectives of the KC-135A tests were to determine the long-term stability and morphology of all sizes of flame balls, and to determine the effects of the coloring agent on the observed behavior.

EXPERIMENTAL PROCEDURE

A cylindrical chamber of 25 cm diameter and 25 cm length (Figure 4) is filled with premixed, weakly combustible gas. The mixture is ignited with an electric spark. A 16 mm film camera is used in the drop tests to visualize the flame. An infrared-sensitive video camera is added for the aircraft experiments, enabling a comparison of flames with and without the coloring agent. In addition to flame imaging, gas temperature, pressure, and composition measurements are taken.

RESULTS

Three weeks of KC-135A flight tests have been conducted. We have found that (1) "flame balls" do indeed exhibit long-term stability, (2) the behavior is qualitatively similar with or without the coloring agent, (3) the "g-jitter" present in the aircraft tests (but not the drop tests) led to the formation of a new type of flame structure consisting of elongated cylinder-like elements of flame (Figure 5), and (4) the effects of dilution, Lewis number, and pressure on these phenomena are in accord with recently developed analytical models. These models indicate the critical role of the interactions of differential diffusion of heat and reactants, flame front curvature, and heat losses due to radiation from the gaseous combusion products.

Our current plans include studying the effects of radiative heat loss and re-absorption using gas mixtures seeded with inert, radiating particles. At small particle loadings it is expected that heat loss will be increased, leading to greater instability and narrower ranges of flammability mixtures, whereas at high particle loadings it is expected that much of the emitted radiation will be re-absorbed by other particles, leading to less instability. Furthermore, we intend to study the effects of stoichiometry in two-reactant flames, as theory predicts the effects of stoichiometry are quite different for "flame balls" and conventional propagating flames.

REFERENCES

Buckmaster, J. D., G. Joulin, and P. D. Ronney, "Structure and Stability of Non-Adiabatic Flame Balls: II. Effects of Far-Field Losses," Combustion and Flame, 84, 411-422 (1991).

Abbud-Madrid, A. and P. D. Ronney, "Effects of Radiative and Diffusive Transport on Premixed Flames Near Flammability Limits," in Twenty-Third Symposium (International) on Combustion

tion Institute, pp. 423-431 (1990).

Farmer, J. N. and P. D. Ronney, "A Numerical Study of Unsteady Nonadiabatic Flames," Combustion Science and Technology, 73, 555-574 (1990).

Ronney, P. D., "Near-Limit Flame Structures at Low Lewis Number," Combustion and Flame, 82, 1-14 (1990).

Buckmaster, J. D., G. Joulin, and P. D. Ronney., "Effects of Heat Loss on the Structure and Stability of Flame Balls," Combustion and Flame, 79, 381-392 (1990).

Whaling, K. N., A. Abbud-Madrid, and P. D. Ronney, "Structure and Stability of Near-Limit Flames with Low Lewis Number," Fall Technical Meeting, Combustion Institute, Western States Section, October 15-16, La Jolla, CA (1990).

Ronney, P. D. and G. I. Sivashinsky, "A Theoretical Study of Propagation and Extinction of Nonsteady Spherical Flame Fronts," SIAM J. Appl. Math., 49, 1029-1046 (1989).

Ronney, P. D., "On the Mechanism of Flame Propagation Limits and Extinction Processes at Microgravity," in Twenty-Second Symposium (International) on Combustion, Combustion Institute, pp. 1615-1623 (1988).

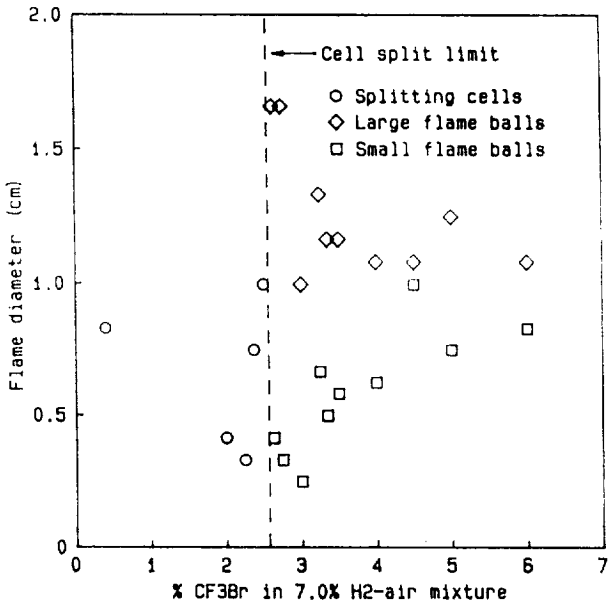

Figure 2. Size of flame balls as a function of gas composition showing two distinct sizes of balls.

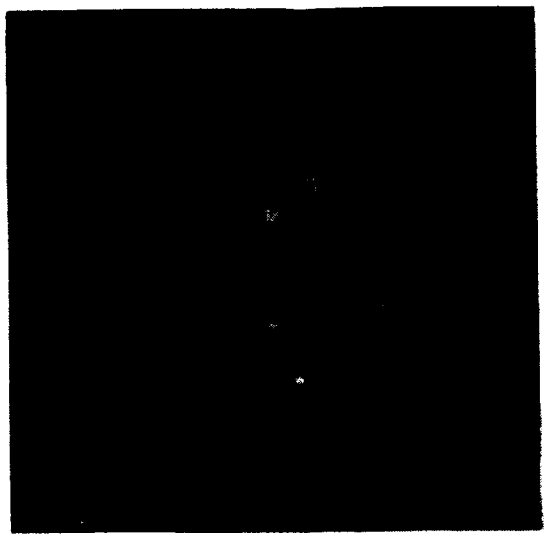

Figure 1. Direct photograph of "flame balls" at microgravity.

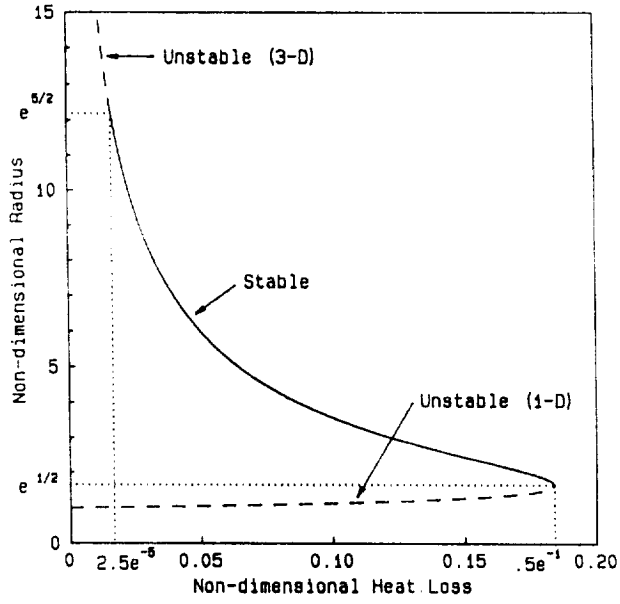

Figure 3. Theoretical prediction of flame ball sizes and stability limits in the presence of heat losses.

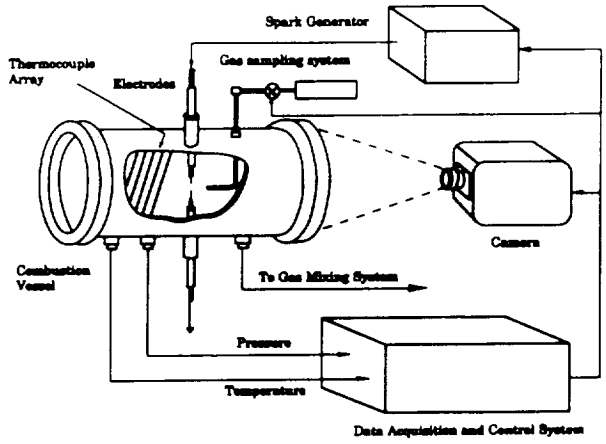

Figure 4. Experimental apparatus block diagram.

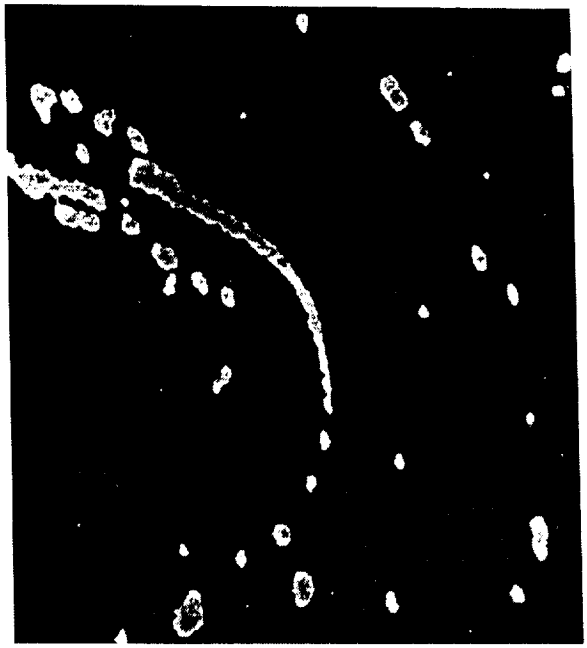

Figure 5. Infrared image of a "flame cylinder" resulting from g-jitter in KC-135A aircraft.

5. CONTAINERLESS PROCESSING

PRECEDING PAGE BLANK NOT FILMED

INTENTIONALLY BLANK

CONTAINERLESS PROCESSING OF BEAM HEATED SAMPLES USING ACOUSTIC LEVITATION

Investigators: Charles A. Rey and Dennis R. Merkley, Intersonics, Inc., North Beach, PA; Edwin C. Ethridge, Space Science Laboratory, NASA, Marshall Space Flight Center, Huntsville, AL

OBJECTIVES

The objective of the High Temperature Acoustic Levitator (HAL) KC-135 testing was to demonstrate the capability of positioning beam heated samples in low gravity using acoustic forces. Results of these experiments would demonstrate the feasibility of using this technique for high temperature containerless materials processing in low gravity.

EQUIPMENT DESCRIPTION AND PROCEDURE

HAL is a three-axis acoustic levitator designed to position solid or liquid samples of 2 to 5 mm nominal diameter at high temperatures. It incorporates sample position detectors which are used in a feedback system to enhance sample positioning stability and, in this work, to provide sample position data for evaluation of positioning performance. The levitator also provides manually-operated control of specimen spin and position.

The HAL is also equipped with three, 1 kW xenon arc lamps for sample heating, an optical pyrometer, two video cameras, and an automated sample injection and retrieval system.

During flight operations, samples were released into the acoustic positioning zone immediately following the transition into low gravity. Tests were performed to establish the effects of sample heating, the effectiveness of the spin and position control, the ability to position samples of various densities, and the effects of acoustic amplitude on the positioning capabilities.

RESULTS

The feasibility of acoustic positioning combined with beam heating has been demonstrated in a low-gravity environment aboard the KC-135. Experiments with and without heating were performed on various samples ranging in density from ≈ 0.1 gm/cm^3 to 22 gm/cm^3. Aluminum was melted and ceramic samples were heated to ≈ 1400 °C. Positioning capabilities were established for a variety of operating conditions, and the effect of feedback control on positioning was demonstrated.

Ground-based experiments have included the successful positioning and melting of liquid aluminum oxide at temperatures up to 2700 °K. This suggests that levitation with the HAL is not limited by specimen temperature.

REFERENCES

Rey, Charles A., et al., "Acoustic Levitation Materials Processing Systems," 17th Aerospace Sciences Meeting, AIAA, New Orleans (1979).

Rey, C. A., T. J. Danley, D. R. Merkley, and G. R. Hammarlund, "A New Acoustic Levitation Device Using the Interference Sound Field from Two Opposed Radiators," 114th Annual Meeting of Acoustical Society of America (1987).

Rey, C. A., D. R. Merkley, G. R. Hammarlund, and T. J. Danley, "Acoustic Levitation Technique for Containerless Processing at High Temperature in Space," Metal. Trans., 19A, 2619-2623 (1988).

Rey, C. A., and D. E. Day, "Glass Formation in Microgravity," Mat. Res. Soc. Symp. Proc., 87, 239-251 (1987).

Rey, C. A., D. R. Merkley, G. R. Hammarlund, and T. J. Danley, "Specimen Translational Control Capabilities Using an Opposed Radiator Acoustic Levitation System," 114th Annual Meeting of Acoustical Society of America (1987).

Rey, C. A. and D. R. Merkley, "Initial Report on HAL KC-135 Test," NASA/MSFC, July 11, 1989.

90 INTENTIONALLY BLANK
PRECEDING PAGE BLANK NOT FILMED

Rey, C. A. and D. R. Merkley, "Final Report," Contract NAS8-33742, NASA/MSFC, August 24, 1989.

Rey, C. A., "Final Report," Contract NAS8-37592, NASA/MSFC, March 28, 1991.

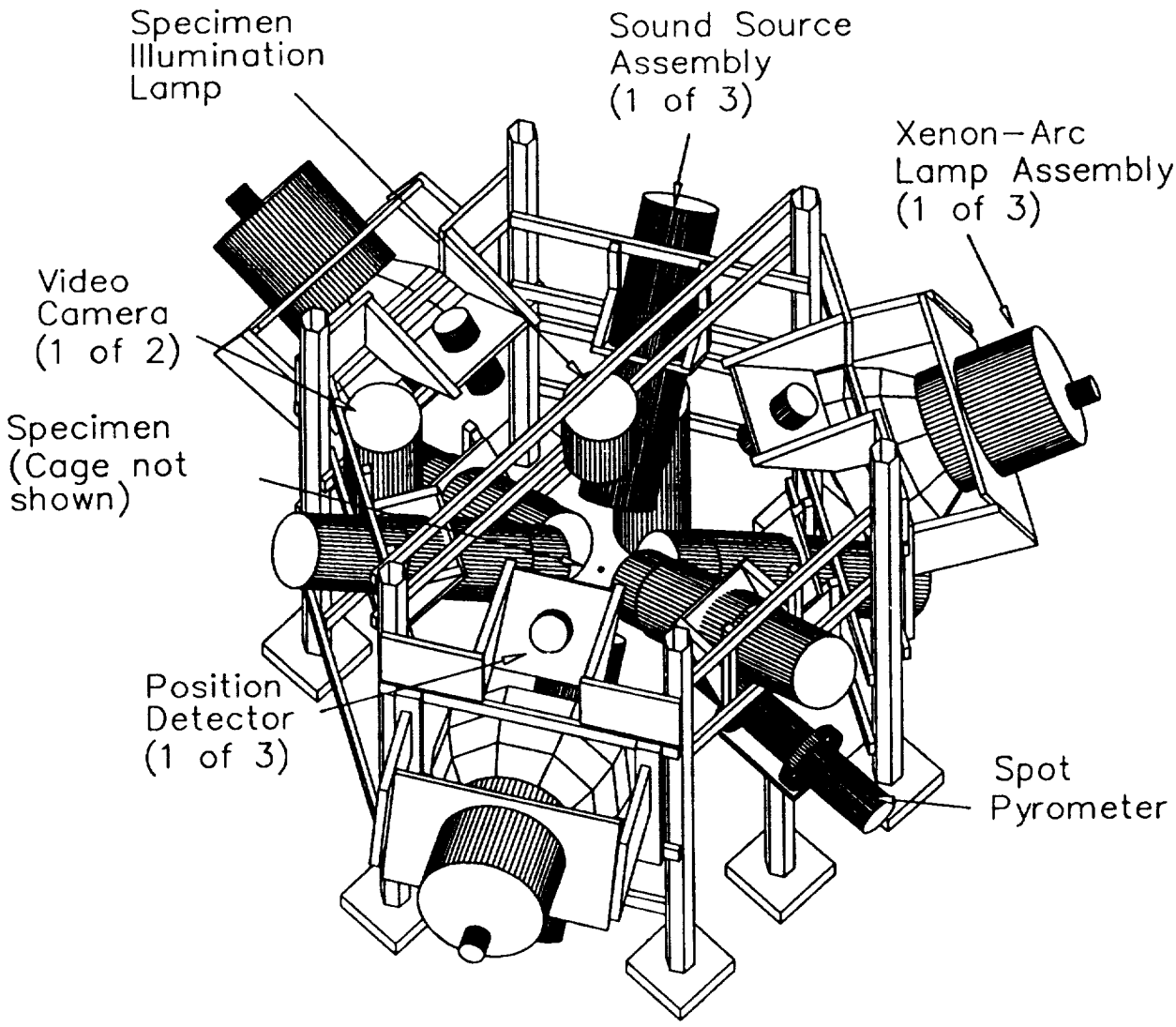

Figure 1. High Temperature Acoustic Levitator (HAL).

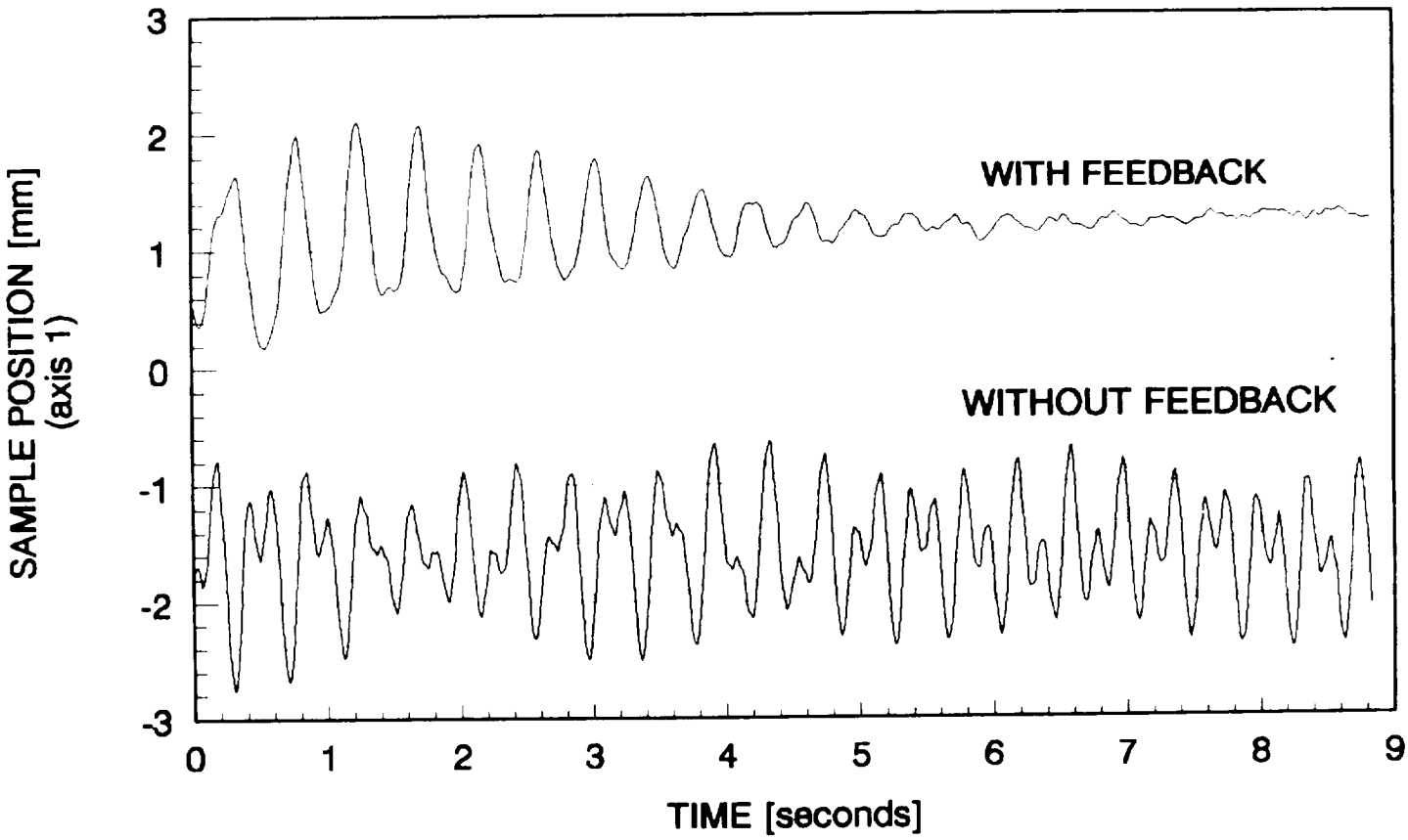

Figure 2. Sample positioning stability. This figure indicates the enhanced position stability that can be achieved with HAL when closed-loop feedback is applied.

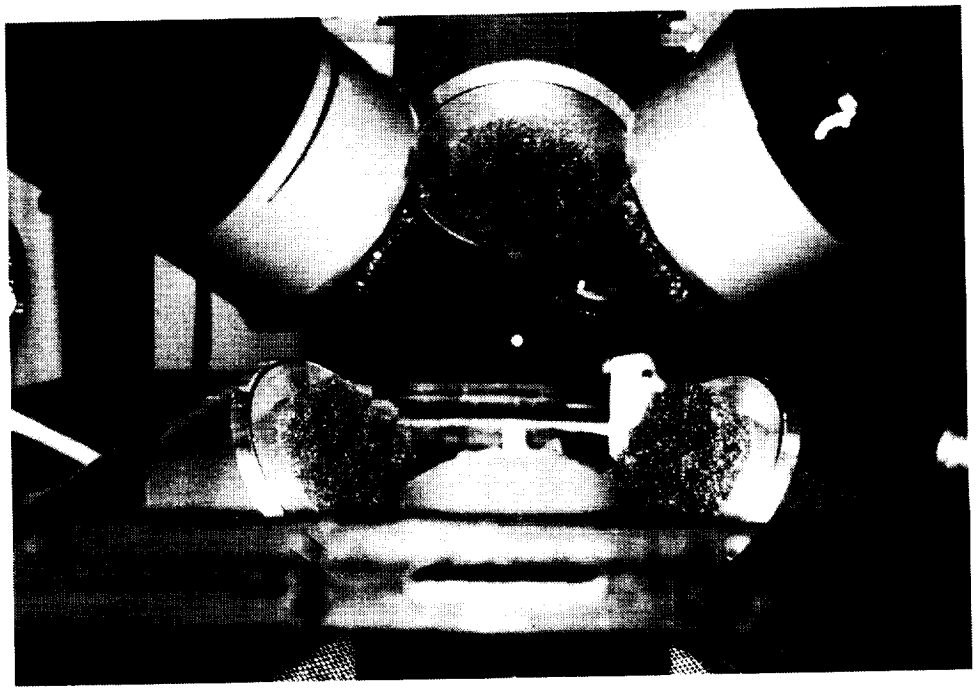

Figure 3. Sample (Al_2O_3, 3 mm diameter) being positioned by the HAL.

ORIGINAL PAGE
BLACK AND WHITE PHOTOGRAPH

CONTAINERLESS STUDIES OF MATERIALS USING ULTRASONIC LEVITATION IN LOW GRAVITY

Investigator: E. H. Trinh, Jet Propulsion Laboratory, California Institute of Technology, Pasadena, CA

OBJECTIVES

The behavior of ultrasonically levitated samples in the liquid state and during melting and solidification is the primary subject of interest of this task. In addition, the degree of interaction between the levitating field and the sample as a function of the level of residual gravitational acceleration is also an emphasized area of investigation. The fundamental objectives of these low-gravity studies are to provide experimental data for comparison with results obtained in terrestrial laboratories using the same apparatus; the only variable being the intensity of the levitating field, this intensity being directly related to the residual gravitational acceleration.

EXPERIMENTAL PROCEDURES AND RESULTS

Several ultrasonic levitators operating in air between 20 and 45 kHz have been integrated into a rack-mounted optical breadboard also used for the positioning of video cameras, xenon arc lamps for non-contact melting of levitated samples, and other various sample deployment apparatuses. Laser illumination for flow visualization studies within and outside of the liquid samples has also been implemented for low-gravity flight experiments. Figure 1 is a photograph of one version of the test breadboard. All experiments have been carried out with the breadboard bolted to the airplane floor and have been manually operated by the investigator. The size of the samples investigated have varied between 2 and 8 mm in diameter for near-spherical specimens, and the samples are generally levitated during the normal and high- and low-gravity parts of the parabola.

Shape of Levitated Simple and Compound Drops

High intensity sound waves allow the levitation of liquid droplets, but also distort their shape due to the action of acoustic radiation stresses. The fundamental requirement for quiescent containerless processing calls for spherical liquid samples, and consequently a quantitative verification of the theoretical predictions of negligible distortion in microgravity must be obtained. Figure 2 displays measured levitated drop shapes in 1 g for different drop sizes. Figure 3 reproduces photographs of drops levitated during different periods of a KC-135 parabola at different acceleration levels. Spherical and compound drops have also beeen levitated during short periods of low gravity, and a demonstration of the capabilities of ultrasonic positioners to process 8 mm diameter spherical samples has also been provided. Figure 4 reproduces photographs of a liquid shell in low gravity at different sound intensities.

Acoustic Streaming Flows and Internal Flows

High intensity sound waves also induce steady-state streaming flows in the environment outside of the levitated sample which could influence its behavior. Measurement of these flows in 1 g have resulted in velocities as high as 50 cm/sec, but these velocities have been determined to be less than 1 mm/sec when liquid samples of density of about 1 g/cc were levitated during a low-gravity parabola. Table 1 summarizes these results and compares data in 1 g and low gravity. The internal flow within the levitated sample could not be measured during the approximately 20 seconds of low gravity due to their low magnitude, but a

94

PRECEDING PAGE BLANK NOT FILMED

quantitative measure of the reduction in uncontrolled rotation of the sample has been obtained (see Table 1).

Containerless Melting Using Beam Heating

Ultrasonically levitated samples of organic compounds have been melted and resolidified using consecutive parabolas and a xenon arc lamp. Samples melting below 200 °C could be accommodated with a single focussed lamp, and pure indium samples have been melted while levitated during the low-gravity periods. The reduction of the acoustic intensity and the accompanying reduction of acoustically forced convective flows have been shown to allow more efficient coupling of the radiant energy into the sample with fixed emissivity. Figure 5 reproduces the stages of melting and solidification of a sample of paraffin wax.

SUMMARY

Low-gravity experiments have allowed the verification of extrapolations dealing with the effects of ultrasonic levitating on a molten sample: spherical simple and compound drop shapes can be obtained in low gravity, forced convective flows are drastically reduced, uncontrolled sample rotation greatly diminishes, and containerless melting and solidification in 0.05 have been demonstrated. The ability to ulilize the same experimental apparatus in low gravity as in 1 g allows the valid comparison of the results and the extrapolation to the true microgravity conditions of low-Earth orbit. Another major practical advantage resides in the ability to levitate samples even during the high-gravity periods of the parabolas, thus allowing more flexibility in experimenting and enhancing the reproducibility of the results.

ACKNOWLEDGMENTS

We thank the low-gravity test projects at Marshall Space Flight Center and at Johnson Space Flight Center for accommodating the flights of our equipment on the KC-135. This task is part of a ground-based research RTOP effort funded by the Microgravity Science and Applications Division of the National Aeronautics and Space Administration. The results described here were obtained during flights in FY87 to FY89, and further studies will take place in FY92.

REFERENCES

Trinh, E. H., "Levitation Studies of the Physical Properties and Nucleation of Undercooled Liquids," ESA SP-295, p. 503 (1990).

Trinh, E. H., "Fluid Dynamics and Solidification of Levitated Drops and Shells," Progress in Astronautics and Aeronautics, 130, 515 (1991).

Trinh, E. H. and C. J. Hsu, "Equilibrium Shapes of Acoustically Levitated Drops," J. Acoust. Soc. Am., 79, 1335 (1986).

Trinh, E. H., J. L. Robey, A. Arce, and M. Gaspar, "Experimental Studies in Fluid Mechanics and Materials Science Using Acoustic Levitation," Mat. Res. Soc. Symp. Proc., 87, 57 (1986).

ORIGINAL PAGE
BLACK AND WHITE PHOTOGRAPH

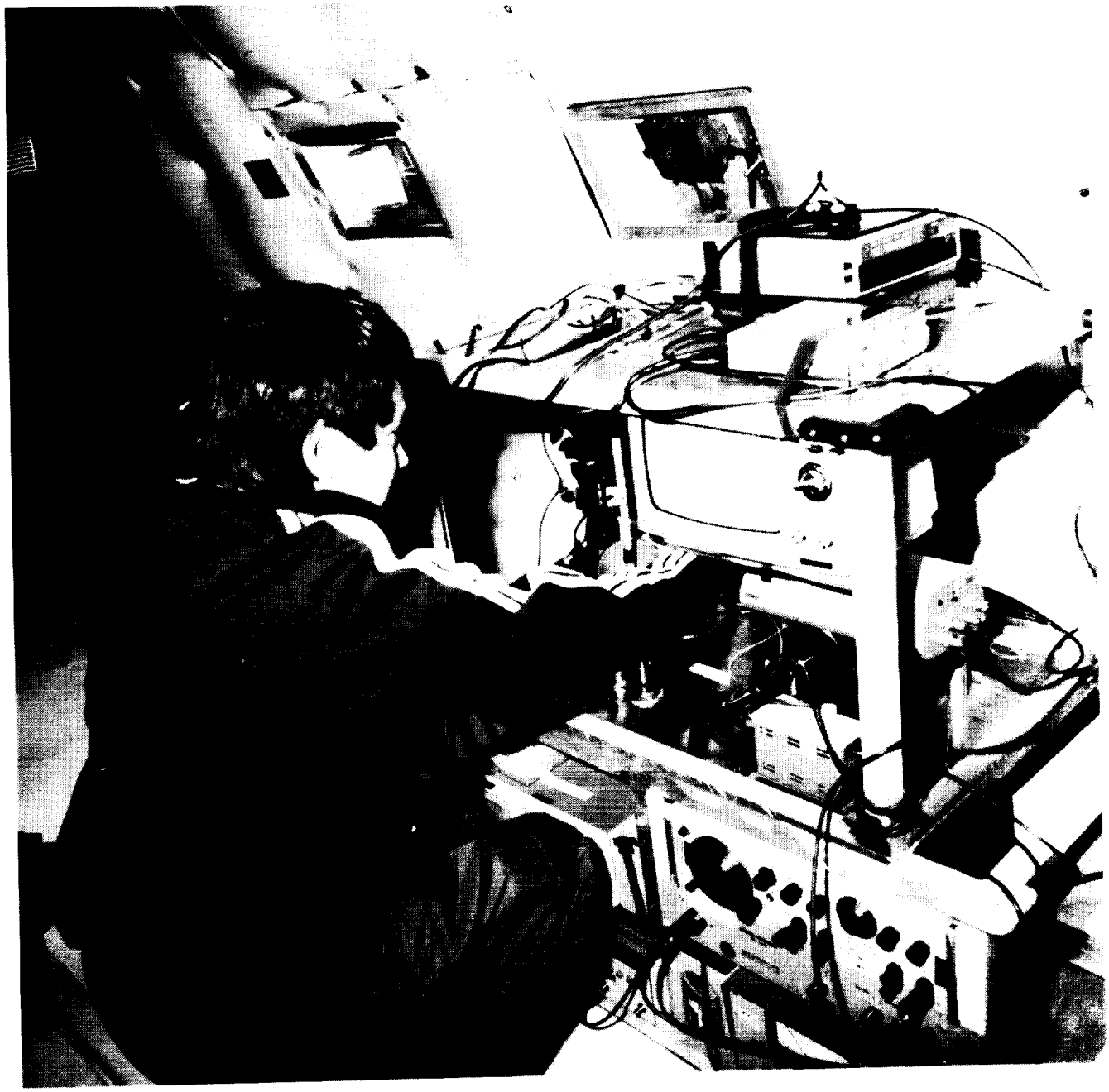

Figure 1. KC-135 test breadboard for experiments of equilibrium shapes of free drops and shells.

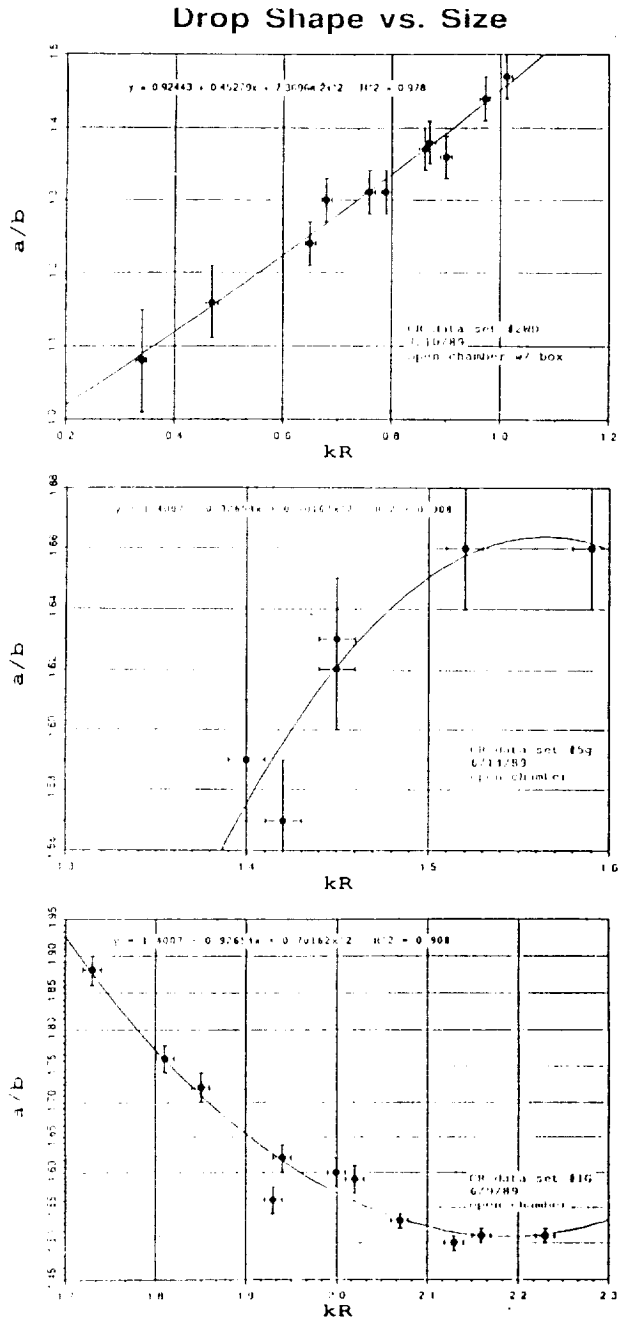

Figure 2. Results of measuremens of the static shape of acoustically levitated droplets in 1 g. The acoustic frequency is 37 kHz, and the sound pressure level is fixed around 159 dB for the data in the kR range between 0.2 and 1.6. The SPL is 163 dB for the last set of data at high kR values. The principal result is the evidence that it is possible to levitate samples with diameters that are comparable to the acoustic wavelength with relatively small sample flattening, even in a one-dimensional sound field.

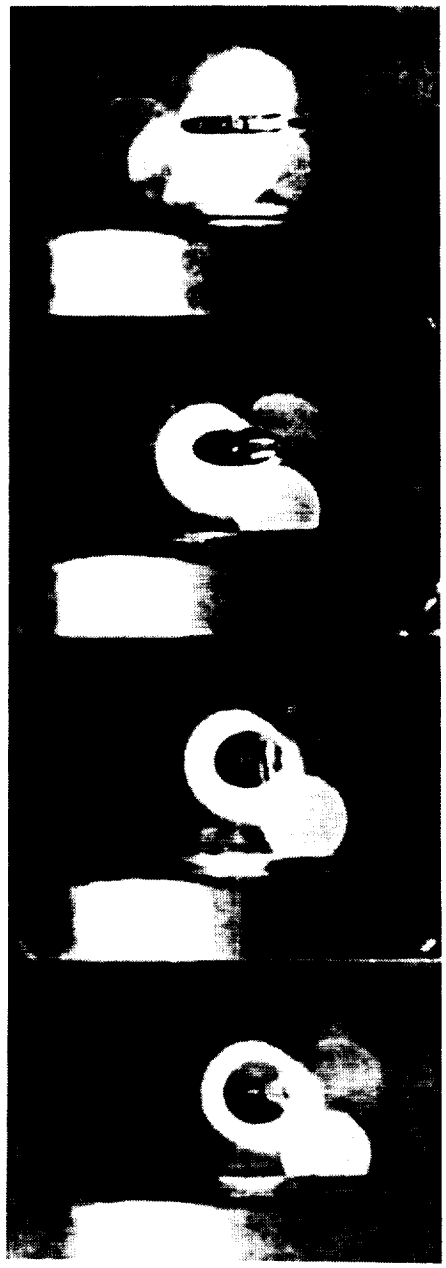

Figure 3. Photographs of 5 mm diameter droplets levitated during a low-gravity period provided by the KC-135 airplane. A wide range of drop shapes can be investigated since the acoustic pressure level can be greatly reduced to compensate for the the decrease of two orders of magnitude in the gravitational field. Drop deformation will thus be negligible during experiments in microgravity.

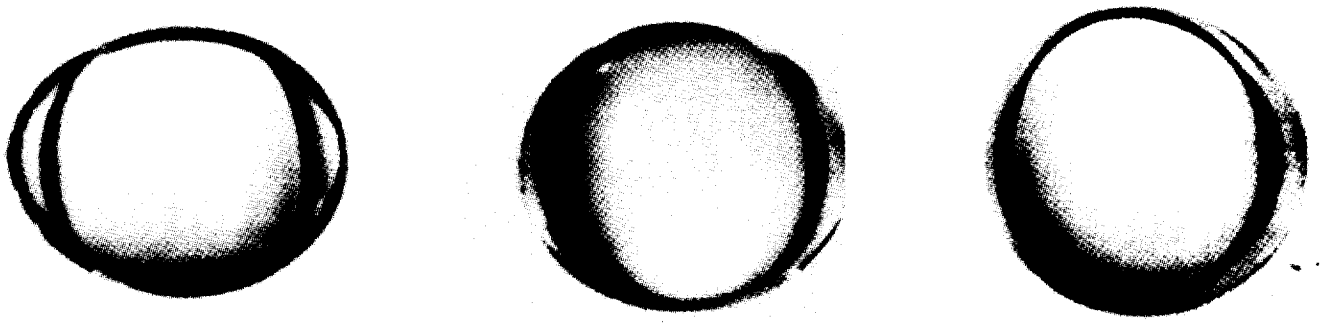

Figure 4. Liquid shell in low gravity at decreasing sound intensity. The reduction of the gravitational acceleration allows the study of the dynamics of virtually undeformed liquid shells even though their position remains fixed by the sound field.

Table 1. Comparison of Conditions for Levitation in 1 g and in 0.05 g

	1 g Laboratory	KC-135 Low Gravity
Sound Pressure Level Required for Levitation (25 kHz)	165 dB	142 dB
Streaming Velocity	19-50 cm/sec	< 1 mm/sec in host gas
Liquid Sample Deformation (A/B Ratio)	1.2	1.0
Sample Uncontrolled Rotation Rate	3-5 rps	< 0.1 rps

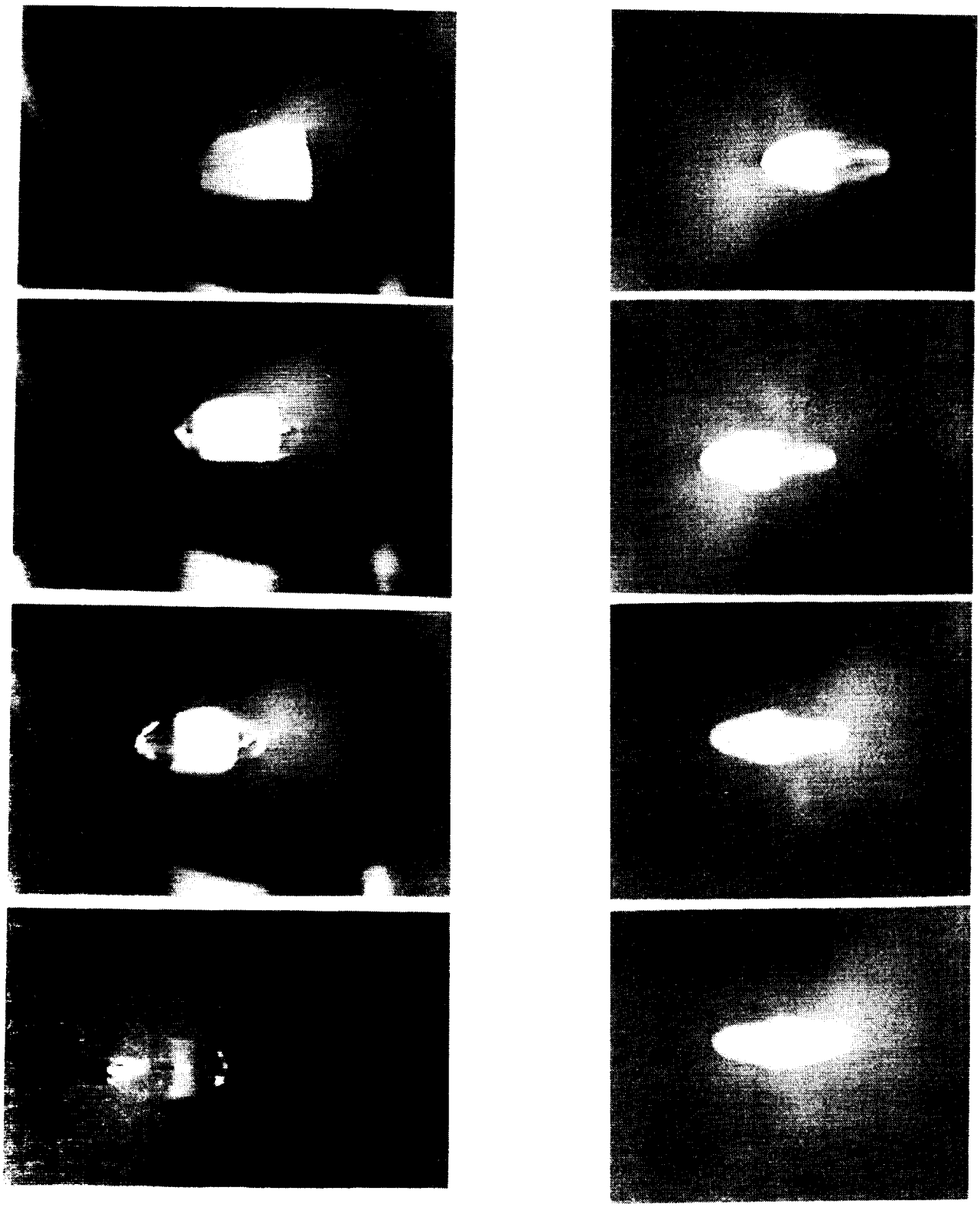

Figure 5. Melting and solidification of levitated samples of Paraffin in low gravity aboard the KC-135. The samples are melted by radiant heating from a focussed Xenon arc lamp while levitated by an ultrasonic field.

6. SOLIDIFICATION WITH FREE SURFACE (WELDING)

EVALUATION OF HYPERMONOTECTIC ALLOYS SOLIDIFIED IN THE MICROGRAVITY ENVIRONMENT PROVIDED BY NASA'S KC-135

Investigators: Richard N. Grugel, Vanderbilt University, Center for Microgravity Research and Applications, Nashville, TN; Richard Poorman, NASA, Marshall Space Flight Center, Huntsville, AL

OBJECTIVE

Hypermonotectic Cu-Pb and Al-In alloys were melted and resolidified during the ~20 seconds of available low-gravity time on NASA's KC-135 aircraft with the intent of comparing the resultant microstructure to those similarly processed under unit gravity. Such comparison will promote our knowledge of factors which contribute to the liquid I and liquid II phase separation and subsequent distribution. Furthermore, these experiments should provide insight regarding solidification behavior prior to processing these alloys aboard, e.g., the STS or Space Station Freedom. Please note that a complete report of this work is given by Grugel and Poorman.[1]

EXPERIMENTAL PROCEDURE

Alloys composed of Al-68 wt pct In and Cu-50 wt pct Pb were investigated. The pure metal components were conventionally alloyed and subsequently prepared for processing as specified in Figure 1.

To work within the microgravity time available on the KC-135, alloy melting and resolidification must be completed within ~20 seconds. This was accomplished by positioning and striking an arc and rotating it about the sample end (Figure 1). Ground-based samples were processed in positions both vertically up and down with respect to the gravity vector; positioning of the samples to be processed in microgravity should be irrelevant. A thermocouple was inserted into some of the ground-based samples as schematically shown in Figure 1. This allowed, at best, determination of the maximum temperature to which the sample was exposed. After processing, the alloys were sectioned along their length and prepared by conventional metallographic means for macroscopic examination.

RESULTS

Figure 2 is characteristic of the Al-In alloy processed vertically upward in unit gravity. The remelted zone shows a finer, better distribution of the indium phase, but a considerably smaller volume fraction. Some indium coalescence is noted in the bottom right corner of the "cap" but the majority, not seen, has collected and run down the sample rod.

Figure 3 is representative of a Cu-Pb alloy processed vertically downward. Here the liquid fell from the sample rod and, again, the volume fraction of the Pb (dark) phase is less than in the as cast material. Figure 3 also shows the apparent settling of considerably larger, lead rich droplets prior to solidification of the liquid which maintained contact with the sample.

The samples processed in the low-gravity environment provided by the KC-135 are shown in Figures 4 and 5. The remelted zone assumes the expected bulbous shape. However, as in the ground-based samples, both the alloys show considerable segregation of L_{II}.

The macrosegregation observed in Figures 2-5 is likely due to a number of interacting mechanisms. The rotating arc probably induces convection in the liquid which would promote collisions and coalescence of the L_{II} droplets. Convection in the liquid will also be initiated by density differences arising from temperature and concentration gradients. Segrega-

PRECEDING PAGE BLANK NOT FILMED

tion from gravity-driven sedimentation due to density differences between the liquids is evidenced in Figures 3-5. Coalescence and coarsening of L_{II} droplets can also result from the gravity independent processes of Marangoni convection and Ostwald ripening. Furthermore, the observed segregation may be a consequence of pushing excess L_{II} ahead of the $L_I = S_I + L_{II}$ reaction interface,[2-3] the extent of which may depend on the preferred wetting of S_I by either L_I or L_{II}.[4-6] Finally, the consequence of different processing positions and environments results in three different cooling and solidification rates.

Ground-based, unit-g, and KC-135 low-gravity processing of hypermonotectic Al-In and Cu-Pb alloys both exhibited massive segregation due to the coalescence of the L_{II} phase. It also noted that the resultant macrostructures are similar to those which have been processed in low gravity for longer times and with better controlled conditions.

ACKNOWLEDGMENTS

This work was supported by the NASA Office of Space Science and Applications.

REFERENCES

1. Grugel, R. N. and R. Poorman, in Materials Science Forum, Materials Processing in Space, Vol. 50, Trans Tech Publications, Ltd., N. B. Singh, V. Laxmanan, and E. W. Collings, eds., pp. 89-100 (1989).
2. Uhlmann, D. R., B. Chalmers, and K. A. Jackson, J. App. Phys., 35(10), 2986-2993 (1964).
3. Chattopadhyay, K., and P. Ramachandrarao, J. Mat. Sci., 15, 685-692 (1980).
4. Chadwick, G. A., Brit. J. Appl. Phys., 16, 1095-1097 (1965).
5. Cahn, J. W., Metall. Trans. A, 10A, 199-121 (1979).
6. Grugel, R. N. and A. Hellawall, Metall. Trans. A, 12A, 669-681 (1981).

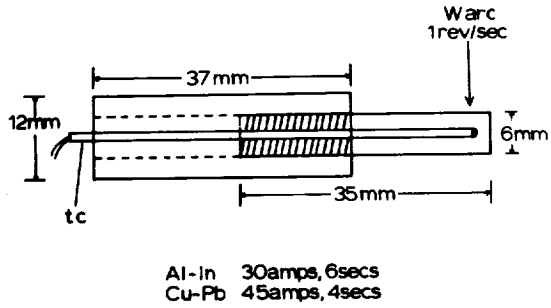

Figure 1. Schematic drawing denoting the dimensions of the sample and sample holder.

Figure 2. Aluminum-indium alloy processed vertically upward in unit gravity.

Figure 3. Copper-lead alloy processed vertically downward in unit gravity.

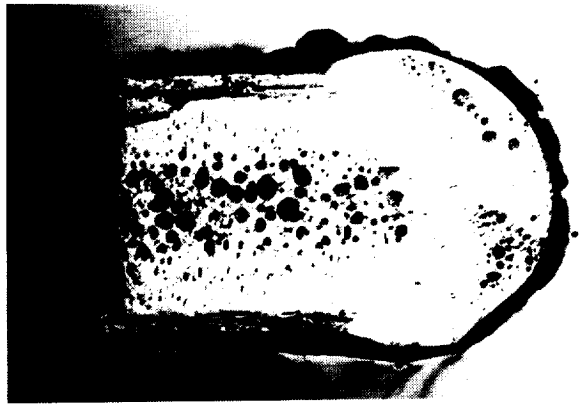

Figure 5. Longitudinal section of a hypermonotectic Cu-Pb alloy processed on the KC-135.

Figure 4. Longitudinal section of a hypermonotectic Al-In alloy processed on the KC-135.

ZERO GRAVITY SOLIDIFICATION OF CAST IRON

Investigators: R. Kazares and L. Lanier, Central Engineering Laboratories, Santa Clara, CA

SUMMARY OF RESULTS

Samples representing three heats of 65-45-12 ductile iron were furnished for metallographic examination. Several of the 3-inch long, 0.21-inch diameter samples contained zones that had been remelted and solidified under low-gravity conditions in a NASA research aircraft. These samples were compared to another sample from one of the heats which had been remelted and solidified by the same procedure under 1 g conditions. The purpose of this experiment was to determine if melting and resolidification at low gravity would affect graphite morphology or distribution.

This examination revealed no significant differences in the morphology or distribution of the remelted zone graphite in any of the as-received or regraphitized samples. Remelting completely dissolved the graphite in all samples and rapid cooling, due to the short duration of the experiment, caused all of the samples to resolidify as white iron. Regraphitizing at 1650 °F for 2 hours caused the graphite to reform with no observable differences between the low gravity and 1 g samples.

Photomicrographs of the as-received samples and regraphitized samples are attached as Figures 1 through 6.

Other information supplied, including process parameters and mechanical properties of base material, is reported in Tables 1 and 2.

PRECEDING PAGE BLANK NOT FILMED

106 INTENTIONALLY BLANK

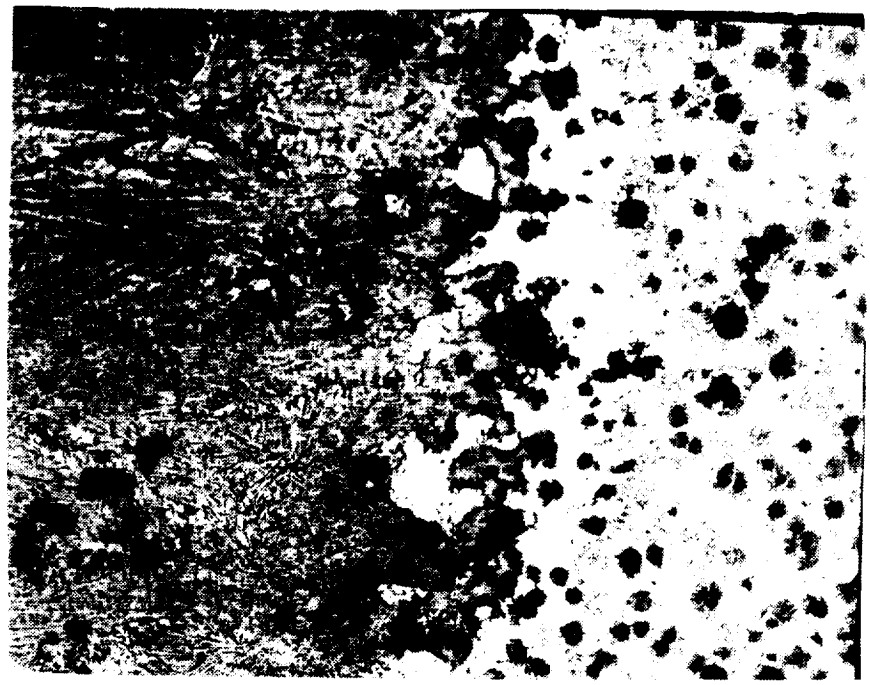

Remelted Zone Heat Affected Zone

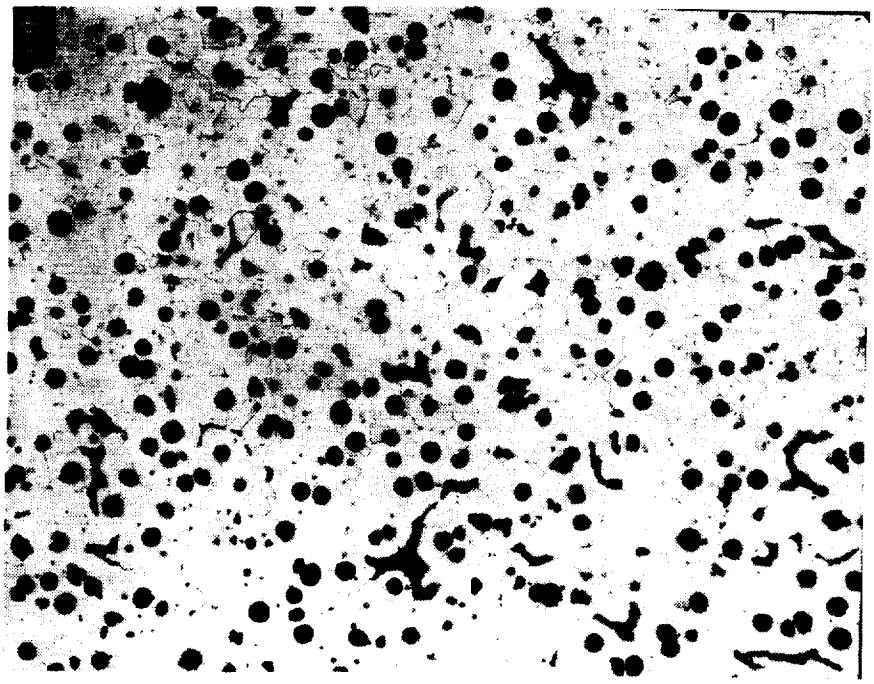

Base Metal

Figure 1. MAG = 50X (nital), heat 2906 - as processed (70 amps, 5 sec), low gravity.

C-2

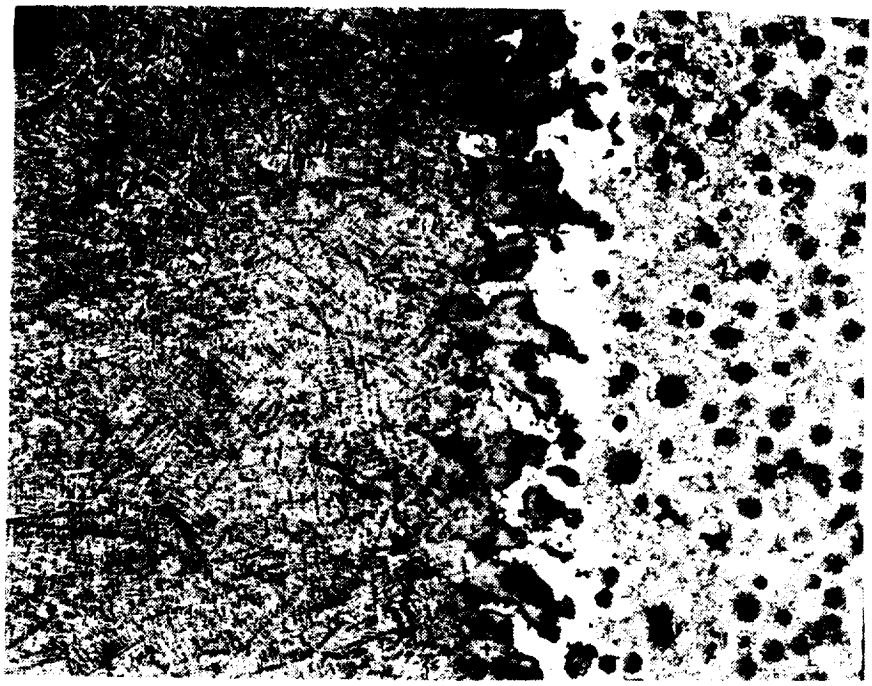

Remelted Zone Heat Affected Zone

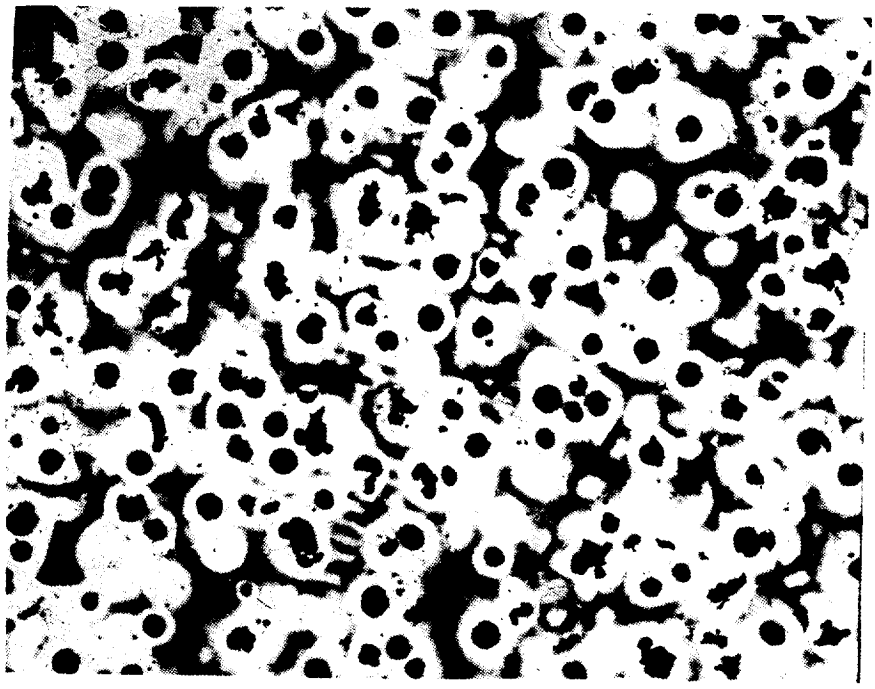

Base Metal

Figure 2. MAG = 50X (nital), heat 2918 - as processed (80 amps, 5 sec), low gravity.

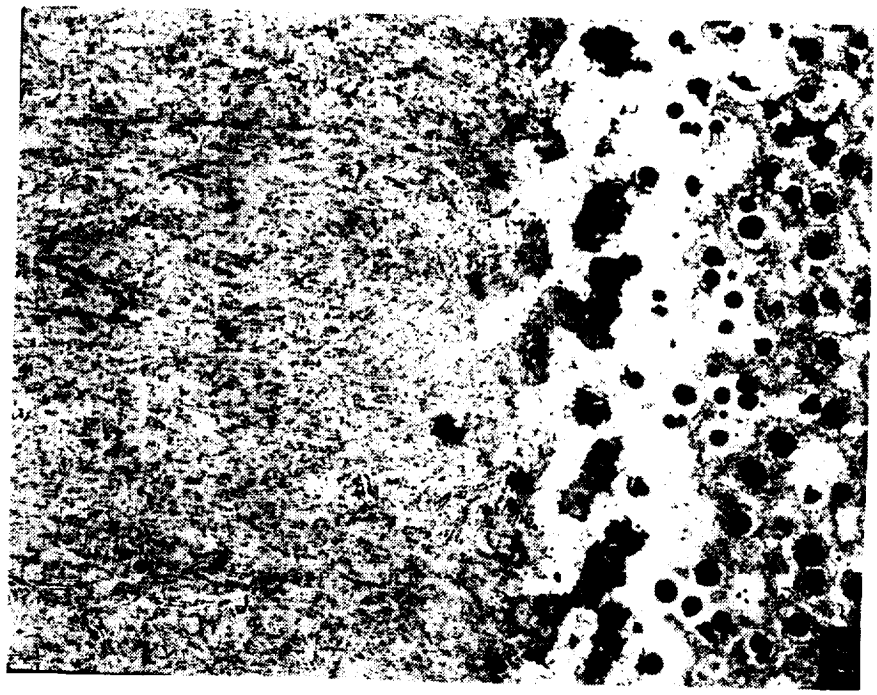

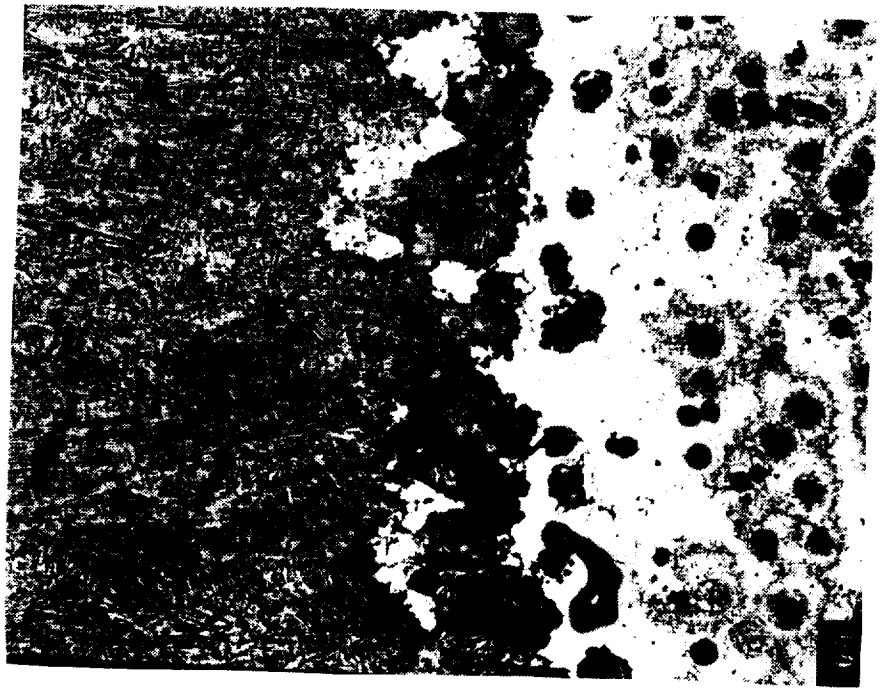

Figure 3. MAG = 50X (nital), heat 2910 - as processed (80 amp, 5 sec), low gravity (top), 1 g (bottom).

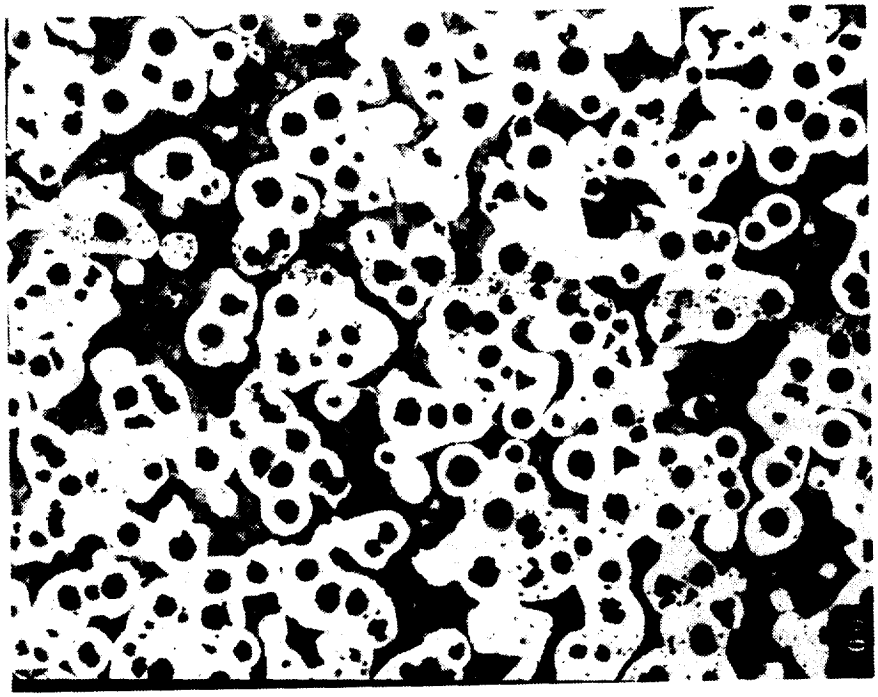

Figure 4. MAG = 50X (nital), heat 2910 - as processed (80 amp, 5 sec), base metal.

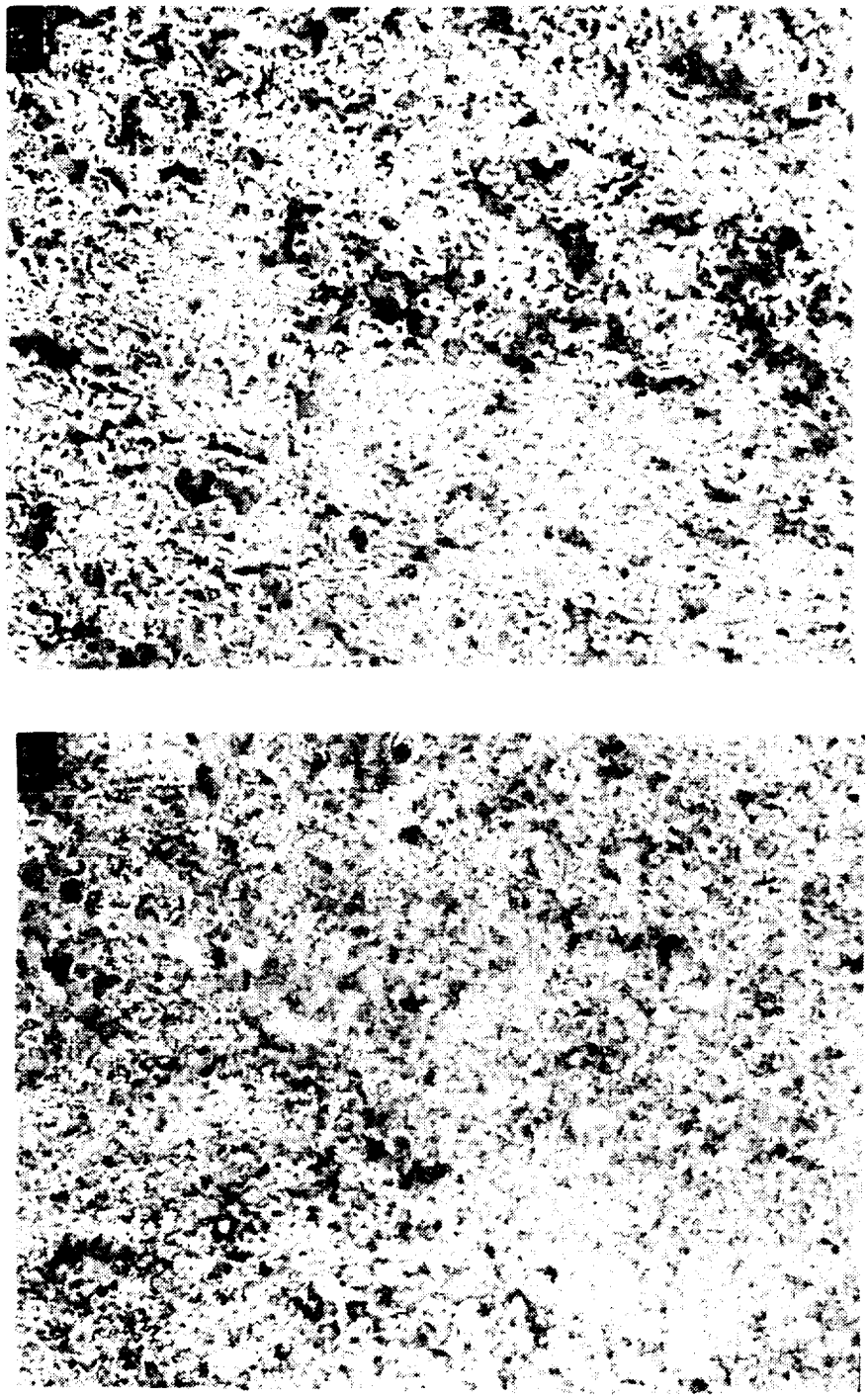

Figure 5. MAG = 250X (nital), heat 2910 remelted zone - regraphitized at 1650 °F for 2 hours, air cooled, low gravity (top), 1 g (bottom).

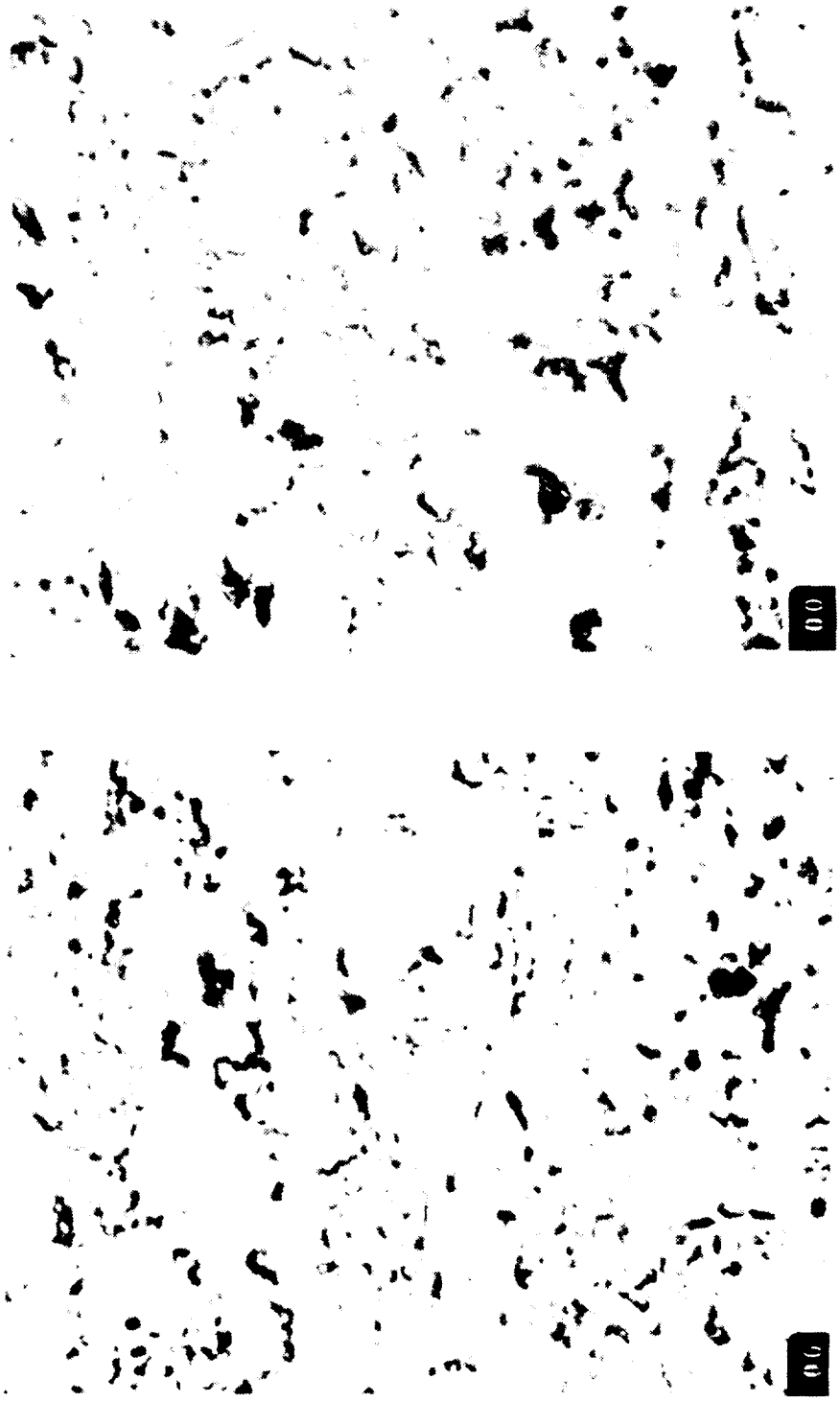

Figure 6. MAG = 1000X (unetched), same as Figure 5, low gravity (top), 1 g (bottom).

Table 1. Processing Parameters (Procedure 2003)*

Heat	Amps	Duration (sec)
2906	70	5
2918	80	5
2910	80	5

*Reported by an unidentified independent laboratory

Table 2. Base Metal Mechanical Properties*

Heat	Ultimate Tensile Strength (psi)	Tensile Yield Strength (psi)	Elongation (%)
2906	69,500	49,500	19.7
2918	76,900	53,500	16.2
2910	78,400	53,100	13.5

*Reported by an unidentified independent laboratory

LASER WELDING EXPERIMENTS IN REDUCED GRAVITY

Investigators: Gary L. Workman and William F. Kaukler, The University of Alabama in Huntsville, Huntsville, AL

OBJECTIVES

To study the effects of reduced gravity on laser welding processes in stainless steel and other materials. The reduced gravity environment will allow simplification of the heat tranpsort and fluid flow parameters affecting melting and solidification phenomena experienced during laser welding of materials. Further elucidation of these parameters in space-based experiments will be useful in both space manufacturing and repair and maintenance of space structures.

EXPERIMENTAL PROCEDURE AND RESULTS

Laser welding experiments using a low power (10-18 watts) Nd-YAG laser have been performed on the NASA KC-135, which flies parabolic maneuvers to achieve reduced gravity conditions. Experiments with 0.005 to 0.020 inch thick stainless steel samples have produced samples showing a pronounced change in convective flows and surface tension with gravity. Reduced gravity processing on the KC-135 has resulted in smaller weld beads, deeper penetration, and increased surface ripple in comparison with 1 g processing. Metallurgical analysis of the weld beads has shown that solidification in reduced gravity has a more radial microstructure while the high g portions of the welds show more dendritic nucleation. A mechanical analysis of the specimens indicated a 10% increase in microhardness and tensile strength in the portions of the weld beads solidified in 0.01 g over those portions of the weld beads which solidified in 1.8 g.

In order to understand the phenomenological aspects of the laser melting process and convective flows in reduced gravity, the study has been extended to include laser processing of single-crystal stainless steel and of thicker samples by using the same laser system with an organic model, succinonitrile. The single crystal samples are currently being analyzed by Dr. Lynn Boatner at Oak Ridge Laboratories.

Succinonitrile is transparaent to the laser energy, but it can be doped with graphite particles to achieve an absorbing condition. The weld volume of this organic material which can be used to model metallic crystals is much larger than that obtained with stainless steel; however, similar results are obtained. However, in order to better compare the results of succinonitrile experiments to the metallic materials above, a mechanism to maintain an adequate temperature gradient across the solidification zone is needed.

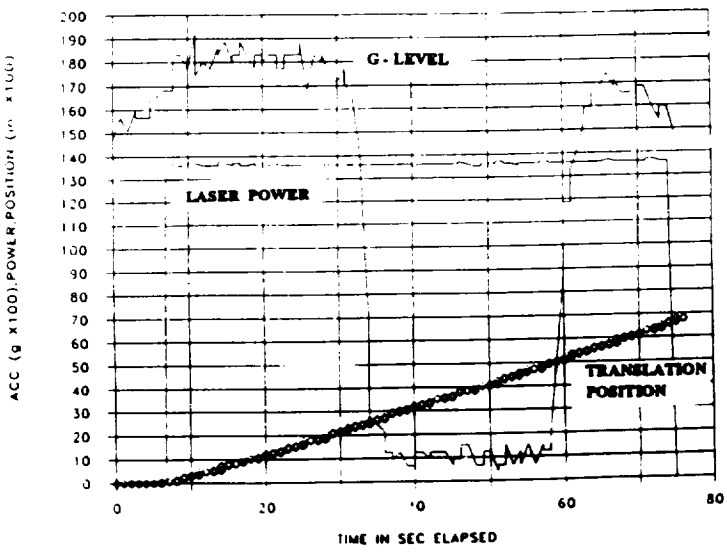

Figure 1. Display of typical laser welding experiment parameters on KC-135.

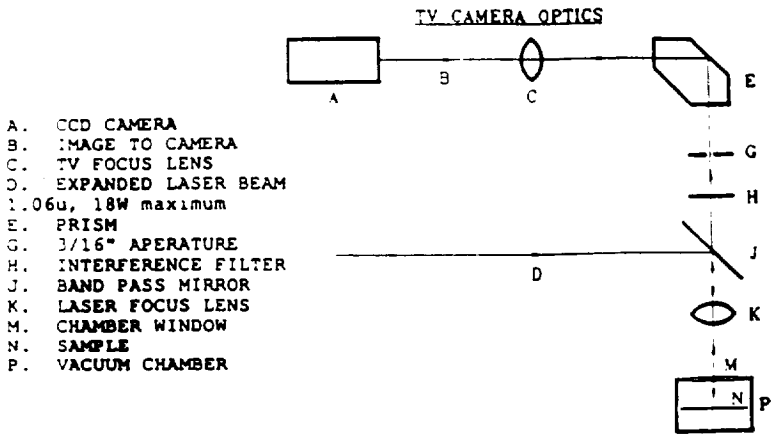

Figure 2. Optical arrangement used in laser welding experiment apparatus.

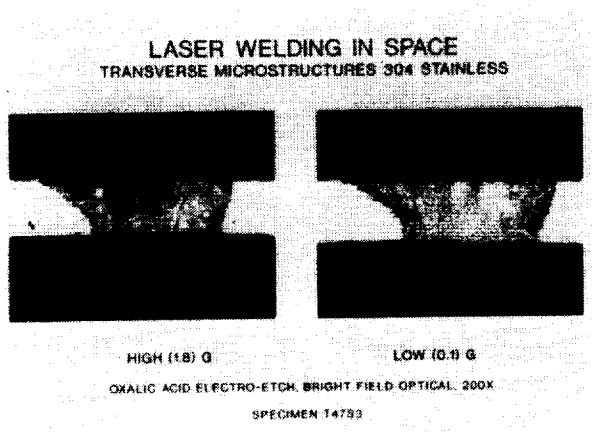

Figure 3. Typical microstructural analysis of stainless steel samples.

7. MELT/CRUCIBLE INTERACTIONS

INFLUENCE OF GRAVITY LEVEL AND INTERFACIAL ENERGIES ON DISPERSION FORMING TENDENCIES IN HYPERMONOTECTIC Cu-Pb-Al ALLOYS

Investigators: J. B. Andrews, Department of Materials Science and Engineering, University of Alabama at Birmingham, Birmingham, AL;
A. C. Sandlin, National Research Council, 2001 Wisconsin Ave., N.W., Washington, D.C.;
P. A. Curreri, NASA, Marshall Space Flight Center, Huntsville, AL

OBJECTIVES

To determine the relative importance of interfacial energy and crucible wetting tendencies in determining the ability to form dispersions in immiscible alloys during low-gravity processing.

EXPERIMENTAL PROCEDURE

Alloys in the Cu-Pb-Al ternary system were utilized to provide samples which exhibited a range of interfacial energies between the immiscible liquid phases. This variation in interfacial energy was accomplished by varying the Al content in the ternary alloys.

The dispersion forming tendencies were evaluated by processing several hypermonotectic alloys under low-gravity conditions. Alloys were heated into the single-phase liquid region, allowed to equilibrate, and were then solidified by cooling at a controlled rate while in a low-gravity environment. One-g processed control samples were used for comparison purposes.

RESULTS

Complete separation due to sedimentation occurred in all ground based control samples. An example is shown in Figure 1a. The results from low-gravity processing were found to be strongly dependent upon alloy composition.

The first samples investigated using low-gravity processing had a low aluminum content (0.9 wt.% Al) and as a result had a low interfacial energy between the immiscible liquid phases. Low-gravity processing of these alloys did prevent sedimentation of the higher density L_2 phase. However, a dispersed microstructure was not obtained. Instead, macroscopic separation and coalescence of the L_2 liquid took place during processing. The resulting structure is shown in Figure 1b. This result was somewhat surprising since the driving force for coalescence, minimization of free energy through reduction of L_1-L_2 interfacial area, would be relatively low in this alloy because of the low interfacial energy. It was also apparent that there was a tendency for the lead-rich hypermonotectic liquid phase to wet the walls of the alumina crucible.

Low-g processing of a high aluminum content (4.2 wt. % Al) alloy resulted in the formation of a completely dispersed microstructure. This alloy was expected to have a higher interfacial energy between the immiscible phases and, as a result, would have a higher driving force for separation and coalescence of the phases. The hypermonotectic liquid phase did not appear to wet the crucible walls.

In summary, for the Cu-Pb-Al alloy system, the alloys that were expected to have a low interfacial energy between the immiscible phases tended to separate macroscopically due to coalescence and crucible wetting when processed under low-gravity conditions. On the other hand, dispersions of the hypermonotectic

PRECEDING PAGE BLANK NOT FILMED
INTENTIONALLY BLANK

phase were obtained when alloys thought to exhibit a high interfacial energy between phases were solidified under low-gravity conditions.

This result is contrary to that normally anticipated. It is usually assumed it should be difficult to obtain dispersions in high interfacial energy alloys, but easy in low interfacial energy alloys. This argument is based on the driving force for coalescence. A higher interfacial energy implies a larger driving force for minimization of interfacial area. Since a dispersed structure will have a higher L_1-L_2 interfacial area than a segregated structure, it has been assumed that dispersions will be less likely to form when the interfacial energy is high.

Obviously, other factors must also be considered. In this system it appears the controlling factor involves the tendency for the hypermonotectic phase to separate and coalesce when it wets the walls of the container. Therefore, for the Cu-Pb-Al alloys investigated, macroscopic separation related to the hypermonotectic liquid wetting the walls of the alumina crucibles appears to be more important in determining the final microstructure during low-gravity solidification than free energy considerations based on the L_1L_2 interfacial energy.

REFERENCES

Andrews, J. B., A. C. Sandlin, and P. A. Curreri, "The Influence of Gravity Level and Interfacial Energies on Dispersion Forming Tendencies in Hypermonotectic Cu-Pb-Al Alloys," Metall. Trans. A, 19A, 2645-2650 (1988).

Sandlin, A. C., J. B. Andrews, and P. A. Curreri, "The Influence of Interfacial Energies and Gravitational Levels on the Directionally Solidified Structures in Hypermonotectic Alloys," Metall. Trans. A, 19A, 2665-2669 (1988).

Andrews, J. B., C. J. Briggs, and M. B. Robinson, "Containerless Low-Gravity Processing of Immiscible Gold-Rhodium Alloys," Materials and Fluid Sciences in Microgravity, ESA Publications Division, ESTEC, Noordwijk, The Netherlands, pp. 1121-1126 (1990).

Sandlin, A. C., J. B. Andrews, and P. A. Curreri, "Directional Solidification of Immiscible Cu-Pb-Al Alloys Under Alternating High-G/Low-G Conditions," Materials and Fluid Sciences in Microgravity, ESA Publications Division, ESTEC, Noordwijk, The Netherlands, pp. 127-133 (1990).

Andrews, J. B., A. C. Sandlin, and R. A. Merrick, "Directional Solidification in Immiscible Systems: The Influence of Gravity," Advances in Space "Research, 11(7), 291-295 (1991).

Andrews, J. B., A. C. Sandlin, R. A. Merrick, Z. B. Dwyer, A. L. Schmale, and C. N. Buckhalt, "Solidification in Immiscible Systems," in Proceedings of the IKI/AIAA Microgravity Science Symposium, Moscow, USSR, pp. 238-246 (1991).

Andrews, J. B., R. A. Merrick, Z. B. Dwyer, A. C. Sandlin, and M. B. Robinson, "The Effect of Processing Conditions on Solidified Microstructures in Immiscible Systems," Materials Science Forum, 77, 269-282 (1991).

Andrews, J. B., A. L. Schmale, and A. C. Sandlin, "The Influence of Gravity Level During Directional Solidification of Immiscible Alloys," Journal of Crystal Growth, in press (1992).

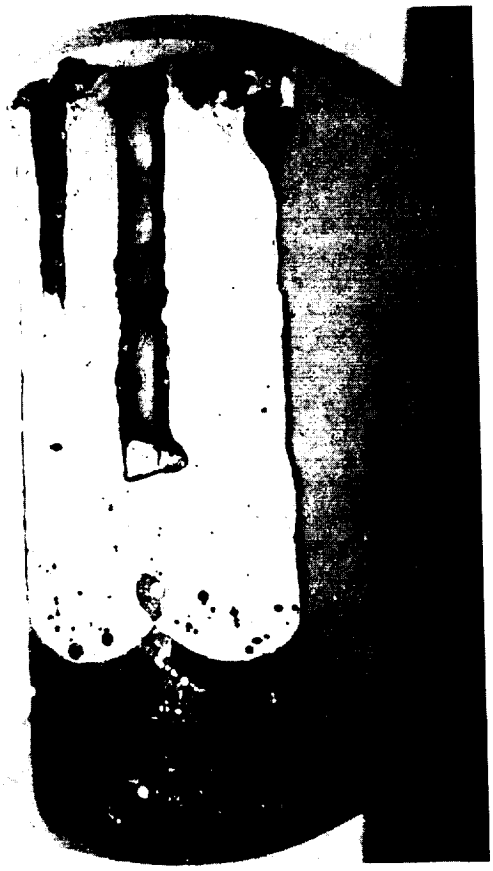

(a)

(b)

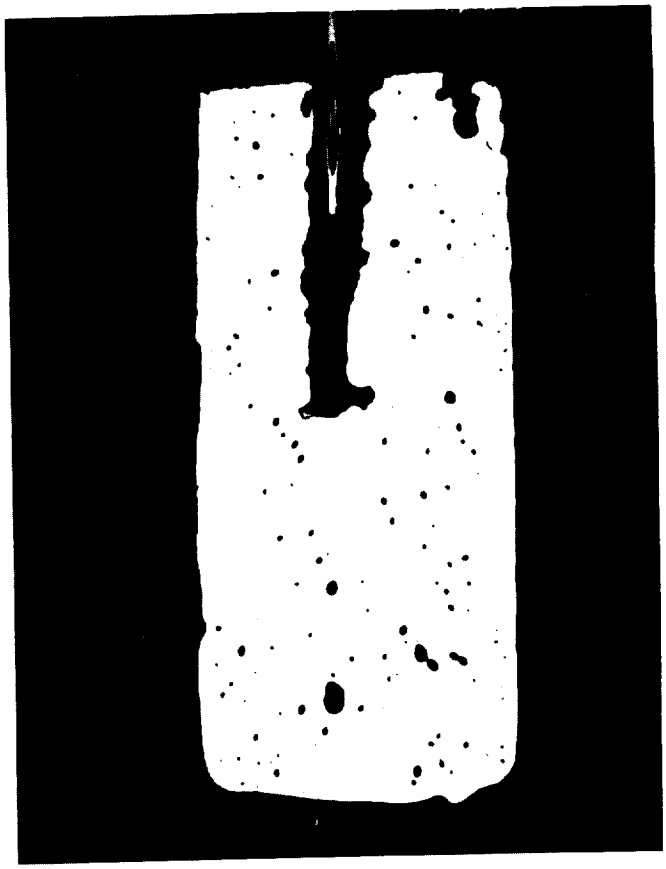

(c)

Figure 1. A comparison of microstructures obtained in the hypermonotectic Cu-Pb-Al alloys investigated. (a) separation due to sedimentation when solidified under 1-g conditions. (b) separation due to crucible wetting and coalescence in a low Al content low-gravity processed sample. (c) dispersion formation in a high Al content, low-gravity processed sample.

ORIGINAL PAGE
BLACK AND WHITE PHOTOGRAPH

CdTe DEWETTING BEHAVIOR IN MICROGRAVITY

Investigators: Gary Bostrup, Ratnakar Neurgaonkar, and April Collins, Rockwell International Science Center, 1049 Camino Dos Rios, Thousand Oaks, CA; Gary Rosen and Fred Carlson, MAE Dept., Center for Advanced Material Processing, Clarkson University, Potsdam, NY; Guy Smith and Gary Workman, Johnson Research Center, The University of Alabama in Huntsville, Huntsville, AL 35899

OBJECTIVES

Cadmium telluride crystal growth in space offers an entire host of advantages not available in a 1-g environment. Without the detrimental influence of gravity such things as hydrostatic forces, confinement effects, and convection will all be significantly reduced. The mitigation of crystalline strain, spurious nucleation, and container-born contamination all depend on the degree of material "dewetting" that occurs in microgravity. Once in the liquid state, cadmium telluride must pull away and exhibit a very low affinity for its ampoule walls. Enhancing this behavior in our USML-1 experiment requires first establishing an Earth-bound microgravity data base. By studying CdTe's reactions to various ampoule shapes and internal surfaces, we hope to discover the best overall configuration that promotes dewetting. Holding material surface contact to a minimum also promises to attenuate any g gitter brought on by accelerations to the spacecraft.

EXPERIMENTAL PROCEDURE AND RESULTS

Due to CdTe's low heat conductivity conventional crystal growth is impossible in the 25 sec of low gravity provided by the KC-135; liquid samples simply cannot nucleate and grow significantly to provide any appreciable material to study. Our procedure relies instead on quenching relatively small charges (6 gm) of cadmium telluride and preserving the effects of low gravity in the morphology of the solidified ingot. This strategy dictates that a 1-g baseline be established first and act as a comparison to all comparable KC-135 run samples. Utilizing the Isothermal Casting Furnace (ICF) provided by Marshall Space Flight Center (MSFC) and The University of Alabama, Huntsville (UAH), small samples could be run both on the ground and later in the aircraft. The ICF could liquefy and later cool CdTe ingots within the low-gravity window aboard the KC-135. Accelerometer and thermocouple data were also provided and noted respectively the low-gravity level along three axes and the internal ampoule temperature (Figs. 1 and 2).

Ampoules (Fig. 3) with smooth and sandblasted pyrolytic internal surfaces were first loaded with CdTe, evacuated, and then sealed. Sister samples were then either run in 1 g as a baseline or flown aboard the KC-135 and quenched in low gravity. Accelerometer and thermocouple data indicated that the material was quenched completely within the 25-sec window and at g levels of approximately 10^{-2}. Experiments performed on over 20 flights indicated that under favorable conditions dewetting can be enhanced significantly. Samples run with smooth pyrolytic surfaces demonstrated a morphology brought on by a low affinity for the ampoule wall. Sandblasted ampoules with pyrolytic surfaces promised an even higher degree of dewetting. Preliminary measurements indicate very high contact angles with CdTe. Several flight samples with a roughened surface have yet to be analyzed.

122 INTENTIONALLY BLANK PRECEDING PAGE BLANK NOT FILMED

REFERENCES

Avduyevsky, V. S., S. D. Grishin, L. V. Leskov, V. I. Polezhayev, and V. V. Savitchev, "Manufacturing in Space: Processing Problems and Advances," MIR Publishers (1984).

Bostrup, G., J. Viola, and E. Gertner, "Experimental Ground-Based Bridgman CdTe Growth in NASA's Advanced Directional Solidification Furnace," AIAA-88-0251 (1988).

Sen, Radha and W. R. Wilcox, "Behavior of a Non-Wetting Melt in Free Fall: Experimental," J. of Crys. Growth, 74, 591-596 (1986).

Sen, Radha, and W. R. Wilcox, "Behavior of a Non-Wetting Melt in Free Fall: Theoretical," J. of Crys. Growth, 78, 129-134 (1986).

Ofitserov, A. A., A. V. Vanyukov, V. V. Golubtsov, M. N. Dubrovin, and A. M. Sokolov, "Method of Measuring the Surface Tension of Decompsoing Compounds," Zavodskaya Laboratoriya, 40(3) 266-268 (1974).

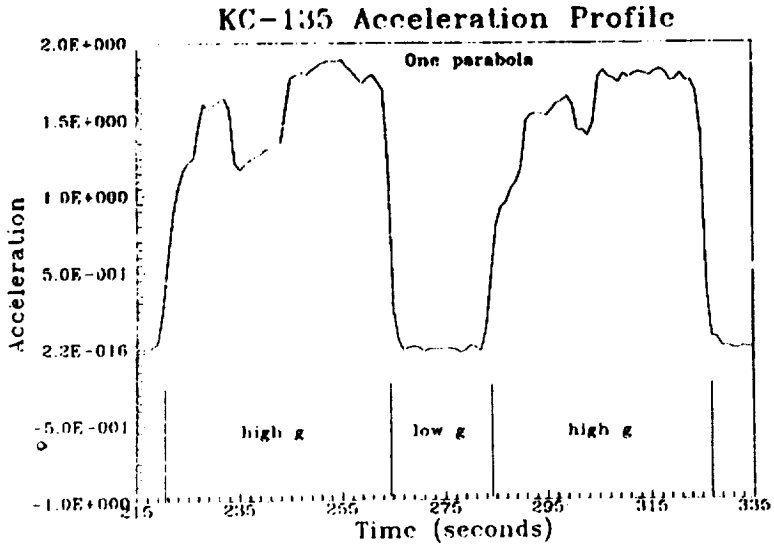

Figure 1. KC-135 sample acceleration profile.

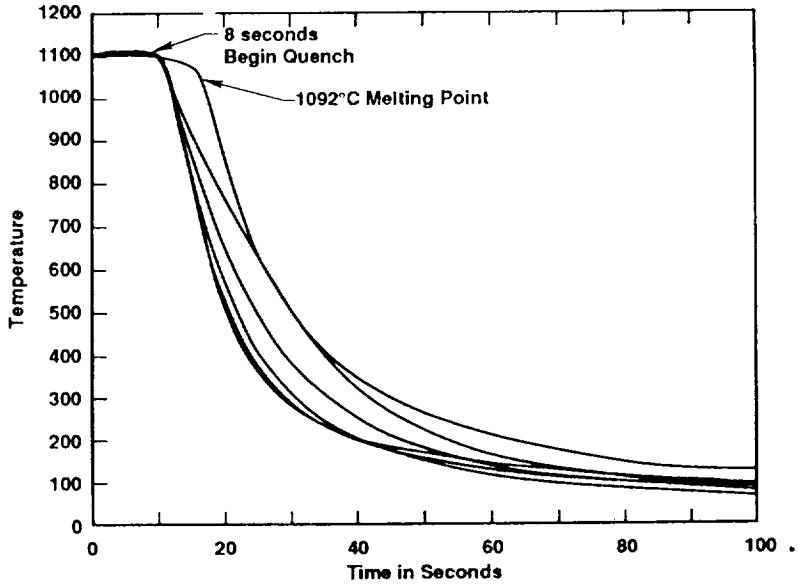

Figure 2. CdTe cooling curve data (ICF flight runs).

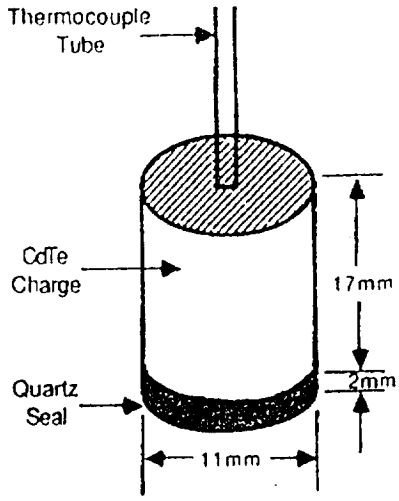

Figure 3. Ampoule configuration (smooth inner wall - pyrolized; sandblasted inner wall - pyrolized).

SEMICONDUCTOR GROWTH AND WETTING BEHAVIOR IN A REDUCED GRAVITY ENVIRONMENT

Investigators: D. H. Matthiesen,
M. J. Wargo, and A. F. Witt,
Massachusetts Institute of
Technology, Cambridge, MA

OBJECTIVES

The primary objective of this series of exploratory experiments was to establish a data base for the design and conduct of semiconductor crystal growth research aboard the shuttle system. Focus was placed on getting more insight into the wetting behavior of semiconductor melts under reduced gravity conditions. Compound semiconductor samples (doped InSb and Be) were molten and resolidified in quartz confinement under parabolic flight trajectories. The resolidified samples were subjected to post-growth analyses.

EXPERIMENTAL PROCEDURE AND RESULTS

This series of experiments was an integral part of a ground-based research program in which the effectiveness of magnetic fields for melt stabilization during Bridgman-type crystal growth of semiconductors was investigated. The KC-135 experiments provided the basis for a comparative analysis.

Undoped and Te-doped ($10^{18}/cm^3$) InSb and Ga-doped ($10^{19}/cm^3$) germanium charges of 6 mm diameter and 30 mm length were placed into a quartz ampoule and sealed in an argon atmosphere. The samples were positioned in the ADSF facility which provided for an axial temperature gradient (at the critical growth position) of about 58 °C/cm as measured in empty configuration. With the furnace at temperature and in predetermined starting position, the inserted samples were subjected to a 10-minute thermal equilibration. Crystal growth was subsequently initiated and sustained for 12 min through furnace translation in the upward direction at a rate of 83.3 μm/s. During the growth period the KC-135 executed six parabolic trajectories providing intermittent g levels as low as 10^{-3}. The samples were removed from the ADSF facility and analyzed.

Figure 1 establishes the correspondence of growth during high and low g values of the g vector for Ga-doped germanium. Details of the surface morphology of the grown samples are observed in Figure 2 which presents low g growth on the lower segment and high g growth on the upper segment. Conspicuous in the lower segment is the "free solidification" (non-wetting) behavior which reveals through striations the characteristics of growth and the changing morphology of the growth interface. Significant is the non-planar growth interface morphology which reflects deficiencies in the thermal boundary conditions provided by the ADSF. The experiments show also the occurrence of noticeable melt back associated with the transition from low to high g growth. The experiment indicates the establishment of non-wetting conditions for melts of Te-doped InSb and Ga-doped Ge suggesting the viability of KC-135 experiments for enlarging the data base related to solidification in a reduced gravity envirmonent. The experiments revealed, moreover, deficiencies in the available hardware.

REFERENCES

Witt, A. F., H. C. Gatos, M. Lichtensteiger, M. Lavine, and C. J. Herman, "Crystal Growth and Steady State Segregation Under Zero Gravity: InSb," J. Electrochem. Soc., 122, 276-283 (1975).

Witt, A. F., H. C. Gatos, M. Lichtensteiger, M. Lavine, and C. J. Herman, "Crystal Growth and Steady State Segregation Under Zero Gravity: Ge," J. Electrochem. Soc., 125, 1832-1840 (1978).

126 INTENTIONALLY BLANK PRECEDING PAGE BLANK NOT FILMED

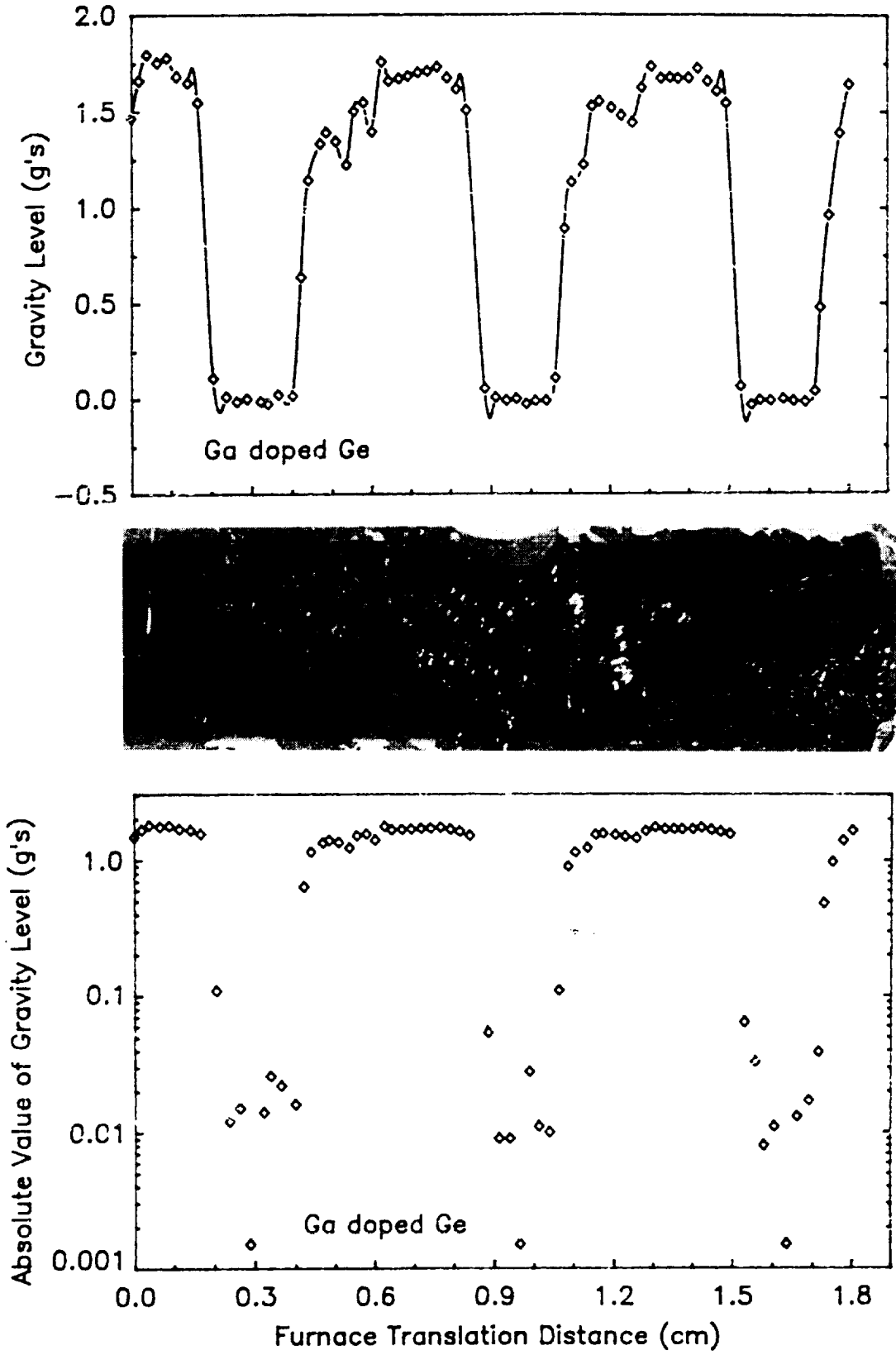

Figure 1. Gravity level as a function of furnace translation for the second Ga/Ge flight sample. Photograph is through the quartz ampoule.

Figure 2. Photomicrographs of the as-grown surface of the first Ga/Ge flight sample. Magnification clearly indicates the morphological change during the transition from low to high gravity level (15 mm = 10 μm).

INDIUM ANTIMONIDE SOLIDIFICATION IN TRANSPARENT FURNACE KC-135

Investigators: W. R. Wilcox, R. Derebail, and B. Hoekstra, Center for Crystal Growth in Space, Clarkson University, Potsdam, NY; M. Vlasse, Space Science Laboratory, NASA, Marshall Space Flight Center, Huntsville, AL

OBJECTIVES

The objective of this study is to observe behavior of melt during directional solidification in a partially filled and poorly wet ampoule.

EXPERIMENTAL PROCEDURE AND RESULTS

Indium antimonide was directionally solidified in partially filled silica ampoules. The melt and solid adjacent to the solid-liquid interface were observed and video taped.

The melt never pulled away from the ampoule wall and the solid remained in contact with the wall. Gas bubbles on the ampoule wall moved toward the solid-liquid interface when the interface contacted them. This was explained by considering the melt-ampoule and melt-interface contact angles.

The microstructure (grain and twin boundary counts) was compared with that of samples grown in the same apparatus on Earth and with samples solidified in large centrifuges. No firm conclusions could be reached.

REFERENCES

Ramnath Derebail, M.S. Thesis, Clarkson University, "Study of Indium Antimonide Solidification Under Low, High, and Normal Gravity" (1990).

130 INTENTIONALLY BLANK
PRECEDING PAGE BLANK NOT FILMED

8. CONTAINED DIRECTIONAL SOLIDIFICATION

132 PRECEDING PAGE BLANK NOT FILMED

DIRECTIONAL SOLIDIFICATION OF Cu-Pb-Al HYPER-MONOTECTIC ALLOYS UNDER ALTERNATING GRAVITY LEVELS

Investigators: J. B. Andrews, Dept. of Materials Science and Engineering, University of Alabama in Birmingham, Birmingham, AL; A. C. Sandlin, National Research Council, 2001 Wisconsin Ave., N.W., Washington, D.C.; P. A. Curreri, Space Science Laboratory, NASA, Marshall Space Flight Center, Huntsville, AL

OBJECTIVES

The objective of this study was the determination of the influence of gravity level on the morphology developed during directional solidification of hypermonotectic immiscible alloys.

EXPERIMENTAL PROCEDURES AND RESULTS

Several different Cu-Pb-Al alloy compositions were directioinally solidified on NASA's KC-135 aircraft during parabolic maneuvers using the Automatic Directional Solidification Furnace (ADSF). The Cu-Pb-Al system was utilized to permit a systematic variation in the miscibility gap height of the alloys investigated.

The Cu-Pb system forms a low-dome-height monotectic while the Al-Pb binary is a high-dome-height monotectic. As Al is added to the Cu-Pb binary, the dome height increases in a smooth manner, thereby providing a range of dome heights within one system.

For proecessing, hypermonotectic samples were placed in the ADSF which was already heated to the operating temperature. The entire sample was held in the hot zone of the furnace for a minimum of 10 min to aid homogenization. Samples were then processed using furnace translation rates of 0.3, 0.6, 1.0, 2.0, 3.0, or 5.0 mm/min.

After processing samples were longitudinally sectioned and prepared for metallaographic analysis, correlations were made between the microstructures obtained and the gravity level during processing.

The directionally solidified low Al-content (i.e., low dome height) hypermonotectic samples exhibited irregular microstructures which decreased in scale as the solidification rate increased. At high furnace translation rates (5.0 and 3.0 mm/min) no apparent variations in structure were observed with gravity level. However, samples procesed at 2.0 mm/min exhibited a measurable decrease in mean particle size during the low-gravity segments of solidification. A plot of the mean particle size versus distance along the sample is shown in Figure 1 along with the variation in gravity level during processing. The cyclic variation in mean particle size appears to correspond to the cyclic variation in gravity level, with the minimum in particles size corresponding to the low-gravity portion of the maneuver.

Dramatically different structures were obtained in high-dome-height (high Al content) samples of specific compositions. When processed at high translation rates (5.0 mm/min), the structure consisted of elliptically-shaped, large droplets of the hypermonotectic constituent superimposed upon a dispersion of small spheres. There was a strong correlation between the occurrence of the large droplets and gravity level. In the portion of the samples solidified under low-gravity conditions, no

134 INTENTIONALLY BLANK PRECEDING PAGE BLANK NOT FILMED

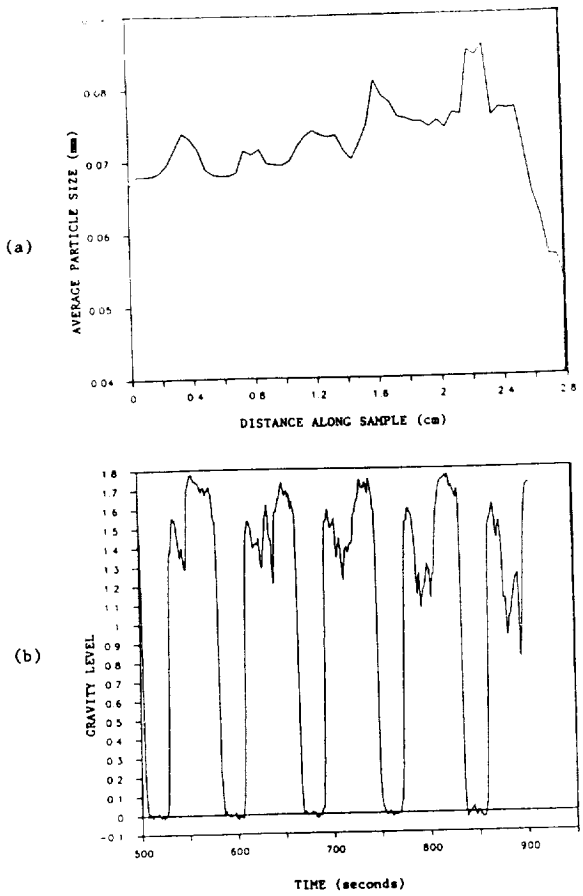

Figure 1. (a) Variation in the mean particle size of the hypermonotectic constituent versus distance on a low-Al content alloy directionally solidified under alternating gravity level conditions; (b) variation in gravity level versus time.

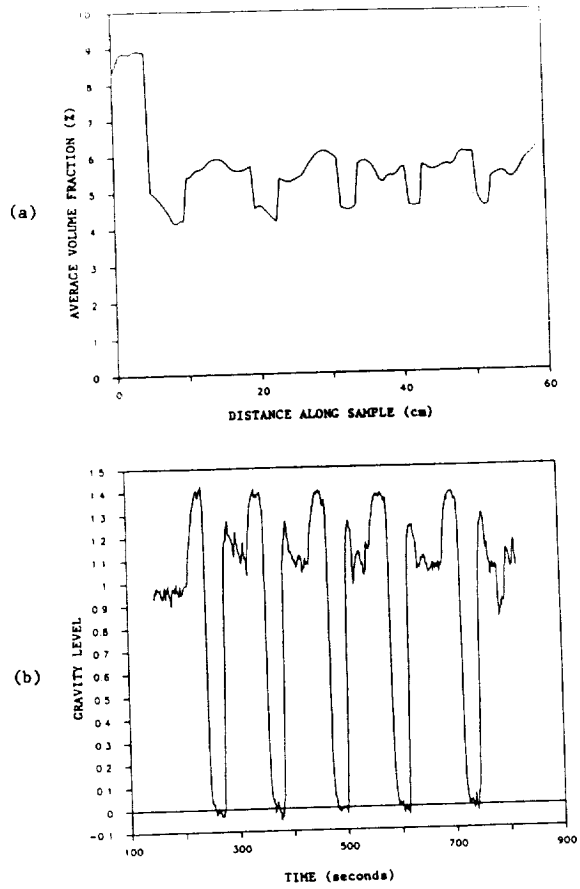

Figure 2. (a) Variation in the volume fraction of the hypermonetectic phase with distance in a slowly solidified high-Al content alloy; (b) plot of gravity level variation as a function of time.

droplets were present. However, a high concentration of large droplets was observed for every high-gravity period during processing. The variation in volume fraction of the hypermonotectic constituent is shown quantitatively in Figure 2 which also plots the gravity level variations with time.

At lower solidification rates (less than 1.0 mm/min) fibrous microstructures were obtained in these high-dome-height samples. While research is still under way in this area, several alloy compositions revealed a transition from fibrous growth to the formation of a dispersion with gravity level with the fibrous structures being formed during low-gravity conditions. Figure 3 shows the microstructural variations observed with gravity level in a sample processed at a furnace transition rate of 0.6 mm/min.

REFERENCES

Andrews, J. B., A. C. Sandlin, and P. A. Curreri, "The Influence of Gravity Level and Interfacial Energies on Dispersion Forming Tendencies in Hypermonotectic Cu-Pb-Al Alloys," Metall. Trans. A, 19A, 2645-2650 (1988).

Sandlin, A. C., J. B. Andrews, and P. A. Curreri, "The Influence of Interfacial Energies and Gravitational Levels on the Directionally Solidified Structures in Hypermonotectic Alloys," Metall. Trans. A, 19A, 2665-2669 (1988).

Andrews, J. B., C. J. Briggs, and M. B. Robin-

son, "Containerless Low-Gravity Processing of Immiscible Gold-Rhodium Alloys," in Materials and Fluid Sciences in Microgravity, ESA Publications Division, ESTEC, Noordwijk, The Netherlands, pp. 1121-1126 (1990).

Sandlin, A. C., J. B. Andrews, and P. A. Curreri, "Directional Solidification of Immiscible Cu-Pb-Al Alloys Under Alternating High-G/Low-G Conditions," in Materials and Fluid Sciences in Microgravity, ESA Publications Division, ESTEC, Noordwijk, The Netherlands, pp. 127-133 (1990).

Andrews, J. B., A. C. Sandlin, R. A. Merrick, Z. B. Dwyer, A. L. Schmale, and C. N. Buckhalt, "Solidification in Immiscible Systems," in Proceedings of the IKI/AIAA Microgravity Science Symposium, Moscow, USSR, pp. 238-246 (1991).

Andrews, J. B., R. A. Merrick, Z. B. Dwyer, A. C. Sandlin, and M. B. Robinson, "The Effect of Processing Conditions on Solidified Microstructures in Immiscible Systems," Materials Science Forum, 77, 269-282 (1991).

Andrews, J. B., A. L. Schmale, and A. C. Sandlin, "The Influence of Gravity Level During Directional Solidification of Immiscible Alloys," Journal of Crystal Growth, in press (1992).

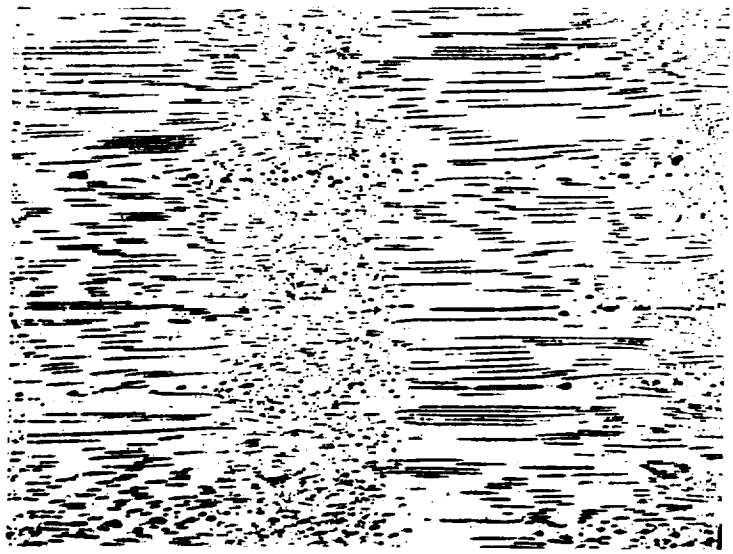

Figure 3. Variation in structure from an aligned fibrous composite to a dispersion as gravity level alternates from low g to high g.

INFLUENCE OF MICRO-GRAVITY ON THE SOLIDIFICATION BEHAVIOR OF METAL MATRIX COMPOSITES

Investigators: D. E. Morel, Applied Research Laboratory, Arlington, VA; D. M. Stefanescu, Dept. of Metallurgical Engineering, University of Alabama in Tuscaloosa, Tuscaloosa, AL; K. C. Russell Dept. of Nuclear, Engineering, Massachusetts Institute of Technology, Cambridge, MA; P. A. Curreri, Space Science Laboratory, NASA, Marshall Space Flight Center, Huntsville, AL

OBJECTIVES

The primary objective of this program is to investigate the effect of gravity level on microstructure development in ceramic reinforced metal matrix composites. The research currently in progress combines theoretical modeling of composite solidification with an experimental program utilizing the ADSF (Automated Directional Solidification Furnace) and the newly developed RMRQ (Rapid Melt/Rapid Quench) Furnace.

EXPERIMENTAL PROCEDURE AND RESULTS

The composite system under investigation in this study consists of the following: aluminum/nickel matrix; particulate silicon carbide, alumina, and calcia stabilized zirconia reinforcement; aluminum indium matrix; particulate, whisker, and continuous fiber silicon carbide reinforcement. Samples for solidification aboard the KC-135 aircraft are prepared by melt casting or powder processing (depending on the desired composition) and machined into rods 0.40 cm in diameter ranging from 4 cm to 8 cm in length. During the parabolic maneuvers performed by the KC-135, the furnace is translated along the sample axis at preselected velocities. Accelerometers measure gravity level as a function of time so that the position of the solidification front can be correlated with gravity level, time, and temperature during the experiment. All data are automatically recorded by computer during teach sample run.

Experimental efforts to date have focused on the Ni-Al alloy system (6.1 and 86.7 wt. % Ni) reinforced with particulate SiC (<7 micron in diameter and 50-150 micron). The solidification behavior of composite samples has been studied as a function of gravity level, particle size, furnace translation rate, and temperature gradient.

Microstructural development in these materials during solidification is strongly influenced by gravity level. When the advancing solidification front encounters a ceramic particle, particle engulfment is favored under high gravity levels where Stokes forces act to push the ceramic into the solidifying melt. High-gravity forces also tend to produce particle agglomeration so that a uniform distribution of the ceramic is difficult to achieve. Conversely, at low-gravity levels larger interparticle spacings and more uniform dispersions are observed (Figure 1). Theoretical modeling of particulate behavior of the melt/ceramic interface by Stefanescu et al. indicates that heat transfer conditions across the interface and the thermophysical properties of the ceramic and melt are important factors in determining reinforcement distribution in the final composite. The nature of particle shape and size also impacts engulfment but at present is not well understood. Future experiments will focus on modeling and the Al-In system.

138 INTENTIONALLY BLANK PRECEDING PAGE BLANK NOT FILMED

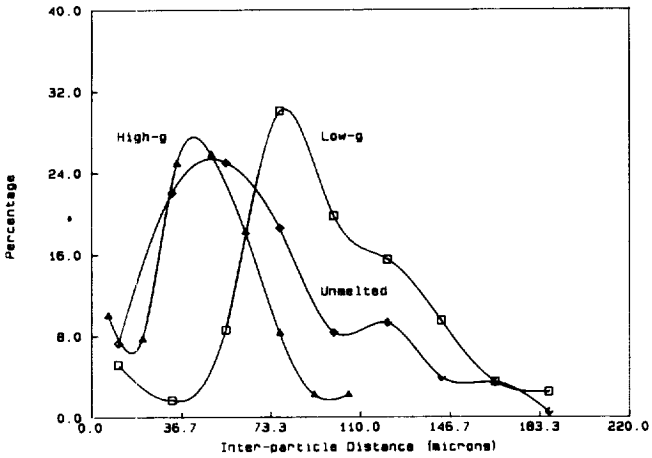

Figure 1. Interparticle spacings for a typical sample solidified under varying g levels aboard the KC-135.

REFERENCES

Stefanescu, D. M., A. Moitra, A. S. Kacar, and B. K. Dhindaw, "The Influence of Buoyant Forces and Volume Fraction of Particles on the Particle Pushing/Entrapment Transition During Directional Solidification of Al/SiC and Al/Graphite Composites," Metall. Trans., 21(A), 231 (1990).

Morel, D. E., "Microgravity Processing of Composite Materials," Proc. ACS 200th Meeting (1990).

Dhindaw, B. K., A. Moitra, D. M. Stafanescu, and P. A. Curreri, "Directional Solidification of Al-Ni/Sic Composites During Parabolic Trajectories," Metall. Trans., 19(A), 1899 (1988).

Moral, D. E., D. M. Stefanescu, and P. A. Curreri, "Microgravity Processing of Particulate Reinforced Metal Matrix Composites," in 21st International SAMPE Technical Conference, 21, 678 (1990).

Stefanescu, D. M., B. K. Dhindaw, S. A. Kacar, and A. Moitra, "Behavior of Ceramic Particles at the Solid-Liquid Metal Interface in Metal Matrix Composites," Metall. Trans., 19(A), 2847 (1988).

Stefanescu, D. M., and B. K. Dhindaw, "Behavior of Insoluable Particles at the Solid/Liquid Interface," Handbook: Metals Handbook: Casting, Vol. 15, p. 142 (1988).

Curreri, P. A., and D. M. Stefanescu, "Low Gravity Effects During Solidification," Metals Handbook: Casting, Vol. 15, pp. 147-158 (1988).

Frier, N., Y. Shiohara, and K. C. Russell, "Solidification Processing of a Monotectic Alloy Matrix Composite," Fall TMS-AIME Meeting, Chicago, September 1988.

Russell, K. C., N. Frier, and Y. Shiohara, "Overview of Monotectic Solidification and Related Microgravity Efforts," Symposium on Materials Processing in Spacer, ASM World Conference, Chicago, September 1988.

Russell, K. C., N. Firer, A. Mortensen, and P. A. Curreri, "Directional Solidification of Fiber Reinforced Composites," Fall TMS-AIME Meeting, Indianapolis, October 1989.

Cu-Pb AND Bi-Ga MONOTECTIC ALLOY DIRECTIONAL SOLIDIFICATION DURING PARABOLIC FLIGHT

Investigators: D. M. Stefanescu, B. K. Dhindaw, and A. K. Singh, Dept. of Metallurgical Engineering, University of Alabama, Tuscaloosa, AL; P. A. Curreri, Space Science Laboratory, NASA, Marshall Space Flight Center, Huntsville, AL

OBJECTIVES

Production of aligned rod morphologies in monotectic systems in a manner analogous to that in eutectic systems is an attractive goal. While aligned structures have been produced in the most common commercial monotectic systems, Cu-Pb, it is not clear by which mechanism these aligned structures are obtained. Therefore, process control to produce desired structures is difficult. In the present study, the effect of magnitude of gravity during solidification on the microstructure of Cu-Pb and Bi-Ga alloys is examined to better understand the mechanism of formation of aligned structures in these systems.

EXPERIMENTAL PROCEDURE AND RESULTS

The Cu-Pb samples were prepared by melting 99.9% pure lead shots and 99.9% pure copper pellets under argon atmosphere. The samples for directional solidification were vacuum pulled from the melt into 4 mm and 10 mm i.d. quartz tubes and quenched in air. Bi-Ga samples were prealloyed by mixing the appropriate weights of 99.999% pure Ga and Bi metals in a quartz tube which was connected to a high vacuum system with the capability to backfill with inert gas. At a pressure of 10^{-6} Torr, the tube was heated by a torch to a temperature above the Bi-Ga consolute temperature. The ampoule was agitated continuously during heating to achieve a homogeneous mixture. The molten sample was quenched in liquid nitrogen.

Direction solidification was accomplished in a Bridgman-type directional solidification furnace. The furnace used was a Space Applications Rocket Program (SPAR) prototype automatic directional solidification furnace with platinum-rhodium-heating coil and a 5 mm maximum sample diameter. This furnace was used for solidification in 1 g and during aircraft low-gravity maneuvers. The method used in this research for studying the effects of variable gravity level in solidification consists, in principle, of running the directional solidification furnace on a NASA KC-135 aircraft, while flying multiple parabolic trajectories (low-gravity maneuvers) which allow sections of the sample to solidify under alternative low-gravity (20 to 30 sec at 10^{-2} g) and high-gravity (1.5 min of 1 to 1.8 g) conditions.

After directional solidification, the samples were cut along the longitudinal axis, mounted, ground, and polished to be examined under the light microscope and the scanning electron microscope. The low melting point of Ga in Bi-Ga samples necessitated special polishing techniques which essentially involved keeping the samples cold while polishing. The Ga-Bi samples were kept refrigerated subsequent to solidification as well as before and after examination under a microscope.

Samples of hypomonotectic composition directionally solidified under variable gravity levels have microstructure consisting of copper dendrites with trapped intradendritic lead droplets. This structure occurred irrespective of whether solidification was under ground conditions or under low-gravity/high-gravity cycles. Due to the absence of sharp secondary arms of copper dendrites, the structure consisted of almost equiaxed copper crystals with intragranular lead. However, the grain size of

copper solidified in low gravity was larger than that for high-gravity solidification. Figure 1 shows a typical plot of number of grains per mm for regions solidified under low gravity and high gravity.

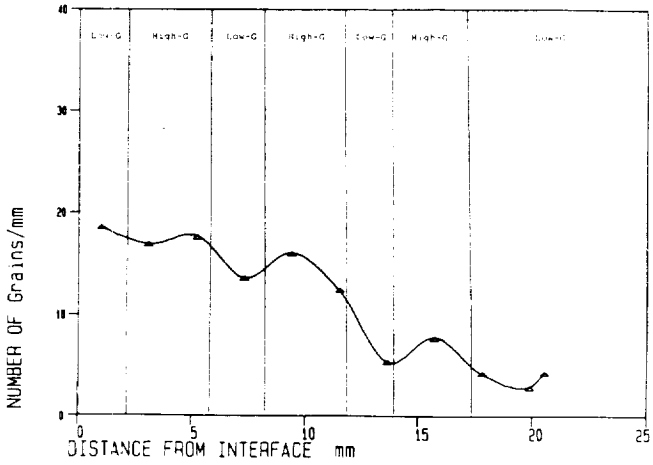

Figure 1. Variation of grain count per mm along Cu-Pb flight sample no. 6, directionally solidified at translation rate of 5 mm/min (temperature gradient of 10 °C/min).

In Cu-Pb alloys of nominal hypermonotectic composition directionally solidified under low-gravity maneuvers at translation rates greater than 10 mm/min, the fiber composite structure was initiated only in portions solidified under high gravity. Low-gravity initiation of directional solidification resulted in a structure consisting of grains of copper with droplets of lead. However, the fiber composite structure once established in the high-gravity regions, continues through the subsequent low-gravity regions.

The interfiber spacings (Figure 2) in samples solidified in low gravity were slightly higher than those for high gravity. Hypomonotectic Cu-Pb alloys showed aligned composite structure in a few areas in portions solidified under high gravity. Hypermonotectic composition solidified parallel to gravity at a rate of 18.7 mm/min and had a structure of large elliptical, randomly-oriented lead droplets near the interface followed by lead-rich bands, indicating lead segregation toward the sample bottom.

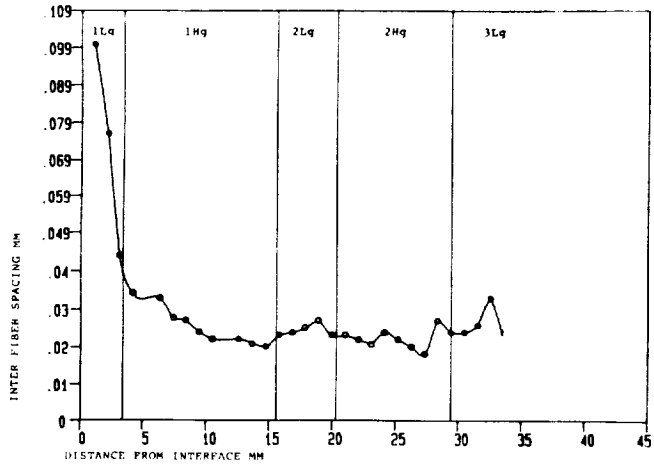

Figure 2. Plot of interfiber spacing versus distance from interface for nominal hypermonotectic Cu-Pb sample solidified at translation rate of 15 mm/min (temperature gradient of 10 °C/min) in parabolic trajectories (sample no. 9).

Four Bi50% Ga samples were directionally solidified in uncoated quartz tubes during low-gravity maneuvers. High solidification rates facilitated short fibrous growth. The gravity level did not seem to affect the structure at high growth rates, but at lower growth rates low gravity seemed to inhibit the short fibrous structures. The structures consisted of Ga droplets dispersed in a Bi matrix. The fiber composite structure observed in Cu-Pb samples was not observed.

Near monotectic and hypermonotectic Cu-Pb alloys, at high growth rates invariably a fiber composite structure is observed which is preceded by a lead-depleted zone. The initial lead fibers are slightly coarser than the subsequent structure. Figure 3 shows a schematic of the proposed model for fibrous composite growth.

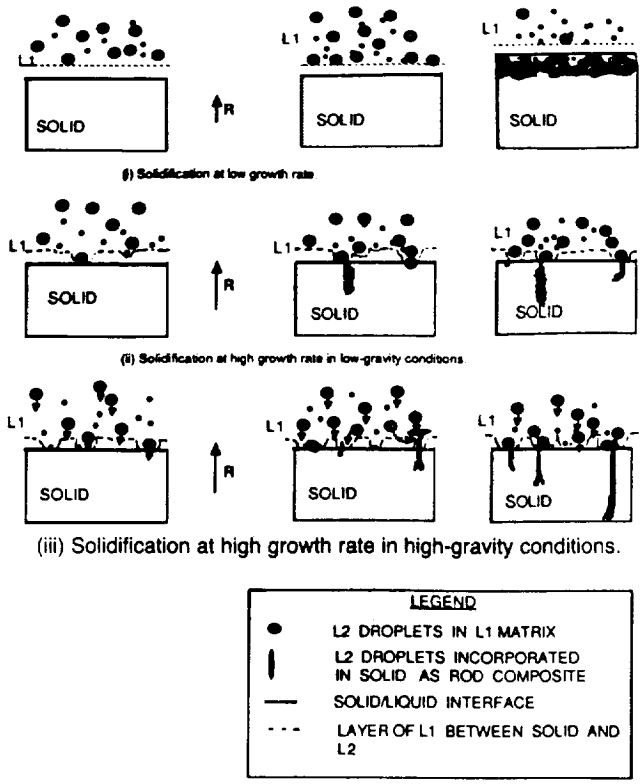

Figure 3. Schematic view of the growth front under varying conditions of solidification as time progresses from left to right: (i) occurrence of Pb-rich transverse bands at low growth rates (< 10 mm/min); (ii) few sites of incorporation of L_2 droplets as rod/fiber-composite; (iii) high rate of penetration of L_1 layer between α and L_2 phase by L_2 droplets, resulting in very prominent rod/fiber-composite structure.

An approximate calculation of the critical rate for engulfment of lead drops into alpha-interface using Chernov's approach gives the following numbers: (a) lead drops 20 microns dia; R_c = 0.0283 mm/min; (b) lead drops 50 microns dia; R_c = 0.00834 mm/min; where R_c = critical solidification rate above which lead droplets are engulfed. At growth rates in this study lead drops should by Chernov's model be engulfed by the interface.

Composite structure was not observed to start in low-g regions; however, once initiated in the high gravity, it continued in the low-gravity regions. Stokes forces in high-gravity solidification in a direction opposite to the gravity vector (Figure 3-iii) contributes to engulfmenet of L_2 drops by helping to overcome the disjoining forces. Stokes forces are insignificant in low-gravity solidification. The Stokes contribution appears to dominate (for the solidification conditions studied) the processes of initiation of composite growth (Figure 3-ii).

Interfiber spacing is higher in the low-gravity regions as compared to the high-gravity regions. This is consistent with decreased nucleation in low-gravity regions; the lead drops do not sedimentate to assist the formation of continuous fibers. Some fibers become truncated and the overall interfiber spacing becomes coarser.

REFERENCES

Dhindaw, B. K., D. M. Stefanescu, A. K. Singh, and P. A. Curreri, "Directional Solidification of Cu-Pb and Bi-Ga Monotectic Alloys Under Normal Gravity and During Parabolic Flight," Metall. Trans. 19A, 2839-2846 (1988).

THE INFLUENCE OF CONVECTION ON THE NUCLEATION AND GROWTH OF EUTECTIC Fe-C ALLOYS

Investigators: D. M. Stefanescu and H. Tian, Dept. of Metallurgical Engineering, University of Alabama, Tuscaloosa, AL; P. A. Curreri, Space Science Laboratory, NASA, Marshall Space Flight Center, Huntsville, AL

OBJECTIVES

For the particular case of stable Fe-C alloys (gray cast iron), which is the material studied in this research, the number of eutectic grains per unit areas (grain density) is a measure of the nuclei available for solidification. In this study heterogeneous nucleation and grain multiplication during solidification of gray cast iron, and the effect of gravitational level on them, have been studied by means of directional solidification on ground and under low-gravity (low-g) and high-gravity (high-g) conditions obtained by aircraft parabolic flights.

EXPERIMENTAL PROCEDURE AND RESULTS

The method used in this research was to have samples directionally solidified aboard the NASA KC-135 aircraft during repetitive low-g maneuvers and on ground. A sample which is being solidified in a Bridgman-type furnace during parabolic flight experiences a repetitive sequence of low-g and high-g forces parallel to the longitudinal growth axis. The acceleration imposed on the sample is monitored by three accelerometers mounted to the furnace assembly on orthogonal axes.

The thermal gradient in the furnace was controlled through the maximum temperature in the isothermal hot zone of the furnace. Thermal gradients were determined in air as well as with samples instrumented with alumina-coated thermocouples. The thermal gradients (crucible i.d. = 0.5 cm) in the liquid zone at the solid/liquid interface were 255 °C/cm and 175 °C/cm when the hot zone temperature was 1500 °C and 1350 °C, respectively. According to these data, it can be extrapolated that for a hot zone temperature of 1300 °C, the external gradient should be around 150 °C/cm.

Through this research, two types of samples were used: uninoculated (prepared at The University of Alabama) and inoculated (prepared at The University of Alabama and at the General Motors Technical Center). The longitudinal insert samples were prepared at General Motors based on the schematic in Figure 1. A core of inoculant alloy A700, with diameter of 1 mm, was inserted in the center of the 4 mm diameter sample. All samples were examined by means of optical microscopy, scanning electron microscopy-energy dispersive analysis by x-ray (SEM-EDAX), and image analysis. One microstructural feature monitored was the eutectic grain density, i.e., the number of grains per unit area. The grains were counted over a given area of the metallographic field, and the resulting number was divided by the surface area of the field to give the grain density (grains/mm^2). The average of the grain density over the four metallographic fields at a given position was considered as the grain density for that position.

Figure 2 shows the morphology of graphite in the low-g and high-g regions. It is obvious that graphite was finer in the high-g region as compared with the low-g region.

For both inoculated samples, the grain density vs. distance curves for the high-g regions parallel the curves for the low-g regions but at higher values (see Figure 3). From micrographs of the graphite morphology (Figure 2) it is clear that the graphite formed during the first low g was coarser than that formed during the first high g. In all cases, it was found that higher number of grains were obtained when

PRECEDING PAGE BLANK NOT FILMED

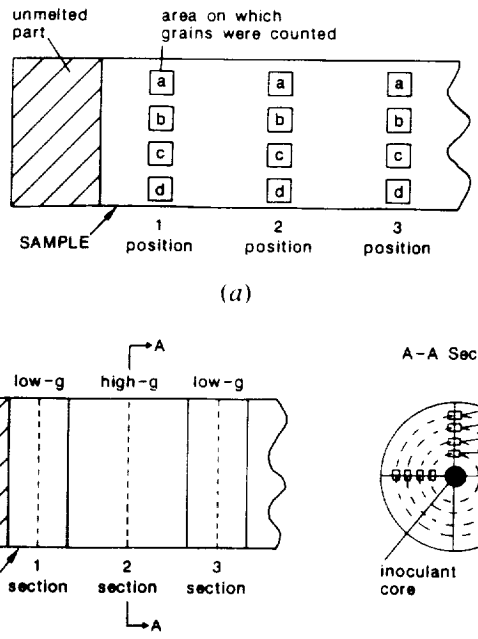

Figure 1. Schematic showing areas on which the number of grains was counted: (a) longitudinal, and (b) transverse counts.

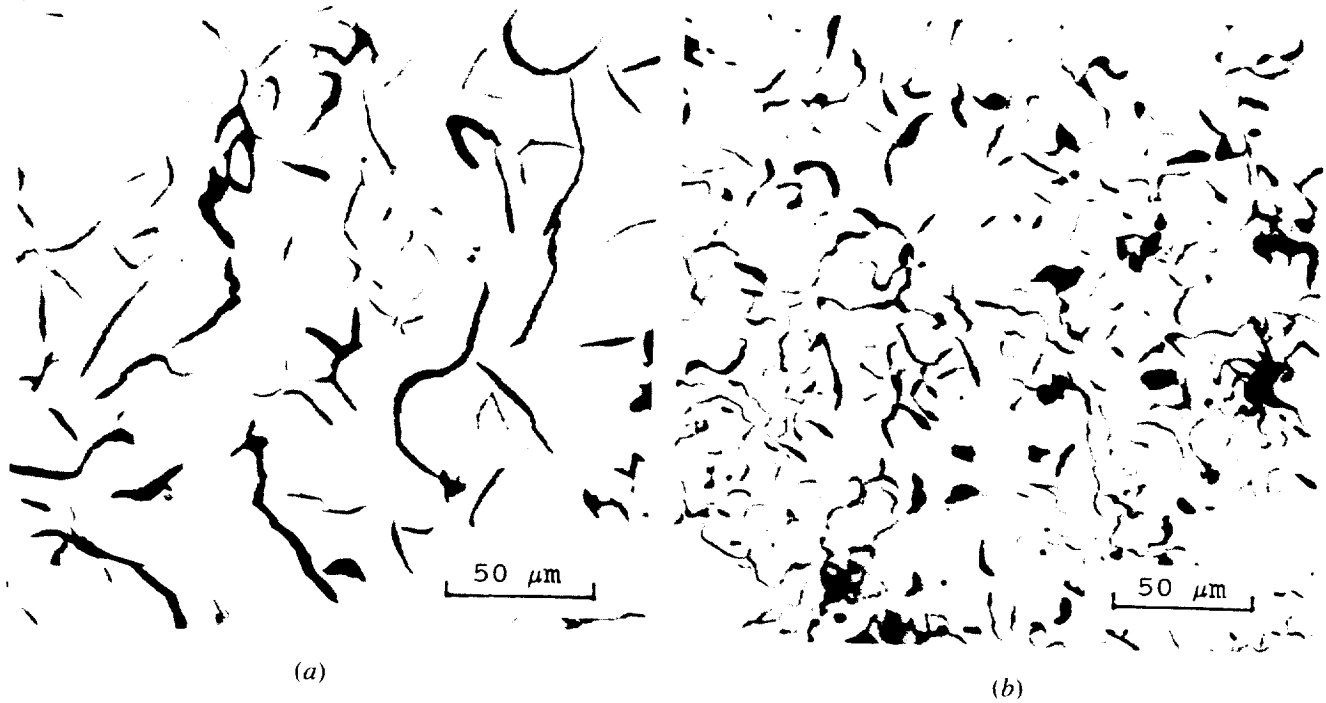

Figure 2. Graphite morphology of sample KC-FL-1: (a) low-g and (b) high-g regions. Magnification = 388.

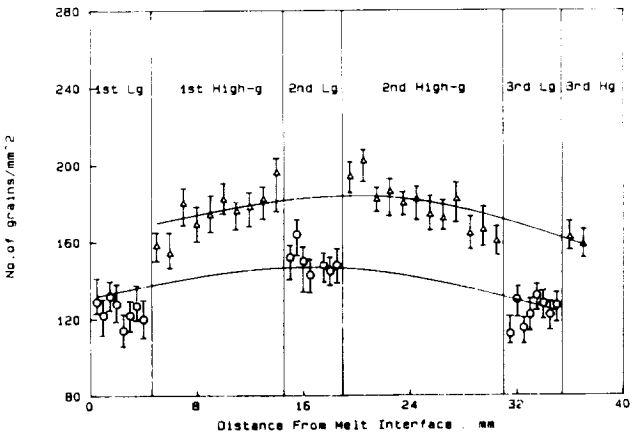

Figure 3. Variation of eutectic grain density with distance from melt interface for sample KC-FL-3, inoculated.

when solidifying in high g as compared with low g. This was attributed to higher convection in high g. It was demonstrated that grain multiplication can contribute 20% to 23% from the total number of grains resulting from heterogeneous nucleation of uninoculated samples for the given experimental conditions. It is proposed that the mechanism for grain multiplication in the case of gray cast iron consist in the breaking of tips of graphite plates, which is the leading phase, transport of these types away from the melt interface, and nucleation of new grains by these graphite fragments.

For the case of inoculated samples, it was shown that the contribution of the kinetics of chemical reactions to the convection-induced nucleation can be as high as 30% but can be nil at very low or very high grain numbers. This contribution is explained in terms of increased convection and diffusion in high g as compared with low g. To confirm these data, more experimental results are necessary.

Enough data were collected to demonstrate the viability of such an approach in the study of heterogeneous nucleation of metallic alloys. Also, the experimental parameters (soak time and temperature, temperature gradient, furnace translation rate, sample composition, and inoculation method) for a definitive space shuttle experiment were established.

The authors would like to acknowledge the direct participation and many helpful suggestions and advice they received from Norman Lillybeck (John Deere and Company) and from Michael Shea (General Motors).

REFERENCES

Tian, H., D. M. Stefanescu, and P. A. Curreri, "Influence of Low-Gravity Solidification on Heterogeneous Nucleation in Stable Iron-Carbon Alloys," Metall. Trans., 21A, 241 (1990).

Curreri, P. A., D J. Larson, and D. M. Stefanescu, "Influence of Convection on Eutectic Morphology," in Solidification Processing of Eutectic Alloys, D. M. Stefanescu, G. J. Abbaschian, and R. Bayuzick, eds., TMS Warrendale, PA, pp. 47-64 (1988).

Curreri, P. A., D. M. Stefanescu, "Low-Gravity Effects During Solidification," Metals Handbook: Casting, Ninth Edition, ASM, Vol. 15, p. 147 (1988).

SUPERCONDUCTING TRANSITION TEMPERATURE OF Al-In-Sn ALLOY DIRECTIONALLY SOLIDIFIED IN HIGH AND LOW GRAVITATIONAL FIELDS

Investigators: M. K. Wu, National Tsing Hua University, Hsinchu, Tiwan/ Republic of China; P. A. Curreri Space Science Laboratory, NASA, Marshall Space Flight Center, Huntsville, AL; W. F. Kaukler, Dept. of Chemistry, The University of Alabama in Huntsville, Huntsville, AL

OBJECTIVES

In an attempt to gain more insight into the low-gravity processing on the materials properties of immiscible alloys, we decided to carry out a systematic study of materials solidified directionally in a Bridgman furnace on NASA's KC-135 aircraft. The advantages of using KC-135 are that it is relatively inexpensive, has a short turnaround time, and provides the capability when combined with unidirectional solidification of having in one sample a series of identifiable sections grown in low gravity (low g) or high gravity (high g). The material chosen in this study is the ternary Al-In-Sn alloy. This alloy was chosen because the Al-In binary has been well studied and the addition of Sn to Al-In binary would alter the interphase interfacial energy and the morphology of the solid-liquid interface and therefore the cast structure. The study would then help to identify the role of interphase interfacial energies during solidification with varying g levels. In addition, the electrical properties of the binary Al-In, Al-Sn, and In-Sn alloys have been extensively studied. Therefore, an extention of the study to the ternary system is a logical choice.

EXPERIMENTAL PROCEDURES AND RESULTS

A sample which is being solidified experiences a repetitive sequence of low-gravity (low-g) and high-gravity (high-g) forces parallel to the longitudinal growth axis. The acceleration during processing is monitored by three accelerometers mounted on the furnace on orthogonal axes with one parallel to the longitudinal growth axis. The growth rate used for the experiments with Al-18In-14Sn alloy was 0.5 cm/min. This resulted in low-g sections of about 2.5 mm alternating with high-g sections of about 7.0 mm. The samples were positioned relative to the thermal gradient of the furnace to allow about 2 cm of the sample to remain unmolten prior to directional solidification. A photomicrograph of a longitudinal section of the Al-18.9In-14.6Sn flight sample for which properties data are reported here is shown in Figure 1.

Samples of different gravity level were sectioned using a diamond saw, and smaller samples of dimension 1 mm x 1 mm x 3 mm were cut and used for electrical and magnetic properties measurements. An ac inductance bridge operated at 40 Hz was used to measure the magnetic susceptibility. At this measurement frequency and sample size, it is expected that the measurements represent the bulk properties of the sample. The resolution of the measurements as determined by the use of standard samples for resistivity and magnetic susceptibility is within 0.1%. Transverse sections of different gravity level were mounted and polished for optical and scanning electron microscopy (SEM) study. Figures 2(a) and 2(b) give representative optical micrographs for transverse sections of the third high-g and fourth low-g zones. A SEM photograph showing the composite structure of the In-Sn particles is given in Figure 2(c). Wavelength dispersive x-ray (WDX) analysis was employed to determine the chemical composition of the samples.

148 INTENTIONALLY BLANK
PRECEDING PAGE BLANK NOT FILMED

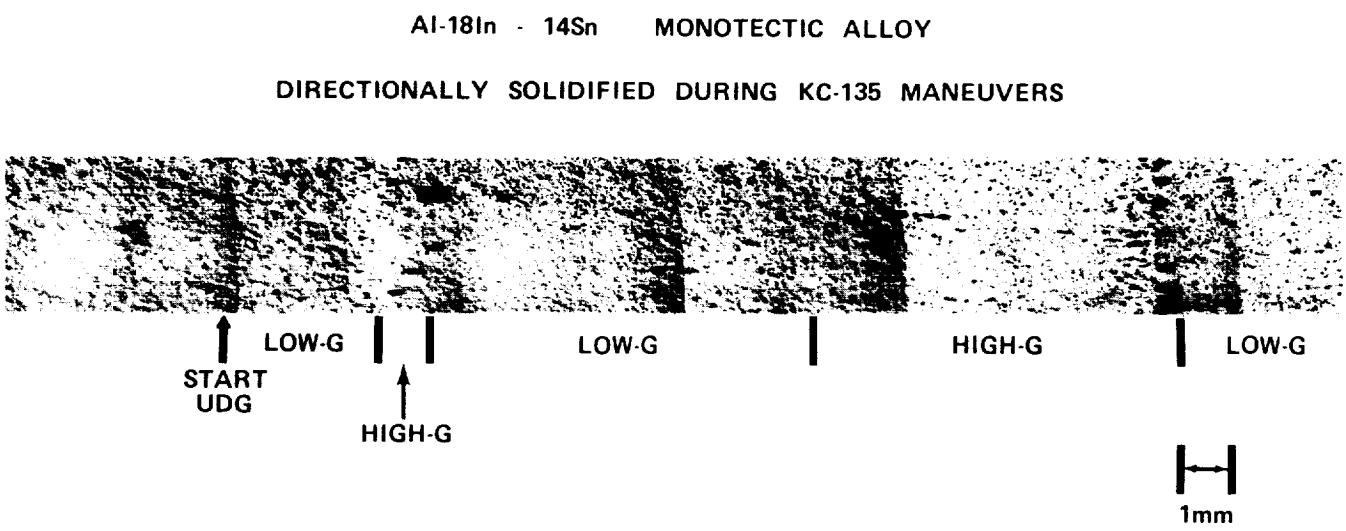

Figure 1. Photomicrograph of Al-18.9In-14.6Sn along longitudinal growth axis showing the microstructure of the sample up to the third low-g zone.

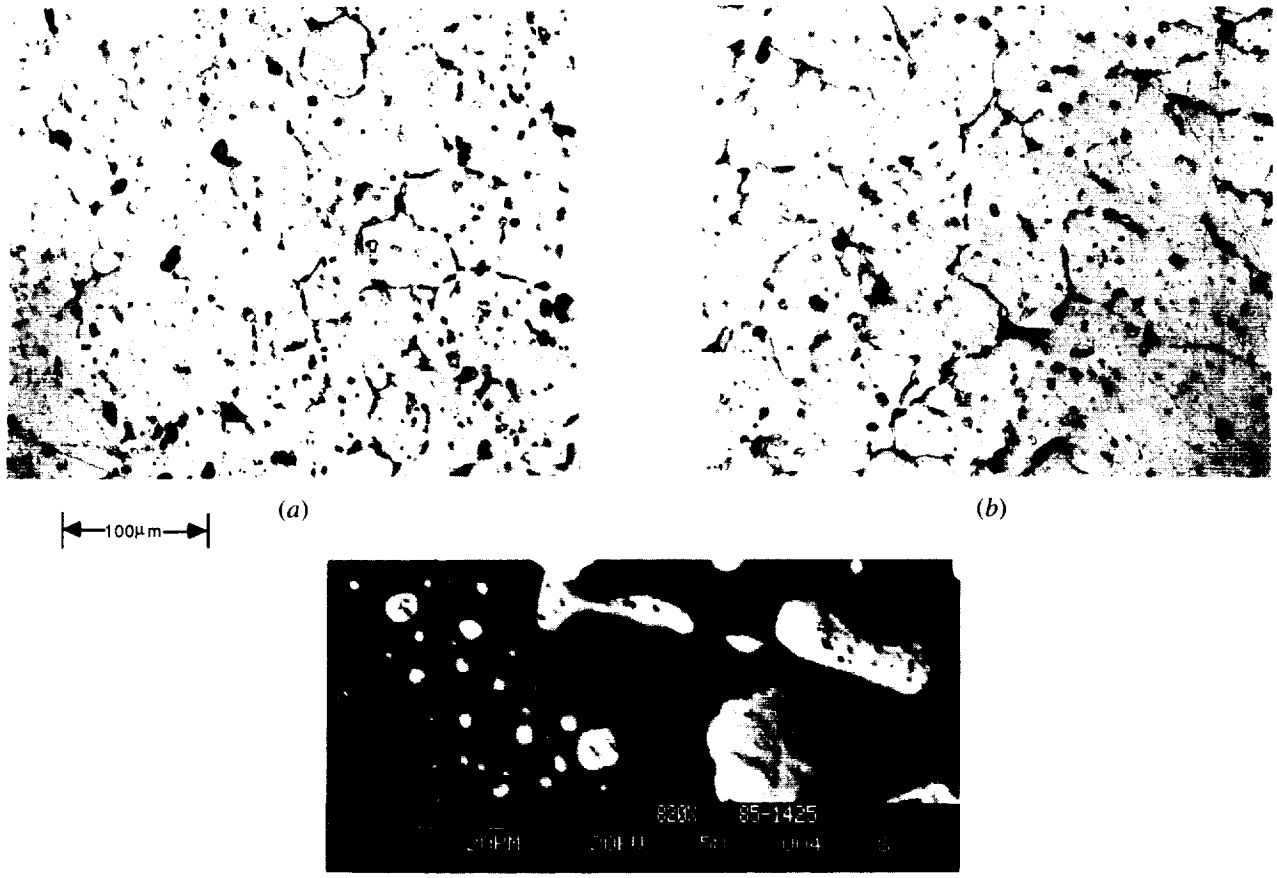

Figure 2. Photomicrographs of unetched sections. (a) and (b) representative optical micrographs of third high-g (sample 6) and fourth low-g (sample 7) zones, respectively, (c) SEM photograph showing the composite structure of In-Sn particles in the aluminum matrix.

Typical resistances R of samples solidified at different gravity levels are shown in Figure 3 as a function of temperature. It can be seen that resistance of low-g samples is less temperature-dependent. The resistance ratio of high-g samples is larger than that of low-g samples. On the other hand, the room temperature resistivity of the low-g samples is about a factor of 10 larger than that of the high-g samples. Results given in Figure 3 in comparison to the characteristic curves clearly indicate that the low-g sample behaves more like a semi-metal while the high-g sample is essentially metallic.

All samples studied become superconducting with an onset temperature ranging from 7.8 K to 6.3 K. Figure 4 shows the temperature dependence of the resistance and magnetic susceptibility at low temperature for high- and low-g section. The average transition width is 3 K, showing the inhomogeneous character of our material. T_c, resistance ratio, and the gravitational acceleration parallel to the growth axis during solidification as plotted vs. sample position are shown in Figure 5.

Microstructure and chemical composition analyses If the samples have been performed using SEM fitted with a WDX analyzer. The micrographs clearly show that samples consist of 3 to 50 micrometer particles embedded in the aluminum matrix. The average size and volume fraction (in the absence of macrosegregation) for In-Sn particles remained relatively constant for high- and low-g sections and was 4 microns and 0.6 microns, respectively. It is found that these are two different phases in these particles, viewed as dark and light phases in light field

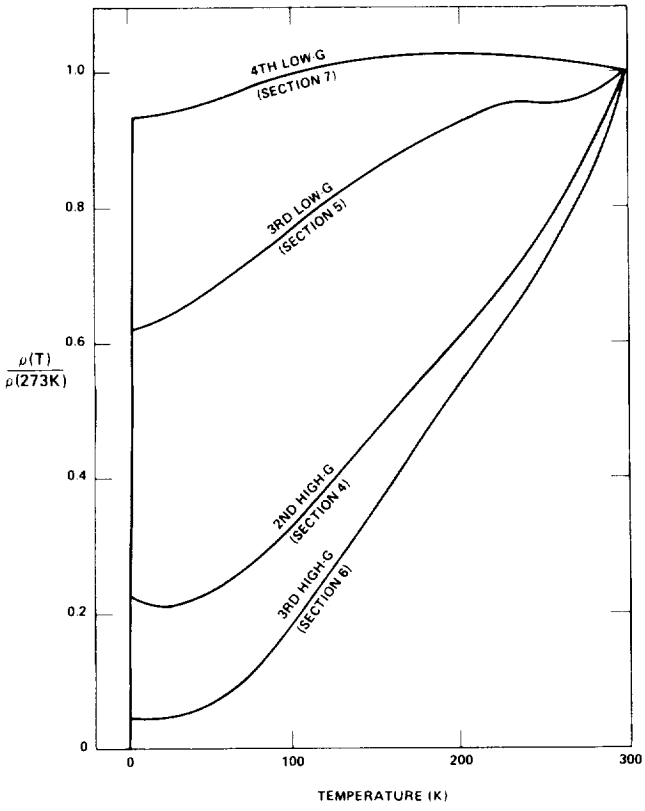

Figure 3. Normalized resistivity ρ(T)/ρ(300 K) as a function of temprature of Al-18.9In-14.6Sn solidified with different levels of acceleration.

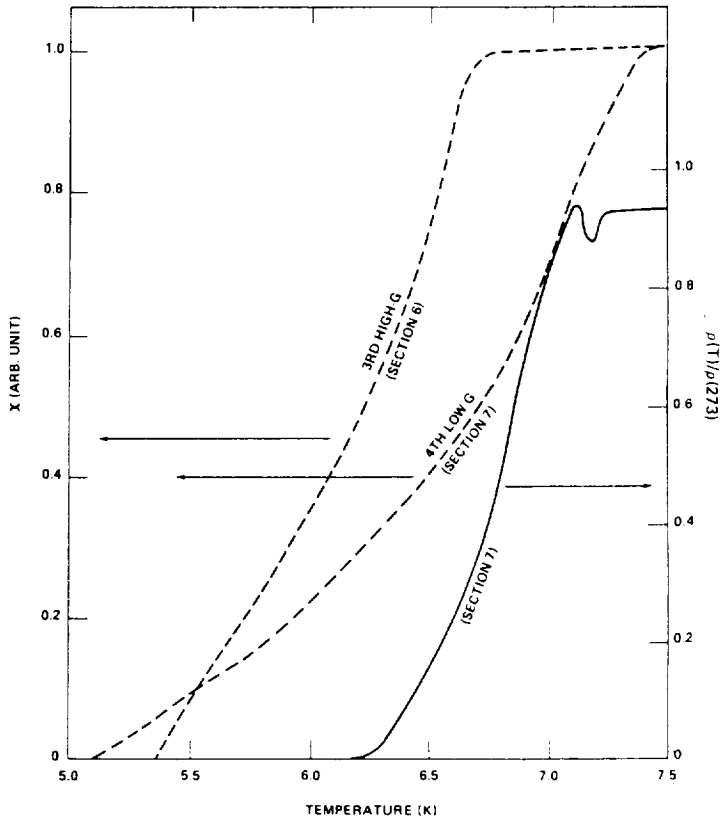

Figure 4. Electrical resistivity and magnetic susceptibility at low temperature of Al-18.9In-14.6Sn solidified with different levels of acceleration.

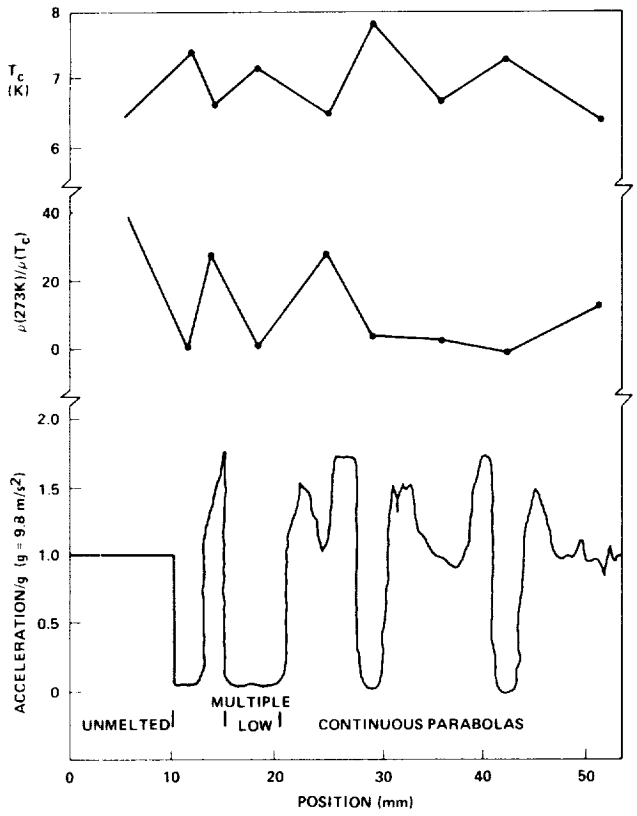

Figure 5. T_c, $\rho(300\ K)/\rho(T_c)$, and gravitational acceleration along longitudinal growth axis as a function of sample position.

SEM. The apparent volume fraction of the dark phase is about one-third of the particle. These particles are made almost entirely of In and Sn. The dark phase of the particles consists on In-Sn with 25 wt%. Sn and the Sn content doesn't change with g level during solidification. On the other hand, the Sn concentration of the light phase of the particles does appear to vary with gravity level. The low-g light phase is mainly In-Sn 25 wt% Sn.

The superconductivity observed is attributed to the presence of the In-Sn phase. Superconductivity of the In-Sn system has been extensively studied. It was found that T_c of the quenched samples varied from 7.8 K occurs at the bata phase with composition of 30 wt% Sn, while gamma phase alloys have T_c on the order of 6 K. Superconducting transition temperature of In-Sn alloys as a function of Sn content along

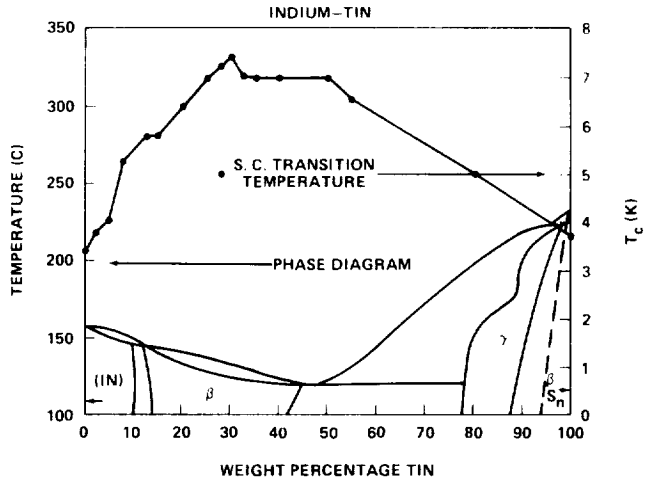

Figure 6. Superconducting transition temperature plotted vs. Sn concentration and phase diagram of In-Sn alloys.

with the In-Sn binary phase diagram is shown in Figure 6. This is consistent with our observations that low-g samples have T_c about 1 K higher than that of the high-g samples, and our hypothesis based on WDX analysis that low-g particle are essentially bata phase while high sections contain mainly gamma phase particles.

REFERENCES

Wu, M. K., J. R. Ashburn, P. A. Curreri, and W. F. Kaukler, "Electrical Properties of Al-In-Sn Alloys Directionally Solidified in High and Low Gravitational Fields," Metall. Trans., 18A, 1511-1517 (1987).

Wu, M. K., J. R. Asburn, C. J. Torng, P. A. Curreri, and C. W. Chu, "Pressure Dependence of the Electrical Properties of GaBi Solidified in Low Gravity," in Materials Processing in the Reduced Gravity Environment of Space, Vol. 87, eds., R. H. Doremus and P. C. Nordine, MRS North-Holland, pp. 77-84 (1987).

Curreri, P. A., P. N. Peters, P. T. Leong, H. Chou, M. K. Wu, and C. Y. Hugan," in High Temperature Superconducting Compounds: Processing and Related Properties, eds., S. H. Whang and A. DasGupta, TMS Warrendale, PA, pp. 143-154 (1989).

Curreri, P. A. P. N. Peters, R. C. Sisk, M. K. Wu, and C. Y. Huang, "High T_c Composite Silver/Oxide Superconductors," Metall. Trans., 21A, 257-260 (1990).

AUTHOR INDEX

SELECTED BIBLIOGRAPHY

Abbud-Madrid, A. and P. D. Ronney, "Effects of Radiative and Diffusive Transport on Premixed Flames Near Flammability Limits," in Twenty Third Symposium (International) on Combustion, Combustion Institute, pp. 423-431 (1990).

Andrews, J. B., C. J. Briggs, and M. B. Robinson, "Containerless Low-Gravity Processing of Immiscible Gold-Rhodium Alloys," Materials and Fluid Sciences in Microgravity, ESA Publications Division, ESTEC, Noordwijk, The Netherlands, pp. 1121-1126 (1990).

Andrews, J. B., A. C. Sandlin, and P. A. Curreri, "The Influence of Gravity Level and Interfacial Energies on Dispersion Forming Tendencies in Hypermonotectic Cu-Pb-Al Alloys, Metall. Trans. A, 19A, 2645-2650 (1988).

Andrews, J. B., A. C. Sandlin, and R. A. Merrick, "Directional Solidification in Immiscible Systems: The Influence of Gravity," Advances in Space Research, 11(7), 291-295 (1991).

Andrews, J. B., A. L. Schmale, and A. C. Sandlin, "The Influence of Gravity Level During Directional Solidification of Immiscible Alloys," Journal of Crystal Growth, in press (1992).

Andrews, J. B., R. A. Merrick, Z. B. Dwyer, A. C. Sandlin, and M. B. Robinson, "The Effect of Processing Conditions on Solidified Microstructures in Immiscible Systems," Materials Science Forum, 77, 269-282, (1991).

Andrews, J. B., A. C. Sandlin, R. A. Merrick, Z. B. Dwyer, A. L. Schmale, and C. N. Buckhalt, "Solidification in Immiscible Systems," in Proceedings of the IKI/AIAA Microgravity Science Symposium, Moscow, USSR, pp. 238-246 (1991).

Bamberger, S., J. M. Van Alstine, D. E. Brooks, J. B. Boyce, and J. M. Harris, in Progress in Low-Gravity Fluid Dynamics and Transport Phenomena, J. N. Koster and R. L. Sani, Eds., AIAA, Washington, pp. 603-630 (1990).

Bamberger, S., J. M. Van Alstine, J. M. Harris, J. K. Baird, R. S. Snyder, J. Boyce, and D. E. Brooks, Sep'n. Sci. and Technol., 23, 17-34 (1987).

Bostrup, G., J. Viola, and E. Gertner, "Experimental Ground-Based Bridgman CdTe Growth in NASA's Advanced Directional Solidification Furnace," AIAA-88-0251 (1988).
(1991).

Boyce, J. F., B. A. Hovanes, J. M. Harris, J. M. Van Alstine, and D. E. Brooks, J. Colloid Interf. Sci., in press (1992).

Buckmaster, J. D., G. Joulin, and P. D. Ronney, "Effects of Heat Loss on the Structure and Stability of Flame Balls," Combustion and Flame, 79, 381-392 (1990).

Buckmaster, J. D., G. Joulin, and P. D. Ronney, "Structure and Stability of Non-Adiabatic Flame Balls: II. Effects of Far-Field Losses," Combustion and Flame, 84, 411-422 (1991).

Cezairliyan, A. and A. P. Miiller, "A Dynamic Technique for Thermophysical Measurements at High Temperatures in a Microgravity Environment," Int. J. Thermophysics, 11, 653-662 (1990).

Curreri, P. A., D. M. Stefanescu, "Low-Gravity Effects During Solidification," Metals Handbook: Casting, Ninth Edition, ASM, Vol. 15, p. 147 (1988).

Curreri, P. A., D J. Larson, and D. M. Stefanescu, "Influence of Convection on Eutectic Morphology," in Solidification Processing of Eutectic Alloys, D. M. Stefanescu, G. J. Abbaschian, and R. Bayuzick, eds., TMS, Warrendale, PA, pp. 47-64 (1988).

Curreri, P. A., P. N. Peters, R. C. Sisk, M. K. Wu, and C. Y. Huang, "High T_c Composite Silver/Oxide Superconductors," Metall. Trans., 21A, 257-260 (1990).

Curreri, P. A., P. N. Peters, P. T. Leong, H. Chou, M. K. Wu, and C. Y. Hugan," in High Temperature Superconducting Compounds: Processing and Related Properties, eds., S. H. Whang and A. Das-Gupta, eds., TMS Warrendale, PA, pp. 143-154 (1989).

Deuser, M. S., J. M. Van Alstine, J. C. Vellinger, F. C. Wessling, and C. A. Lundquist, in Proceedings of the VIIIth European Symposium on Materials and Fluid Sciences Under Microgravity, ESA Publications, Noordwijk (1992).

Dhindaw, B. K., D. M. Stefanescu, A. K. Singh, and P. A. Curreri, "Directional Solidification of Cu-Pb and Bi-Ga Monotectic Alloys Under Normal Gravity and During Parabolic Flight," Metall. Trans., 19A, 2839-2846 (1988).

Farmer, J. N. and P. D. Ronney, "A Numerical Study of Unsteady Nonadiabatic Flames," Combustion Science and Technology, 73, 555-574 (1990).

Gans, R. and F. Leslie, "Low Gravity Liquid Management: A Hydrostatic Stability Problem," 37th Annual Meeting of the Division of Fluid Dynamics, American Physical Society, Providence, RI, November 18-20 (1984).

Gans, R. F. and F. W. Leslie, "Interface Stability in a Slowly Rotating Low Gravity Tank: Theory," AIAA 24th Aerospace Sciences Meeting, January 6-9, 1986, Reno, NV, AIAA-86-0198 (1986).

Gans, R. F. and F. W. Leslie, "Interface Stability in a Slowly Rotating Tank: Theory," J. of Spacecraft and Rockets, 24, 232-235 (1987).

Giarratano, P. J., A. Kumakawa, V. D. Arp, and R. B. Owen, "Transient Heat-Transfer Studies in Low-Gravity Using Optical Measurement Techniques," J. of Thermophysics and Heat Transfer, 4(1), 53-58 (1990).

Grugel, R. N. and A. Hellawall, Metall. Trans. A, 12A, 669-681 (1981).

Grugel, R. N. and R. Poorman, in Materials Science Forum, Materials Processing in Space, Vol. 50, Trans Tech Publications, Ltd., N. B. Singh, V. Laxmanan, and E. W. Collings, eds., pp. 89-100 (1989).

Herren, B. J., S. G. Shafer, J. M. Van Alstine, J. M. Harris, and R. S. Snyder, J. Colloid Interf. Sci., 115, 46-55 (1987).

Hinman, E. M., "Robot-Tended Crystal Growth in a Space-Based Laboratory," International Symposium on Laboratory Automation and Robotics Proceedings (1990).

Hinman, E. M. and G. L. Workman, "Characterizing Microgravity Performance of a Laboratory Robot," to appear in Proceedings of the 1991 International Robots & Vision Automation Conference, Detroit, MI, October 1991.

Hinman, E. M. and G. L. Workman, "Simulations for IVA Robotics," Advances in Intelligent Robotic Systems -- Sensor Fusion IV: Control Paradigns and Data Structures, to appear in Proceedings SPIE, Boston, MA, November 1991.

Hinman, E. M., D. Gilliam, and G. L. Workman, "Physical and Digital Simulations for Space Robotics," The Southeastern Simulation Council - SESC 1990, Society for Computer Simulation, International, October 1990.

Li, Houcheng, G. L. Workman, and E. M. Hinman, "Characterization and Improvement of Robot Dynamics Through Simulation," The Southeastern Simulation Council - SESC 1990, Society for Computer Simulation, International, October 1990.

Karr, L. J., J. M. Harris, S. G. Shafer, J. M. Van Alstine, and R. S. Snyder, J. Chromatog., 442, 219-227 (1987).

Leslie, F. W., "Measurements of Rotating Bubble Shapes in a Low Gravity Environment," J. Fluid Mechanics, 161, 269-279 (1984).

Leslie, F. and R. F. Gans, "Interface Stability in a Slowly Rotating Low Gravity Tank: Experiments," AIAA 24th Aerospace Sciences Meeting, January 6-9, 1986, Reno, NV, AIAA-86-0197 (1986).

Leslie, Fred, Roger Gans, and Charles Schafer, "Fluid Surface Behavior in Low Gravity," NASA TP-2486 (1985).

Leslie, F., C. Schafer, and R. Gans, "Classical Model of Liquid Helium Management for Gravity Probe-B," Proceedings of 1983 Space Helium Dewar Conference, edited by John B. Hendricks and Gerald R. Karr, University of Alabama in Huntsville, 199-210 (1983).

Miiller, A. P. and A. Cezairliyan, "A Dynamic Technique for Measuring Surface Tension at High Temperatures in a Microgravity Environment," Int. J. Thermophysics, 11, 663-674 (1990).

McCay, M. H. and T. D. McCay, "Measurement of Solutal and Thermal Layers in Directional Solidification," AIAA-87-1494 (1987).

McCay, M. H. and T. D. McCay, "Measurement of Solutal Layers in Unidirectional Solidification," J. Thermophysics and Heat Transfer, 2(3) (1988).

McCay, T. D., M. H. McCay, and P. A. Gray, "Experimental Observation of Convective Breakdown of the Diffusion Layer During Alloy Solidifications," Phys. Rev. Lett., 2060-2063 (1989).

McCay, T. D., M. H. McCay, and S. A. Lowry, AIAA 24th Thermophysics Conference, Buffalo, New York, AIAA-89-1755 (1989).

McCay, T. D., M. H. McCay, S. A. Lowry, and L. M. Smith, "Convection Instabilities During Directional Solidification," J. Thermophysics and Heat Transfer, in press (1992).

Noever, D. A., "A Note on the No-Slip Boundary Condition Applied to Diffusing Gases," Phys. Lett. A, 144, 253-255 (1990).

Noever, D. A., "The Baroeffect and an Appropriate Momentum Boundary Condition," Physics of Fluids A: Fluid Dynamics, 2, 863-865 (1990).

Noever, D. A., "The Ternary Baroeffect with a Third, Non-Duffusing Component," Phys. Rev. Lett., 65, 1587-1590 (1990).

Noever, D. A., "Fractal Dimension of Bioconvective Patterns," J. Phys. Soc. Japan, 59, 10-13 (1990).

Noever, D. A., "Bioconvective Patterns, Synchrony and Survival," Phys. Rev. Lett., 65, 1953-1956 (1990).

Noever, D. A., "A Rotating Spectrometer for Separation/Concentration of Bioconvecting Microorganisms," Rev. Scien. Instrum., 62, 229-232 (1991).

Noever, D. A. "Diffusive Slip and Surface Transport Properties," J. Coll. Interfac. Sci., 147(1), 186-191 (1991).

Noever, D. A., "Evolution of Bioconvective Patterns in Variable Gravity," Phys. Rev. A, 44, 5279-5291 (1992).

Noever, D. A. and H. C. Matsos, "The Rotating Spectrometer: New Biotechnology for Cell Separations," NASA TM-103522, November 1990.

Noever, D. A. and H. C. Matsos, "A Biosensor for Cadmium Based on Bioconvective Patterns," NASA TM-103523, November 1990.

Noever, D. A. and H. C. Matsos, "A Bioassay for Monitoring Cadmium Based on Bioconvective Patterns," J. Environ. Sci. Health, A26, 273-286 (1991).

Noever, D. A. and H. C. Matsos, "Calcium Protection Against Cadmium Poisoning: Bioconvective Indicators in Tetrahymena," J. Environ. Sci. Health, A26, 1105-1113 (1991).

Noever, D. A., H. C. Matsos, J. U. Johnson, and R. J. Cronise, "A Decisive Test of Gravity's Role in Biologically Generated Cellular Patterns," Phys. Rev. Lett., submitted (1991).

Rey, C. A., "Final Report," Contract NAS8-37592, NASA/MSFC, March 28, 1991.

Rey, C. A. and D. E. Day, "Glass Formation in Microgravity," Mat. Res. Soc. Symp. Proc., 87 (1987).

Rey, C. A. and D. R. Merkley, "Initial Report on HAL KC-135 Test," NASA/MSFC, July 11, 1989.

Rey, C. A. and D. R. Merkley, "Final Report," Contract NAS8-33742, NASA/MSFC, August 24, 1989.

Rey, Charles A., et al., "Acoustic Levitation Materials Processing Systems," 17th Aerospace Sciences Meeting, AIAA, New Orleans (1979).

Rey, C. A., T. J. Danley, D. R. Merkley, and G. R. Hammarlund, "A New Acoustic Levitation Device Using the Interference Sound Field from Two Opposed Radiators," 114th Annual Meeting of Acoustical Society of America (1987).

Rey, C. A., D. R. Merkley, G. R. Hammarlund, and T. J. Danley, "Specimen Translational Control Capabilities Using an Opposed Radiator Acoustic Levitation System," 114th Annual Meeting of Acoustical Society of America (1987).

Rey, C. A., D. R. Merkley, G. R. Hammarlund, and T. J. Danley, "Acoustic Leviatation Technique for Containerless Processing at High Temperature in Space," Metall. Trans., 19A (1988).

Ronney, P. D., "On the Mechanism of Flame Propagation Limits and Extinction Processes at Microgravity," in Twenty Second Symposium (International) on Combustion, Combustion Institute, pp. 1615-1623 (1988).

Ronney, P. D., "Near-Limit Flame Structures at Low Lewis Number," Combustion and Flame, 82, 1-14 (1990).

Ronney, P. D. and G. I. Sivashinsky, "A Theoretical Study of Propagation and Extinction of Nonsteady Spherical Flame Fronts," SIAM J. Appl. Math., 49, 1029-1046 (1989).

Sandlin, A. C. and R. J. Schaefer, "Surface Energy Reduction in Fibrous Monotectic Structures," Metall. Trans. A (1990).

Sandlin, A. C., J. B. Andrews, and P. A. Curreri, "The Influence of Interfacial Energies and Gravitational Levels on the Directionally Solidified Structures in Hypermonotectic Alloys," Metall. Trans. A, 19A, 2665-2669 (1988).

Sandlin, A. C., J. B. Andrews, and P. A. Curreri, "Directional Solidification of Immiscible Cu-Pb-Al Alloys Under Alternating High-G/Low-G Conditions," in Materials and Fluid Sciences in Microgravity, ESA Publications Division, ESTEC, Noordwijk, The Netherlands, pp. 127-133 (1990).

Sen, Radha and W. R. Wilcox, "Behavior of a Non-Wetting Melt in Free Fall: Experimental," Journal of Crystal Growth, 74, 591-596 (1986).

Sen, Radha and W. R. Wilcox, "Behavior of a Non-Wetting Melt in Free Fall: Theoretical," Journal of Crystal Growth, 78, 129-134 (1986).

Tian, H., D. M. Stefanescu, and P. A. Curreri, "Influence of Low-Gravity Solidification on Heterogeneous Nucleation in Stable Iron-Carbon Alloys," Metall. Trans., 21A, 241 (1990).

Trinh, E. H., "Levitation Studies of the Physical Properties and Nucleation of Undercooled Liquids," ESA SP-295, 503 (1990).

Trinh, E. H., "Fluid Dynamics and Solidification of Levitated Drops and Shells," Progress in Astronautics and Aeronautics, 130, 515 (1991).

Trinh, E. H. and C. J. Hsu, "Equilibrium Shapes of Acoustically Levitated Drops," J. Acoust. Soc. Am., 79, 1335 (1986).

Trinh, E. H., J. L. Robey, A. Arce, and M. Gaspar, "Experimental Studies in Fluid Mechanics and Materials Science Using Acoustic Levitation," Mat. Res. Soc. Symp. Proc., 87, 57 (1986).

Uhlmann, D. R., B. Chalmers, and K. A. Jackson, J. App. Phys., 35(10), 2986-2993 (1964).

Van Alstine, J. M., S. Bamberger, J. M. Harris, R. S. Snyder, and D. E. Brooks, in Proceedings of the VIIth European Symposium on Materials and Fluid Sciences Under Microgravity, ESA Publication SP-295, pp. 399-407 (1989).

Walter, H., D. Fisher, and D. E. Brooks, "Partitioning in Aqueous Two-Phase Systems," Theory, Methods, Uses, and Applications in Biotechnology, Academic Press, Orlando (1986).

Whaling, K. N., A. Abbud-Madrid, and P. D. Ronney, "Structure and Stability of Near-Limit Flames with Low Lewis Number," Fall Technical Meeting, Combustion Institute, Western States Section, October 15-16, La Jolla, CA (1990).

Witt, A. F., H. C. Gatos, M. Lichtensteiger, M. Lavine, and C. J. Herman," Crystal Growth and Steady State Segregation Under Zero Gravity: InSb," J. Electrochem. Soc., 122, 276-283 (1975).

Witt, A. F., H. C. Gatos, M. Lichtensteiger, M. Lavine, and C. J. Herman, "Crystal Growth and Steady State Segregation Under Zero Gravity: Ge," J. Electrochem. Soc., 125, 1832-1840 (1978).

Workman, G. L., Contract Final Report, NAS8-36955, D. O. 72.

Workman, G. L. and W. F. Kaukler, "Convective Flow Analysis on the KC-135 Aircraft," AIAA-92-0844.

Workman, G. L., T. Grisham, E. Hinman, and C. Coker, "Robot Dynamics in Reduced Gravity Environment," Fifth Conference on Artificial Intelligence for Space Applications, NASA CP-3073 (1990).

Wu, M. K., J. R. Ashburn, P. A. Curreri, and W. F. Kaukler, "Electrical Properties of Al-In-Sn Alloys Directionally Solidified in High and Low Gravitational Fields," Metall. Trans., 18A, 1511-1517 (1987).

Wu, M. K., J. R. Asburn, C. J. Torng, P. A. Curreri, and C. W. Chu, "Pressure Dependence of the Electrical Properties of GaBi Solidified in Low Gravity," in Materials Processing in the Reduced Gravity Environment of Space, Vol. 87, eds., R. H. Doremus and P. C. Nordine, MRS North-Holland, pp. 77-84 (1987).

SUBJECT INDEX

REPORT DOCUMENTATION PAGE

Form Approved
OMB No 0704-0188

Public reporting burden for this collection of information is estimated to average 1 hour per response, including the time for reviewing instructions, searching existing data sources, gathering and maintaining the data needed, and completing and reviewing the collection of information. Send comments regarding this burden estimate or any other aspect of this collection of information, including suggestions for reducing this burden, to Washington Headquarters Services, Directorate for Information Operations and Reports, 1215 Jefferson Davis Highway, Suite 1204, Arlington, VA 22202-4302, and to the Office of Management and Budget, Paperwork Reduction Project (0704-0188), Washington, DC 20503.

1. AGENCY USE ONLY (Leave blank)	2. REPORT DATE	3. REPORT TYPE AND DATES COVERED
	March 1993	Technical Memorandum

4. TITLE AND SUBTITLE

Materials Science on Parabolic Aircraft - The FY 87-89 KC-135 Microgravity Test Program

5. FUNDING NUMBERS

6. AUTHOR(S)

Peter A. Curreri, Editor

7. PERFORMING ORGANIZATION NAME(S) AND ADDRESS(ES)

George C. Marshall Space Flight Center
Marshall Space Flight Center, AL 35812

8. PERFORMING ORGANIZATION REPORT NUMBER

M-713

9. SPONSORING / MONITORING AGENCY NAME(S) AND ADDRESS(ES)

National Aeronautics and Space Administration
Washington, D.C. 20546

10. SPONSORING / MONITORING AGENCY REPORT NUMBER

NASA TM-4456

11. SUPPLEMENTARY NOTES

Prepared by Space Science Laboratory, Science and Engineering Directorate.

12a. DISTRIBUTION / AVAILABILITY STATEMENT

Subject Category: 29

Unclassified--Unlimited

12b. DISTRIBUTION CODE

13. ABSTRACT *(Maximum 200 words)*

This document covers research results from the KC-135 Materials Science Program managed by MSFC for the period FY87 through FY89. It follows the previous NASA Technical Memorandum for FY84-86 published in August 1988. This volume contains over 30 reports grouped into eight subject areas covering acceleration levels, space flight hardware, transport and interfacial studies, thermodynamics, containerless processing, welding, melt/crucible interactions, and directional solidification. The KC-135 materials science experiments during FY87-89 accomplished direct science, preparation for space flight experiments, and justification for new experiments in orbit.

14. SUBJECT TERMS	15. NUMBER OF PAGES
KC-135, Low Gravity, Materials Science, Parabolic Maneuvers, Microgravity, Containerless Processing	**172**
	16. PRICE CODE: A08

17. SECURITY CLASSIFICATION OF REPORT	18. SECURITY CLASSIFICATION OF THIS PAGE	19. SECURITY CLASSIFICATION OF ABSTRACT	20. LIMITATION OF ABSTRACT
Unclassified	**Unclassified**	**Unclassified**	**Unlimited**

NSN 7540-01-280-5500

Standard Form 298 (Rev 2-89)
Prescribed by ANSI Std Z39-18
298-102

NASA-Langley, 1993